Online ISSN : 2249-4626
Print ISSN : 0975-5896
DOI : 10.17406/GJSFR

GLOBAL JOURNAL

OF SCIENCE FRONTIER RESEARCH: A

Physics and Space Science



Highlights

- Stick-Slip Torsional Vibrations
- Transmission Electron Microscopy
- Elivination of the Contradiction
- Spontaneous Symmetry Transitions

Discovering Thoughts, Inventing Future

VOLUME 22 ISSUE 6 VERSION 1.0

© 2001-2022 by Global Journal of Science Frontier Research, USA

Volume 22 Issue 23 was originally issued as A6

Global Journal of Science Frontier Research: A
Physics & Space Science

Volume 22 Issue 23
Originally issued as A6

Global Journal of Science Frontier Research: A
Physics & Space Science

Volume 22 Issue 6 (Ver. 1.0)

Open Association of Research Society

© Global Journal of Science Frontier Research. 2022.

All rights reserved.

This is a special issue published in version 1.0 of "Global Journal of Science Frontier Research." By Global Journals Inc.

All articles are open access articles distributed under "Global Journal of Science Frontier Research"

Reading License, which permits restricted use. Entire contents are copyright by of "Global Journal of Science Frontier Research" unless otherwise noted on specific articles.

No part of this publication may be reproduced or transmitted in any form or by any means, electronic or mechanical, including photocopy, recording, or any information storage and retrieval system, without written permission.

The opinions and statements made in this book are those of the authors concerned. Ultraculture has not verified and neither confirms nor denies any of the foregoing and no warranty or fitness is implied.

Engage with the contents herein at your own risk.

The use of this journal, and the terms and conditions for our providing information, is governed by our Disclaimer, Terms and Conditions and Privacy Policy given on our website http://globaljournals.us/terms-and-condition/menu-id-1463/

By referring / using / reading / any type of association / referencing this journal, this signifies and you acknowledge that you have read them and that you accept and will be bound by the terms thereof.

All information, journals, this journal, activities undertaken, materials, services and our website, terms and conditions, privacy policy, and this journal is subject to change anytime without any prior notice.

Incorporation No.: 0423089
License No.: 42125/022010/1186
Registration No.: 430374
Import-Export Code: 1109007027
Employer Identification Number (EIN):
USA Tax ID: 98-0673427

Global Journals Inc.

*(A Delaware USA Incorporation with "Good Standing"; **Reg. Number: 0423089**)*
Sponsors: Open Association of Research Society
Open Scientific Standards

Publisher's Headquarters office

Global Journals® Headquarters
945th Concord Streets,
Framingham Massachusetts Pin: 01701,
United States of America
USA Toll Free: +001-888-839-7392
USA Toll Free Fax: +001-888-839-7392

Offset Typesetting

Global Journals Incorporated
2nd, Lansdowne, Lansdowne Rd., Croydon-Surrey,
Pin: CR9 2ER, United Kingdom

Packaging & Continental Dispatching

Global Journals Pvt Ltd
E-3130 Sudama Nagar, Near Gopur Square,
Indore, M.P., Pin:452009, India

Find a correspondence nodal officer near you

To find nodal officer of your country, please email us at *local@globaljournals.org*

eContacts

Press Inquiries: *press@globaljournals.org*
Investor Inquiries: *investors@globaljournals.org*
Technical Support: *technology@globaljournals.org*
Media & Releases: *media@globaljournals.org*

Pricing (Excluding Air Parcel Charges):

Yearly Subscription (Personal & Institutional)
250 USD (B/W) & 350 USD (Color)

Editorial Board

Global Journal of Science Frontier Research

Dr. John Korstad

Ph.D., M.S. at Michigan University, Professor of Biology, Department of Biology Oral Roberts University, United States

Dr. Alicia Esther Ares

Ph.D. in Science and Technology, University of General San Martin, Argentina State University of Misiones, United States

Dr. Sahraoui Chaieb

Ph.D. Physics and Chemical Physics, M.S. Theoretical Physics, B.S. Physics, cole Normale Suprieure, Paris, Associate Professor, Bioscience, King Abdullah University of Science and Technology United States

Tuncel M. Yegulalp

Professor of Mining, Emeritus, Earth & Environmental Engineering, Henry Krumb School of Mines, Columbia University Director, New York Mining and Mineral, Resources Research Institute, United States

Andreas Maletzky

Zoologist University of Salzburg, Department of Ecology and Evolution Hellbrunnerstraße Salzburg Austria, Universitat Salzburg, Austria

Dr. Gerard G. Dumancas

Postdoctoral Research Fellow, Arthritis and Clinical Immunology Research Program, Oklahoma Medical Research Foundation Oklahoma City, OK United States

Dr. Mazeyar Parvinzadeh Gashti

Ph.D., M.Sc., B.Sc. Science and Research Branch of Islamic Azad University, Tehran, Iran Department of Chemistry & Biochemistry, University of Bern, Bern, Switzerland

Dr. Indranil Sen Gupta

Ph.D., Mathematics, Texas A & M University, Department of Mathematics, North Dakota State University, North Dakota, United States

Dr. Richard B Coffin

Ph.D., in Chemical Oceanography, Department of Physical and Environmental, Texas A&M University United States

Dr. A. Heidari

Ph.D., D.Sc, Faculty of Chemistry, California South University (CSU), United States

Dr. Xianghong Qi

University of Tennessee, Oak Ridge National Laboratory, Center for Molecular Biophysics, Oak Ridge National Laboratory, Knoxville, TN 37922, United States

Dr. Vladimir Burtman

Research Scientist, The University of Utah, Geophysics Frederick Albert Sutton Building 115 S 1460 E Room 383, Salt Lake City, UT 84112, United States

Dr. Shyny Koshy

Ph.D. in Cell and Molecular Biology, Kent State University, United States

Dr. Gayle Calverley

Ph.D. in Applied Physics, University of Loughborough, United Kingdom

Dr. Bingyun Li

Ph.D. Fellow, IAES, Guest Researcher, NIOSH, CDC, Morgantown, WV Institute of Nano and Biotechnologies West Virginia University, United States

Dr. Baziotis Ioannis

Ph.D. in Petrology-Geochemistry-Mineralogy Lipson, Athens, Greece

Dr. Matheos Santamouris

Prof. Department of Physics, Ph.D., on Energy Physics, Physics Department, University of Patras, Greece

Dr. Vyacheslav Abramov

Ph.D in Mathematics, BA, M.Sc, Monash University, Australia

Dr. Fedor F. Mende

Ph.D. in Applied Physics, B. Verkin Institute for Low Temperature Physics and Engineering of the National Academy of Sciences of Ukraine

Dr. Moustafa Mohamed Saleh Abbassy

Ph.D., B.Sc, M.Sc in Pesticides Chemistry, Department of Environmental Studies, Institute of Graduate Studies & Research (IGSR), Alexandria University, Egypt

Dr. Yaping Ren

School of Statistics and Mathematics, Yunnan University of Finance and Economics, Kunming 650221, China

Dr. Yilun Shang

Ph.d in Applied Mathematics, Shanghai Jiao Tong University, China

Dr. T. David A. Forbes

Associate Professor and Range Nutritionist Ph.D. Edinburgh University - Animal Nutrition, M.S. Aberdeen University - Animal Nutrition B.A. University of Dublin-Zoology

Dr. Bing-Fang Hwang

Department of Occupational, Safety and Health, College of Public Health, China Medical University, Taiwan Ph.D., in Environmental and Occupational Epidemiology, Department of Epidemiology, Johns Hopkins University, USA Taiwan

Dr. Moaed Almeselmani

Ph.D in Plant Physiology, Molecular Biology, Biotechnology and Biochemistry, M. Sc. in Plant Physiology, Damascus University, Syria

Dr. Giuseppe A Provenzano

Irrigation and Water Management, Soil Science, Water Science Hydraulic Engineering , Dept. of Agricultural and Forest Sciences Universita di Palermo, Italy

Dr. Eman M. Gouda

Biochemistry Department, Faculty of Veterinary Medicine, Cairo University, Giza, Egypt

Dr. Claudio Cuevas

Department of Mathematics, Universidade Federal de Pernambuco, Recife PE, Brazil

Dr. Arshak Poghossian

Ph.D. Solid-State Physics, Leningrad Electrotechnical Institute, Russia Institute of Nano and Biotechnologies Aachen University of Applied Sciences, Germany

Dr. Qiang Wu

Ph.D. University of Technology, Sydney, Department of Mathematics, Physics and Electrical Engineering, Northumbria University

Dr. Lev V. Eppelbaum

Ph.D. Institute of Geophysics, Georgian Academy of Sciences, Tbilisi Assistant Professor Dept Geophys & Planetary Science, Tel Aviv University Israel

Prof. Jordi Sort

ICREA Researcher Professor, Faculty, School or Institute of Sciences, Ph.D., in Materials Science Autonomous, University of Barcelona Spain

Dr. Eugene A. Permyakov

Institute for Biological Instrumentation Russian Academy of Sciences, Director Pushchino State Institute of Natural Science, Department of Biomedical Engineering, Ph.D., in Biophysics Moscow Institute of Physics and Technology, Russia

Prof. Dr. Zhang Lifei

Dean, School of Earth and Space Sciences, Ph.D., Peking University, Beijing, China

Dr. Hai-Linh Tran

Ph.D. in Biological Engineering, Department of Biological Engineering, College of Engineering, Inha University, Incheon, Korea

Dr. Yap Yee Jiun

B.Sc.(Manchester), Ph.D.(Brunel), M.Inst.P.(UK) Institute of Mathematical Sciences, University of Malaya, Kuala Lumpur, Malaysia

Dr. Shengbing Deng

Departamento de Ingeniera Matemtica, Universidad de Chile. Facultad de Ciencias Fsicas y Matemticas. Blanco Encalada 2120, Piso 4., Chile

Dr. Linda Gao

Ph.D. in Analytical Chemistry, Texas Tech University, Lubbock, Associate Professor of Chemistry, University of Mary Hardin-Baylor, United States

Angelo Basile

Professor, Institute of Membrane Technology (ITM) Italian National Research Council (CNR) Italy

Dr. Bingsuo Zou

Ph.D. in Photochemistry and Photophysics of Condensed Matter, Department of Chemistry, Jilin University, Director of Micro- and Nano- technology Center, China

Dr. Bondage Devanand Dhondiram

Ph.D. No. 8, Alley 2, Lane 9, Hongdao station, Xizhi district, New Taipei city 221, Taiwan (ROC)

Dr. Latifa Oubedda

National School of Applied Sciences, University Ibn Zohr, Agadir, Morocco, Lotissement Elkhier N66, Bettana Sal Marocco

Dr. Lucian Baia

Ph.D. Julius-Maximilians, Associate professor, Department of Condensed Matter Physics and Advanced Technologies, Department of Condensed Matter Physics and Advanced Technologies, University Wrzburg, Germany

Dr. Maria Gullo

Ph.D., Food Science and Technology Department of Agricultural and Food Sciences, University of Modena and Reggio Emilia, Italy

Dr. Fabiana Barbi

B.Sc., M.Sc., Ph.D., Environment, and Society, State University of Campinas, Brazil Center for Environmental Studies and Research, State University of Campinas, Brazil

Dr. Yiping Li

Ph.D. in Molecular Genetics, Shanghai Institute of Biochemistry, The Academy of Sciences of China Senior Vice Director, UAB Center for Metabolic Bone Disease

Nora Fung-yee TAM

DPhil University of York, UK, Department of Biology and Chemistry, MPhil (Chinese University of Hong Kong)

Dr. Sarad Kumar Mishra

Ph.D in Biotechnology, M.Sc in Biotechnology, B.Sc in Botany, Zoology and Chemistry, Gorakhpur University, India

Dr. Ferit Gurbuz

Ph.D., M.SC, B.S. in Mathematics, Faculty of Education, Department of Mathematics Education, Hakkari 30000, Turkey

Prof. Ulrich A. Glasmacher

Institute of Earth Sciences, Director of the Steinbeis Transfer Center, TERRA-Explore, University Heidelberg, Germany

Prof. Philippe Dubois

Ph.D. in Sciences, Scientific director of NCC-L, Luxembourg, Full professor, University of Mons UMONS Belgium

Dr. Rafael Gutirrez Aguilar

Ph.D., M.Sc., B.Sc., Psychology (Physiological), National Autonomous, University of Mexico

Ashish Kumar Singh

Applied Science, Bharati Vidyapeeth's College of Engineering, New Delhi, India

Dr. Maria Kuman

Ph.D, Holistic Research Institute, Department of Physics and Space, United States

Contents of the Issue

i. Copyright Notice
ii. Editorial Board Members
iii. Chief Author and Dean
iv. Contents of the Issue

1. Active Control of Stick-Slip Torsional Vibrations of Drill-Strings using Non-Switching Sliding Mode Controller. *1-20*
2. Explanation of Many Natural Phenomena by One Cause. *21-44*
3. Elivination of the Contradiction between Thermodynamics and Evolution. *45-56*
4. Emerging Trends in Transmission Electron Microscopy for Medical Applications. *57-59*
5. Gauge-Theoretic Study of Kundt Tube Experiment and Spontaneous Symmetry Transitions. *61-86*

v. Fellows
vi. Auxiliary Memberships
vii. Preferred Author Guidelines
viii. Index

Global Journal of Science Frontier Research: a Physics and Space Science
Volume 22 Issue 6 Version 1.0 Year 2022
Type: Double Blind Peer Reviewed International Research Journal
Publisher: Global Journals
Online ISSN: 2249-4626 & Print ISSN: 0975-5896

Active Control of Stick-Slip Torsional Vibrations of Drill-Strings using Non-Switching Sliding Mode Controller

By A. Baz

University of Maryland

Abstract- Torsional vibrations of drill-strings are actively controlled using a non-switching sliding mode strategy. The controller is intended also to reject the effect of the interaction between the drill-bit and rock formation which induces non-linear stick-slip friction torque while tracking a desirable constant angular velocity of the drill-string. In order to demonstrate the merits of the proposed control algorithm, it is integrated with a simple two degrees-of-freedom model of the drill-string which is considered as a benchmark model for studying stick-slip induced torsional vibrations. Details of the development of the individual components making up the entire control action of the sliding mode controller (*SMC*) are presented. These components aim at rejecting the effect of the external disturbance of the stick-slip disturbance and tracking a reference angular velocity of the drill-string. Such development of the control action components is established using Lyapunov stability criterion. Numerical examples are presented to demonstrate the effectiveness of the *SMC* controller as influenced by the weight-on-bit (*WOB*), the drill-string rotational speed, and the main parameters of the controller. The stick-slip sensitivity (SSS) maps are developed to illustrate the performance characteristics of the active system for different operating conditions and important design parameters of the *SMC*. The presented active control approach is envisioned to present an invaluable and practical means for effectively mitigating the undesirable effects of stick-slip frictional disturbances on drill-stings.

Keywords: *drill-string torsional vibrations, simple 2 DOF model, active control of torsional vibrations, stick-slip friction, continuous sliding mode controller.*

GJSFR-A Classification: *DDC Code: 620.2 LCC Code: TA355*



Strictly as per the compliance and regulations of:

© 2022. A. Baz. This research/review article is distributed under the terms of the Attribution-NonCommercial-NoDerivatives 4.0 International (CC BY-NC-ND 4.0). You must give appropriate credit to authors and reference this article if parts of the article are reproduced in any manner. Applicable licensing terms are at https://creativecommons.org/licenses/by-nc-nd/4.0/.

Active Control of Stick-Slip Torsional Vibrations of Drill-Strings using Non-Switching Sliding Mode Controller

A. Baz

Abstract- Torsional vibrations of drill-strings are actively controlled using a non-switching sliding mode strategy. The controller is intended also to reject the effect of the interaction between the drill-bit and rock formation which induces non-linear stick-slip friction torque while tracking a desirable constant angular velocity of the drill-string. In order to demonstrate the merits of the proposed control algorithm, it is integrated with a simple two degrees-of-freedom model of the drill-string which is considered as a benchmark model for studying stick-slip induced torsional vibrations. Details of the development of the individual components making up the entire control action of the sliding mode controller (*SMC*) are presented. These components aim at rejecting the effect of the external disturbance of the stick-slip disturbance and tracking a reference angular velocity of the drill-string. Such development of the control action components is established using Lyapunov stability criterion. Numerical examples are presented to demonstrate the effectiveness of the *SMC* controller as influenced by the weight-on-bit (*WOB*), the drill-string rotational speed, and the main parameters of the controller. The stick-slip sensitivity (SSS) maps are developed to illustrate the performance characteristics of the active system for different operating conditions and important design parameters of the *SMC*. The presented active control approach is envisioned to present an invaluable and practical means for effectively mitigating the undesirable effects of stick-slip frictional disturbances on drill-stings.

Keywords: drill-string torsional vibrations, simple 2 DOF model, active control of torsional vibrations, stick-slip friction, continuous sliding mode controller.

I. Introduction

Several passive vibration mitigation approaches have been considered to attenuate the vibration of drill-strings. Distinct among these passive approaches is periodic designs of the drill-string [1-2].

Also, among the adopted advanced active control approaches is the sliding mode control approach (*SMC*) because it is a robust control method that can accommodate the effects of uncertainty of the drill-string parameters and reject the adverse effects of external disturbances. The *SMC* controller has been reported by Navarro-Lopez and Cortes [3], Vaziri *et al*. [4], and Sadeghimehr *et al.* [5]. It has been demonstrated that the method has effectively eliminated the stick-slip vibrations both theoretically and experimentally. The method has also been shown by Navarro-López and Liceaga-Castro [6], to track a desired reference angular velocity in the presence of dry friction due to bit–rock interaction. Also, the authors demonstrated the robustness of the *SMC* algorithm in accommodating uncertainties of the drill-string parameters. Furthermore, Sadeghihr *et al*. [7] have reported the effective use of the *SMC* in controlling the vibration of drill-strings in the presence of input time delays.

It is important to note that in all the above-mentioned studies on the sliding mode control, the adopted method relies in its operation on a switching approach which suffers from the classical problem of "chattering" more and above the associated computational complexities. Several schemes have been proposed to alleviate this problem but these approaches significantly contribute to the complexity of the development and implementation of the controller.

Author: University of Maryland, Department of Mechanical Engineering, University of Maryland, College Park, USA.
e-mail: baz@umd.edu

© 2022 Global Journals

It is therefore, the main objective of this study to eliminate the problems associated with the use of the original sliding mode method (*SMC*) control method by adopting a continuous sliding mode (*CSM*) control algorithm [8]. This algorithm completely eliminates the chattering problem while maintaining the stable and attractive attributes of the sliding mode controller. In the development of the *CSM* controller, no knowledge of the excitation characteristics is needed except for a rough estimate of the maximum value of the excitation force.

The original *CSM* method is modified here in order to provide it with tracking capabilities of reference input commands. With these capabilities, the method becomes suitable to control the speed of drill-stings while rejecting the non-linear effects generated by the stick-slip disturbances acting at the drill bit end.

This paper is organized in six sections. In section 1, a brief introduction is presented about current state-of-the-art of active control of drill-strings. The configuration and the dynamic equations of the benchmark model of the drill-string considered in this paper are described in Section 2 and its mathematical model is described in Section 3. The development of the non-switching sliding mode controller (*CSM*) is outlined in Section 4. The performance characteristics of the actively controlled drill-string are presented in Section 5. Finally, Section 6 summarizes the conclusions and possible recommendations for future studies.

II. The Drill String System

The benchmark 2*DOF* drill-string torsional system sketched in Fig. 1 is considered. The degrees of freedom are θ_{top} and θ_{bit}, which are the rotations of the top-drive and of the bottom-hole-assembly (*BHA*)/bit. A control law is applied at the top-drive to reject the and a nonlinear bit–rock inter-action torque occurs at the bottom of the column. It is assumed that the *BHA* is a rigid body, and that the drill-pipe is flexible. The inertia and the natural frequency of the system are obtained calibrating the model with the field data found in Ritto *et al.* [9].

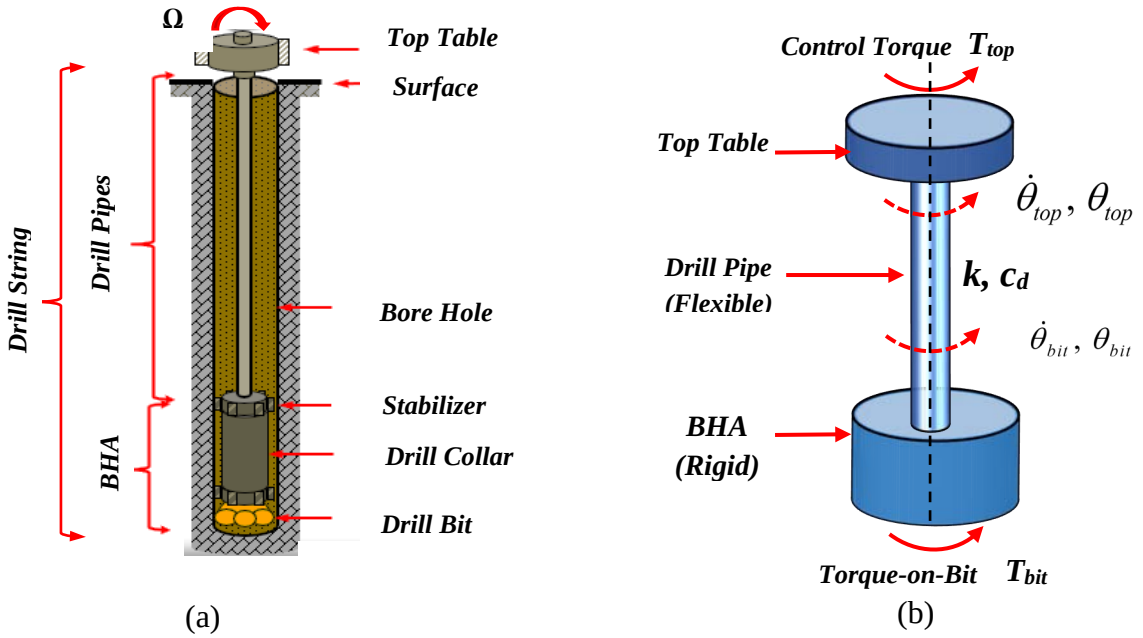

Fig. 1: Drill string under torsional vibrations

© 2022 Global Journals

III. Mathematical Model of the Active Drill-String

a) Full-Order Model

The full-order benchmark linear model of the drill-string, shown in Fig. 1, with linear viscous damping is considered. The drill-string model is subjected to a nonlinear torque T_{bit} resulting from the drill bit–rock interaction and the control torque T_{top}. Hence, the equations of motion of the system are given by:

$$I_{top}\ddot{\theta}_{top} + k\left(\theta_{top} - \theta_{bit}\right) + c_d\left(\dot{\theta}_{top} - \dot{\theta}_{bit}\right) = T_{top}$$

and

$$I_{bit}\ddot{\theta}_{bit} + k\left(\theta_{bit} - \theta_{top}\right) + c_d\left(\dot{\theta}_{bit} - \dot{\theta}_{top}\right) = T_{bit} \tag{1}$$

where I_{top} and I_{bit} are the top-drive and drill-string mass moments of inertia, k is the drill-pipe stiffness, and c_d is the damping parameter.

The torques at the top T_{top} and at the bit T_{bit} are given by [9]:

$$T_{top} = T_{control}, \quad \text{and} \quad T_{bit} = -b_0\left(\tanh(b_1\dot{\theta}_{bit}) + \frac{b_2\dot{\theta}_{bit}}{1 + b_3\dot{\theta}_{bit}^2}\right) \tag{2}$$

in which the torque is given in *N.m* and $\dot{\theta}_{bit}$ in *rad/s*. Also, the parameters of the nonlinear bit–rock interaction model are positive constants b_0 (*N.m*), b_1 (*s*), b_2 (*s*), and b_3 (s^2) which depend on the weight-on-bit, rock properties and cutting characteristics.

Eqs. (1) through (2) are combined to yield the following state-space model of the entire system as follows:

$$\dot{\mathbf{X}} = \mathbf{A}\mathbf{X} + \mathbf{B}u + \mathbf{B_d}d \tag{3}$$

and

$$\mathbf{y} = \mathbf{C}\,\mathbf{X} \tag{4}$$

where $\bar{\mathbf{X}} = \{\theta_{top} \;\; \theta_{bit} \;\; \dot{\theta}_{top} \;\; \dot{\theta}_{bit}\}^T$ is the state vector. Also, $\mathbf{A} = \begin{bmatrix} \mathbf{0}_{2\times2} & \mathbf{I}_{2\times2} \\ -\mathbf{M}^{-1}\mathbf{K}_{2\times2} & -\mathbf{M}^{-1}\mathbf{C_d} \end{bmatrix}$, $\mathbf{B} = \begin{bmatrix} \mathbf{0}_{2\times2} \\ \mathbf{M}^{-1}\mathbf{B}_{top} \end{bmatrix}$, and $\mathbf{B_d} = \begin{bmatrix} \mathbf{0}_{2\times2} \\ \mathbf{M}^{-1}\mathbf{B}_{bit} \end{bmatrix}$ with $\mathbf{B}_{top} = \begin{bmatrix} 1 \\ 0 \end{bmatrix}$ and $\mathbf{B}_{bit} = \begin{bmatrix} 0 & 1 \end{bmatrix}^T$. Also, $u = T_{top}$ denotes the control torque and $d = T_{bit}$ defines the disturbance torque generated by the bit. Furthermore, in state-space equation (3), the mass, damping and stiffness matrices **M, C**$_\mathbf{d}$, and **K** are given by:

$$\mathbf{M} = \begin{bmatrix} I_{top} & 0 \\ 0 & I_{bit} \end{bmatrix}, \; \mathbf{C}_d = \begin{bmatrix} c_d & -c_d \\ -c_d & c_d \end{bmatrix}, \text{ and } \; \mathbf{K} = \begin{bmatrix} k & -k \\ -k & k \end{bmatrix} \tag{5}$$

© 2022 Global Journals

In this paper, the physical parameters of the benchmark drill-string model are listed in Table 1 which are exactly the same parameters used by Ritto *et al.*, [9].

Table 1: The physical parameters of the drill string and bit disturbance [9]

Parameter	k ***(Nm/rad)***	c_d ***(Nms/rad)***	L ***(m)***	I_{top} ***(kgm^2)***	I_{bit} ***(kgm^2)***	b_0 ***(Nm/kN)***	b_1 ***(s)***	b_2 ***(s)***	b_3 ***(s^2)***
Value	276	162	5200	9.58	383	23.14	0.4775	8.7854	4.5595

Based on these parameters, the state-space system matrix A, given by Equation (3), has the following eigenvalues: $[0, \quad 0, \ -1.9093, -15.5068]$ as outlined in Appendix A.

Hence, the system has two rigid body modes which are manifested by the zero eigenvalues. These modes result from the free rotation of the drill-string which result from the singular nature of the stiffness matrix **K**.

Furthermore, checking the controllability and observability matrices of the system as quantified by computing the ranks of these matrices indicates that the system is controllable with its controllability matrix has a full rank (*i.e.,* 4) while the observability matrix of the system has only a rank of 3 (*i.e.*, short rank). These ranks indicate that the system is controllable but not observable. This implies also that the state-space representation of the system is not a minimum realization. The details of these parameters are presented in Appendix A.

Therefore, the state-space representation of the system as given by Eqs. (3) and (4) is reduced first in order to render the reduced-order system to be both controllable and observable. The simultaneous controllability and observability conditions are ensured by reducing the system order by using the minimum realization techniques [10].

b) Reduced-Order Model

The reduced order model is developed using *MATLAB* '***minreal***" command to yield the following system:

$$\dot{\bar{\mathbf{X}}} = \bar{\mathbf{A}}\bar{\mathbf{X}} + \bar{\mathbf{B}}u + \bar{\mathbf{B}}_{\mathbf{d}}d \tag{6}$$

and

$$y = \bar{\mathbf{C}}\bar{\mathbf{X}} \tag{7}$$

where $\bar{\mathbf{X}} = \mathbf{U}^{\mathbf{T}}\mathbf{X}$, $\bar{\mathbf{A}} = \mathbf{U}\mathbf{A}\mathbf{U}^{\mathbf{T}}$, $\bar{\mathbf{B}} = \mathbf{U}\mathbf{B}$, and $\bar{\mathbf{B}}_{\mathbf{d}} = \mathbf{U}\mathbf{B}_{\mathbf{d}}$ with **U** is a transformation matrix obtained by the *MATLAB* "***mineral***" routine.

The reduced order model is rendered to be both controllable and observable. But, it still has one rigid body mode instead of two rigid body modes as the full-order system. It is used later on to effectively design and implement the continuous sliding mode (*CSM*) controller. All the parameters and main features of the reduced order model are presented in Appendix A. These parameters can then be used to reconstruct the entire state variable of the full-order system.

© 2022 Global Journals

The drill-string system is then integrated with the controller as shown in the block diagram of Fig. 2. In this integrated assembly, the controller aims at generating a control action u in order to reject the external disturbance d ($=T_{bit}$) produced by the drill bit and to track a desirable angular velocity $\boldsymbol{\Omega}$ at the top drive end.

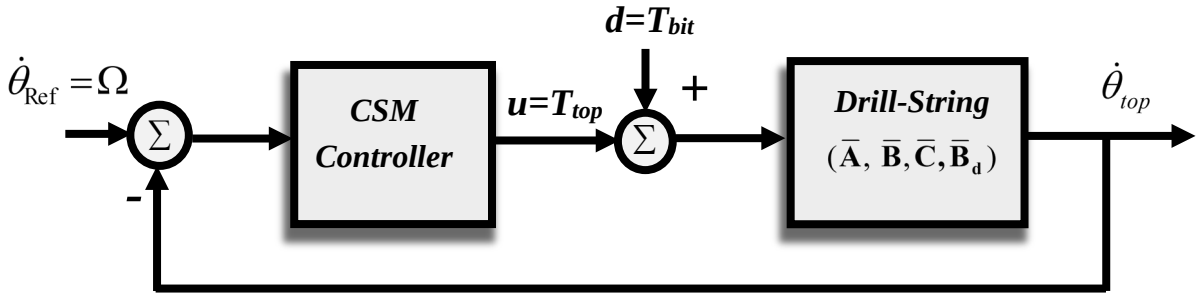

Fig. 2: Block diagram of the control system

IV. The Continuous Sliding Mode Controller with Output Feedback

In this section, the continuous sliding mode (*CSM*) controller is described and its stability is investigated first in order to establish the control structure when the drill-string operates without the influence of the external disturbance generated by the drill bit/rock interaction. Then, the control structure is modified and augmented in order to reject the effect of this disturbance.

a) Without External Disturbance

The dynamic equations of the vibrating drill-string, Eq. (3), is considered first without the effect of the external disturbance (*i.e., d*=0), such that:

$$\dot{\bar{\mathbf{X}}} = \bar{\mathbf{A}}\bar{\mathbf{X}} + \bar{\mathbf{B}}u \text{ , and } y = \bar{\mathbf{C}}\bar{\mathbf{X}} \tag{8}$$

where $(\bar{\mathbf{A}}, \bar{\mathbf{B}}, \bar{\mathbf{C}})$ are the reduced system, control input, and measurement matrices, respectively. Also, $\bar{\mathbf{X}}$ is the reduced state variable vector of the system, $\mathbf{y}$ is the vector of measurements and u is the control force.

The control effort is generated to track a desirable angular velocity $\boldsymbol{\Omega}$ of the upper platform such that the tracking error e is given by:

$$e = \bar{\mathbf{C}}\,\bar{\mathbf{X}} - \Omega \tag{9}$$

Hence, the output feedback control action u is given by:

$$u = u_y + u_e = -\mathbf{K}_{\mathbf{y}}\bar{\mathbf{C}}\,\bar{\mathbf{X}} - \mathbf{K}_{\mathbf{e}}e \tag{10}$$

with $\mathbf{K_y}$ and $\mathbf{K_e}$ are the output and tracking error feedback gains.

© 2022 Global Journals

The structure of the control gains $\mathbf{K_y}$ and $\mathbf{K_e}$ is determined by assuming that the system is to follow the sliding plane:

$$\sigma = \mathbf{p}\,(\bar{\mathbf{C}}\,\bar{\mathbf{X}} - \Omega) = \mathbf{p}\,e \tag{11}$$

where $\mathbf{p}$ is a parameter of the sliding plane σ with e denoting the tracking error.

In order to select the control gains $\mathbf{K_e}$ and $\mathbf{K_y}$ that ensures stability, consider the following Lyapunov function $V = \frac{1}{2}\sigma^2$, then its time derivative $\dot{V}$ is given by:

$$\dot{V} = \sigma\,\dot{\sigma} = \sigma\;\mathbf{p}\,\bar{\mathbf{C}}\,\dot{\bar{\mathbf{X}}} \tag{12}$$

Substituting Eqs. (8) through (10) into Eq. (11) gives:

$$\begin{aligned}\dot{\sigma} &= \mathbf{p}\,\bar{\mathbf{C}}\dot{\bar{\mathbf{X}}} = \sigma\,\mathbf{p}\,\bar{\mathbf{C}}\left[(\bar{\mathbf{A}} - \bar{\mathbf{B}}\,\mathbf{K}_{\mathbf{y}}\,\bar{\mathbf{C}})\bar{\mathbf{X}} - \bar{\mathbf{B}}\mathbf{K}_{\mathbf{e}}e\right] \\ &= \left(\mathbf{p}\,\bar{\mathbf{C}}\bar{\mathbf{B}}\right)\left\{\left[\left(\mathbf{p}\,\bar{\mathbf{C}}\bar{\mathbf{B}}\right)^{-1}\mathbf{p}\,\bar{\mathbf{C}}\bar{\mathbf{A}} - \mathbf{K}_{\mathbf{y}}\,\bar{\mathbf{C}}\right]\bar{\mathbf{X}} - \mathbf{K}_{\mathbf{e}}e\right\}\end{aligned} \tag{13}$$

To ensure system stability, let $\mathbf{K_y}$ be selected such that:

$$\mathbf{K}_y\bar{\mathbf{C}} = \left(\mathbf{p}\,\bar{\mathbf{C}}\bar{\mathbf{B}}\right)^{-1}\mathbf{p}\,\bar{\mathbf{C}}\bar{\mathbf{A}}, \quad \text{Or} \quad \mathbf{K}_y = \left(\mathbf{p}\,\bar{\mathbf{C}}\,\bar{\mathbf{B}}\right)^{-1}\mathbf{p}\,\bar{\mathbf{C}}\bar{\mathbf{A}}\bar{\mathbf{C}}^{\dagger}. \tag{14}$$

where $\bar{\mathbf{C}}^{\dagger}$ is the pseudo-inverse of the output matrix $\bar{\mathbf{C}}$.

Also, let $\mathbf{K_e}$ be selected such that: $\mathbf{K}_e = \left(\mathbf{p}\,\bar{\mathbf{C}}\,\bar{\mathbf{B}}\right)^{-1}\mathbf{p}$. (15)

Then, combining Eqs. (13), (14) and (15) gives: $\dot{\sigma} = -\mathbf{p}e$ (16)

Hence, combining Eqs. (11), (12) and (16) yields:

$$\dot{V} = \sigma\dot{\sigma} = -\mathbf{p}^2\,e^2 < 0. \tag{17}$$

Eq. (17) indicates that the rate of decay of V is strictly negative and stability is guaranteed.

b) With External Disturbance

The equation of the system becomes:

$$\dot{\bar{\mathbf{X}}} = \bar{\mathbf{A}}\bar{\mathbf{X}} + \bar{\mathbf{B}}u + \bar{\mathbf{B}}_{\mathbf{d}}d \quad \text{and} \quad y = \bar{\mathbf{C}}\bar{\mathbf{X}} \tag{18}$$

© 2022 Global Journals

where $\bar{\mathbf{B}}_{\mathbf{d}}$ is the disturbance input matrix and *d* is the external disturbance.

In this case, the control effort *u,* given by Equation (10), is augmented with a disturbance rejection controller u_d such that:

$$u = -\mathbf{K}_{\mathbf{y}}\bar{\mathbf{C}}\bar{\mathbf{X}} + \mathbf{K}_{\mathbf{e}}\, e - u_d \tag{19}$$

where u_d is taken as: $$u_d = \left\{\left[\left(\bar{\beta} + \delta_d\right)/\lambda\right]\left(\mathbf{p}\bar{\mathbf{C}}\bar{\mathbf{B}}\right)\mathbf{p}\right\}\left(\bar{\mathbf{C}}\bar{\mathbf{X}} - \Omega\right), \tag{20}$$

with λ and δ_d are positive numbers. Also, $\bar{\beta}$ is assumed to be given by:

$$\bar{\beta} = \sup[\beta] = \sup\left[\left(\mathbf{p}\bar{\mathbf{C}}\bar{\mathbf{B}}\right)^{-1}\left(\mathbf{p}\bar{\mathbf{C}}\bar{\mathbf{B}}_{\mathbf{d}}\right)d\right]. \tag{21}$$

where *sup*[.] denotes the maximum upper bound of [.].

Eq. (19) indicates that the disturbance rejection control action is put in an output feedback form and Eq. (21) defines the maximum limit of the expected stick and slip torque disturbance.

Stability of the system, subjected to the disturbance *d*, can be checked by considering the Lyapunov function $V = \frac{1}{2}\sigma^2$. It can be easily shown that $\dot{V}$ is given by:

$$\dot{V} = \sigma\dot{\sigma} = -\sigma^2 - \sigma\left(\mathbf{p}^{\mathbf{T}}\bar{\mathbf{C}}\bar{\mathbf{B}}\right)\left\{\left[\left(\bar{\beta} + \delta_d\right)/\lambda\right]\left(\mathbf{p}^{\mathbf{T}}\bar{\mathbf{C}}\bar{\mathbf{B}}\right)\sigma - \beta\right\} \tag{22}$$

The first term on the *RHS* of Eq. (22) corresponds to the undisturbed system and it is negative definite. The second term arises from the effect of the external disturbance *d* and the corresponding disturbance rejection controller u_d.

The second term of Eq. (22) can be made negative definite by selecting λ small enough such that $\left|\left(\mathbf{p}\bar{\mathbf{C}}\bar{\mathbf{B}}\right)\sigma\right|/\lambda >> 1$ then:

a. If $\left(\mathbf{p}^{\mathbf{T}}\bar{\mathbf{C}}\bar{\mathbf{B}}\right)\sigma > 0$ then:

$$-\sigma\left(\mathbf{p}\bar{\mathbf{C}}\bar{\mathbf{B}}\right)\left\{\left[\left(\bar{\beta} + \delta_d\right)\right]\left(\mathbf{p}\bar{\mathbf{C}}\bar{\mathbf{B}}\right)\sigma/\lambda - \beta\right\} < 0 \tag{23}$$

and **b.** If $\left(\mathbf{p}\bar{\mathbf{C}}\bar{\mathbf{B}}\right)\sigma < 0$ then:

$$-\sigma\left(\mathbf{p}\bar{\mathbf{C}}\bar{\mathbf{B}}\right)\left\{\left[\left(\bar{\beta} + \delta_d\right)\right]\left(\mathbf{p}\ \bar{\mathbf{C}}\bar{\mathbf{B}}\right)\sigma/\lambda - \beta\right\} < 0 \tag{24}$$

Under these conditions $\dot{V}$ becomes negative definite and controller will be able to stabilize the system and reject the external disturbance *d*.

© 2022 Global Journals

V. Performance of the Controlled Drill-String

This section summarizes the performance characteristics of the actively controlled drill-string as influenced by the weight-on-bit (*WOB*), the drill-string rotational speed, and the main parameters of the controller. Also, this section includes the extraction of the stick-slip sensitivity (*SSS*) maps which act as metric for evaluating the performance characteristics of the active system for different operating conditions and important design parameters of the *SMC*.

Fig. 3 displays the time response characteristics of reduced order model of the drill string system when it is subjected to initial velocities $\dot{\theta}_0 = -15\,rad/s$ and $\dot{\theta}_b = -15\,rad/s$ with a desired reference angular velocity $\Omega = 50\,rad/s$ when the *WOB* = 200*KN*. The *CSM* parameters are set such that δ_d=2, λ=0.005, and p=10. Fig. 3a shows the disturbance torque T_{bit} generated by the interaction between the bit and the rocks during the angular velocity control of the drill-string. The nonlinear nature of the disturbance torque T_{bit} as a function of the drill bit angular velocity $\dot{\theta}_b$ is evident.

The effectiveness of the *CSM* controller in controlling the drill-string speed and tracking the desired reference command of $\Omega = 50\,rad/s$ is displayed in Fig. 3b. With the set parameters, the controller moves the top end from $\dot{\theta}_0 = -15\,rad/s$ to the desired reference command $\Omega = 50\,rad/s$ in less than 8 *ms* as shown in Fig. 3b. The controller is also able to bring the bit end to track the desired reference velocity as the system matrices *A* and *B* form a controllable pair with controllability matrix that is full rank. However, the settling time is longer than that of the top end as shown in Fig. 3c. The attained settling time is about 14 *s*.

Fig. 3d displays the time history of the bit torque T_{bit} in relation to the required control torque T_{top} (*i.e.*, $T_{control}$). When the two torques match each other, the entire drill-string attains its steady-state mode of operation.

Fig. 4 displays the time response characteristics of drill string system when it is subjected to the same initial and reference angular velocities as that of Fig. 3, but with sliding parameter **p**=4. Under these conditions, the settling time of the top end is much longer reaching 100 *ms* as shown in Fig. 4a.

Fig. 5, shows a different visual comparison between the characteristics of the controller when the sliding parameter **p** is changed from 10 to 4. In the Fig., the phase plane portrait is shown relating the angular velocity at the bit $\dot{\theta}_{bit}$ end to the twist angle $\theta_0 - \theta_{bit}$ experienced by the drill-string. In this approach, the relative twist angle $\theta_0 - \theta_{bit}$ is considered instead of treating the absolute values of θ_0 and θ_{bit} separately. In this manner, it is possible to eliminate the rigid body motions associated with each of these two degrees of freedom. Furthermore, the considered visualization approach displays the trajectory followed by the controller to drive the string from its initial position ($\theta_0 = 0^o, \theta_b = 0^o, \dot{\theta}_b = -15\,rad/s$) to achieve steady-state conditions when the angular velocities of both ends assume the desired reference command $\Omega = 50\,rad/s$.

© 2022 Global Journals

The figure shows also that using a *SMC* with sliding parameters p=10 and λ=0.005, the drill string attains the desired reference angular velocity with almost zero steady-state error. At this final angular velocity, the drill-string is twisted such that the steady-state twist angle between the two ends is $\theta_0 - \theta_{bit}$ =18°. Such a twist angle is accompanied with an elastic twist torque that counter balances the difference between the disturbance and control torques as displayed in Fig. 3d.

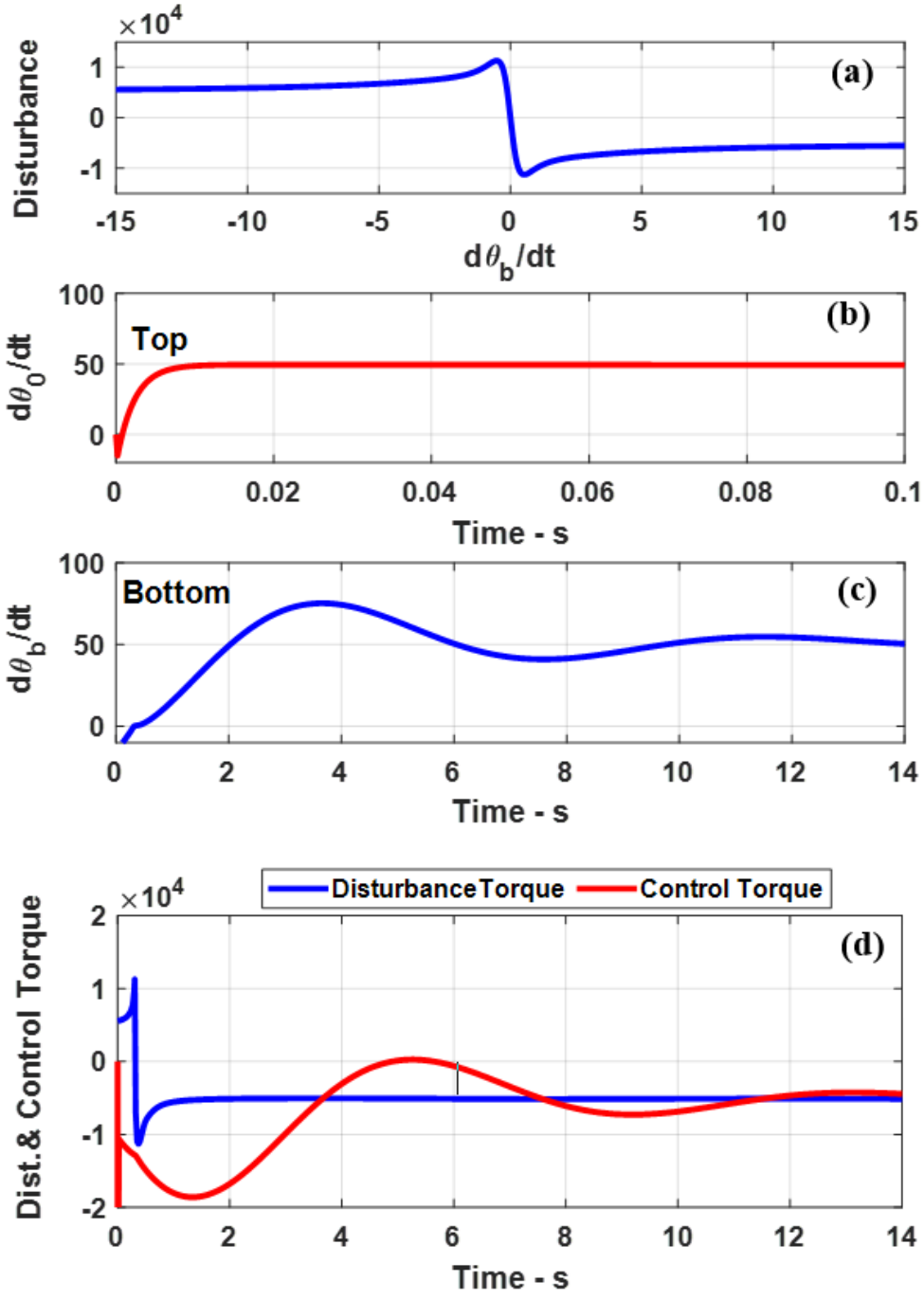

Fig. 3: Performance of the drill string with the *CSM* controller for δ_d=2, λ=0.005, p=10, W=200KN, and Ω=50rad/s

© 2022 Global Journals

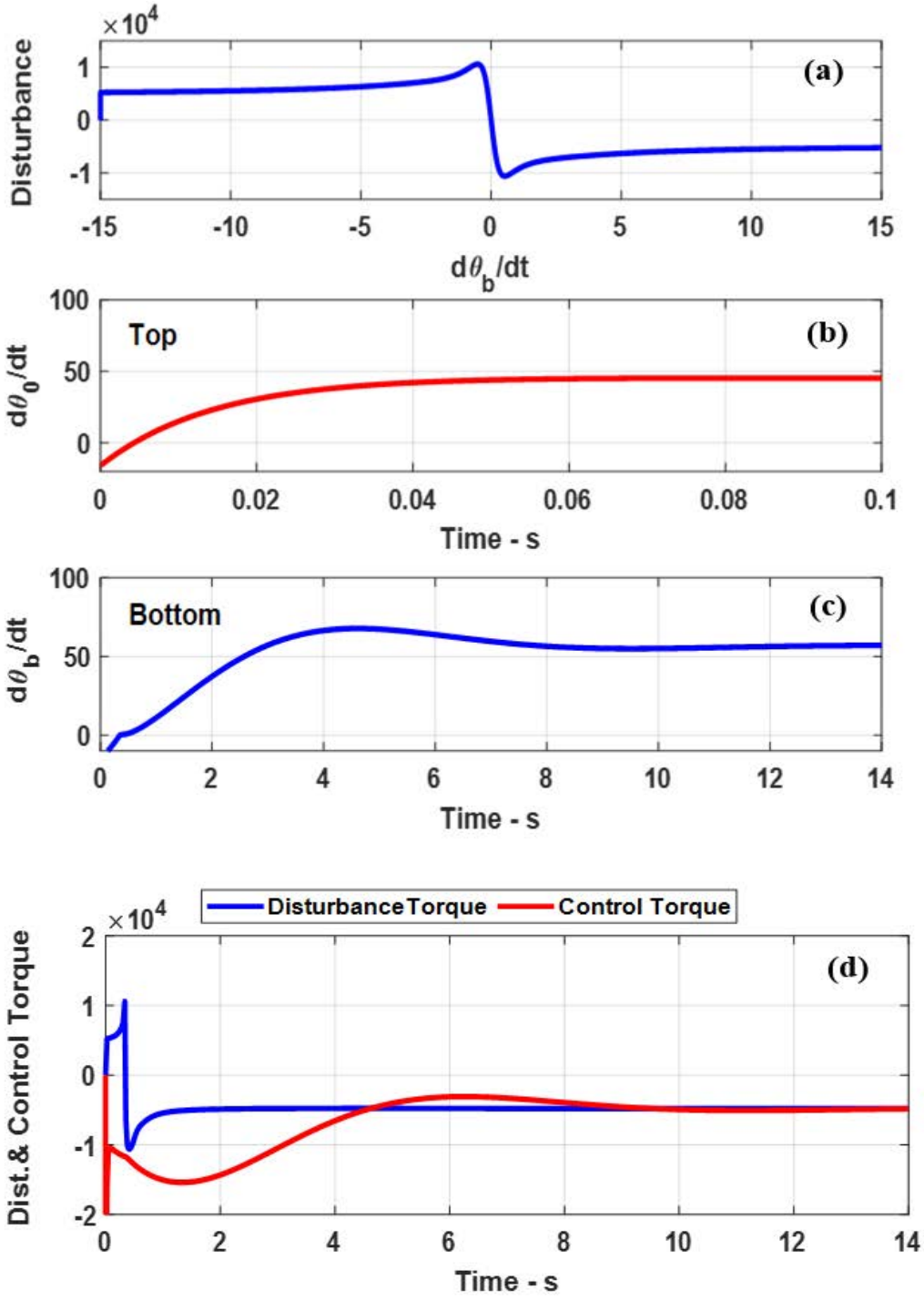

Fig. 4: Performance of the drill string with the *CSM* controller for $\delta_d=2$, $\lambda=0.005$, p=4, $W=200KN$, and $\Omega=50rad/s$

© 2022 Global Journals

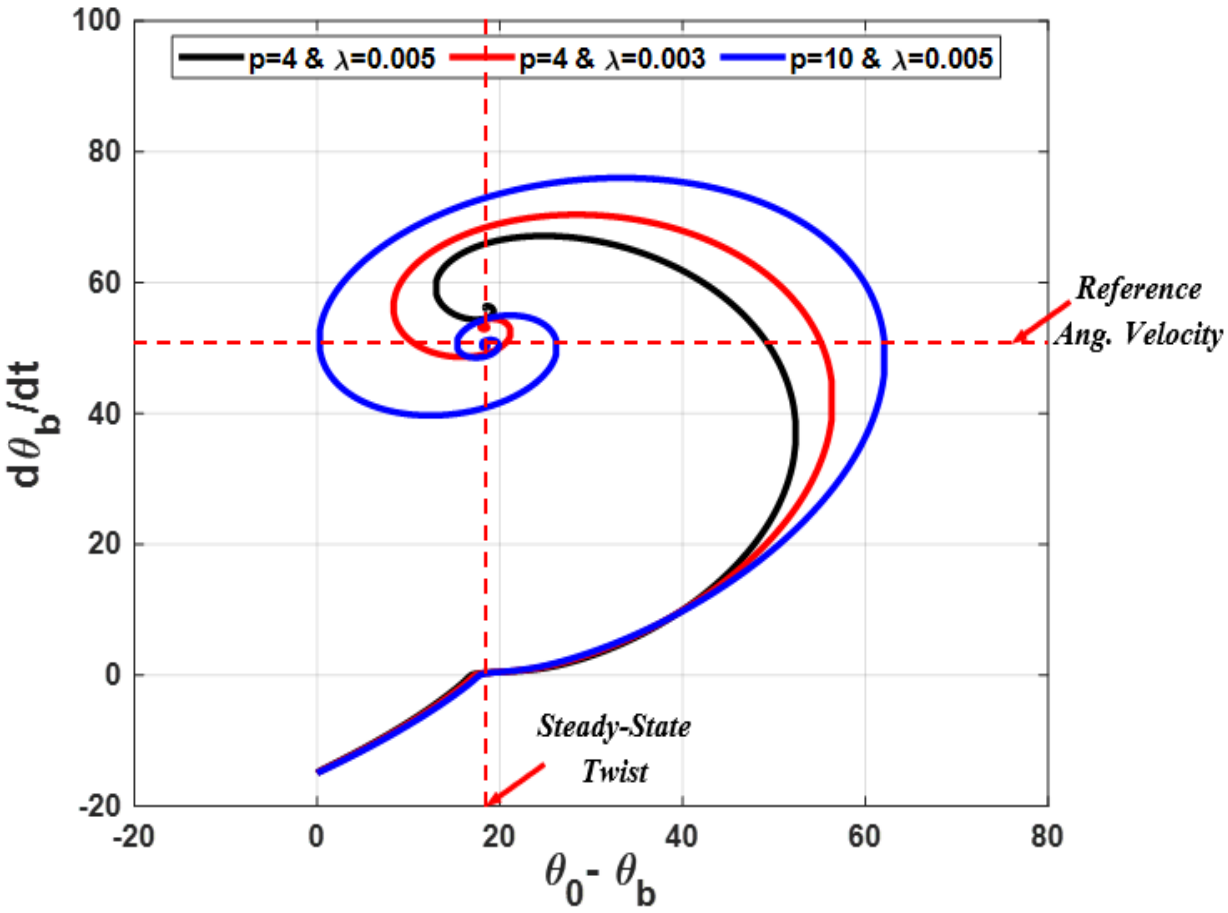

Fig. 5: Phase plane plots of the *CSM* controller for different values of the sliding parameter p with δ_d=2, *W*=200KN, and Ω=50*rad/s*

Note that when the sliding parameters are adjusted such that p=4 and λ=0.005, the drill string did not attain the desired reference angular velocity and a steady-state error of about 5 degrees is observed as shown in Fig. 5. Such steady-state error can be reduced to 2 degrees by reducing the parameter λ from 0.005 to 0.003 as is evident in Fig. 5. Hence, adjustment of the sliding parameters plays an important role in enhancing the performance characteristics of the *SMC* controller.

Fig. 6 displays the corresponding time response of the drill string system when the desired reference angular velocity is changed to $\Omega = 20\,rad/s$ when the $WOB = 200KN$. The *CSM* parameters are set such that $\delta_d = 2$, λ = 0.005, and **p** =10.

© 2022 Global Journals

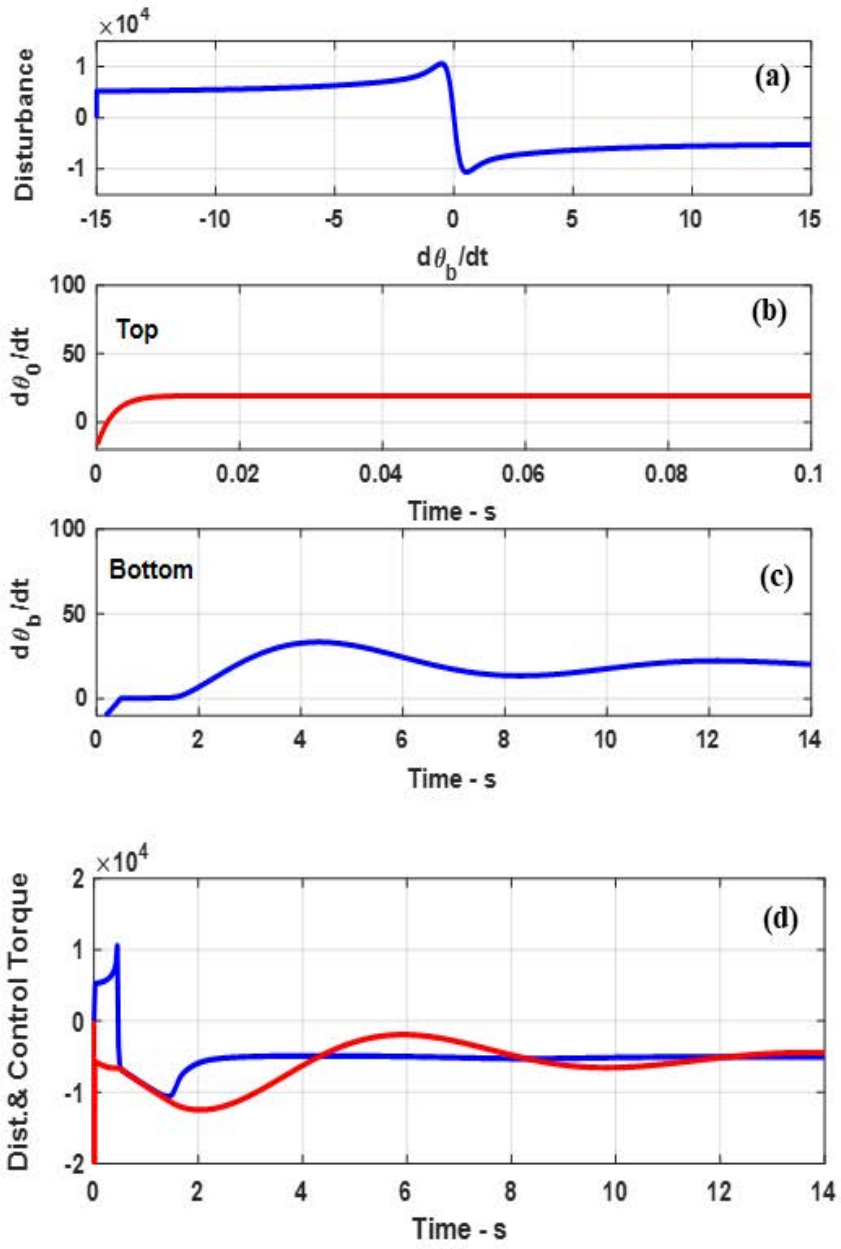

Fig. 6: Performance of the drill string with the *CSM* controller for δ_d=2, λ=0.005, p=10, *W*=200KN, and Ω=20*rad/s*

The displayed results in Fig. 6 indicate that the controller is equally effective in tracking a reference command angular velocity of $\Omega = 20\,rad/s$. The controller behavior is very similar to its performance while tracking a reference command of $\Omega = 50\,rad/s$. The only difference appears in the first 2 seconds which are primarily dominated by the disturbance torque and the attempt of the controller to overcome this torque. However, the control effort in this case is still much lower than that required for the case of $\Omega = 50\,rad/s$.

© 2022 Global Journals

A quantitative way for investigating the effect of the different operating conditions and important design parameters of the *SMC* on the performance characteristics of the actively controlled system is generated by considering the stick-slip sensitivity (*SSS*) maps [Ritto *et al*., [9]. In these maps, the stick-slip sensitivity (*SSS*) metric is defined as:

$$SSS_i = \frac{\dot{\theta}_{i,\max} - \dot{\theta}_{i,\min}}{\Omega} \quad \text{where } i = top \text{ and } bit \tag{25}$$

Equation (25) indicates that the *SSS* metric quantifies the effectiveness of the controller in minimizing the extent of angular velocity variation relative to the desired reference angular velocity. In effect, this metric quantifies the harshness of the stick-slip phenomenon on the effective tracking of a desirable angular velocity.

Fig. 7 displays the combined effect of the sliding parameter **p** and the *WOB* on the *SSS* metric at the top and bit ends when the reference command is $\Omega = 50\,rad/s$. It is evident that reducing the *SSS* metric requires that the *WOB* be low while it is almost independent of the sliding parameter **p**. However, simultaneous increase of the weight-on-bit *WOB* and the sliding parameter **p** increases considerably the *SSS* metric. Note that for the considered ranges of the *WOB* and **p**, the associated *SSS* is observed to be bounded between 1.2 and 2.

The limits bounding the *SSS* metric increase considerably as the desired reference angular velocity **Ω** decreases as shown in Fig. 8. The figure displays the *SSS* map as influenced by the combined effect of the *WOB* and the desired operating angular velocity **Ω**. In this Fig., it can be seen that the bounds limiting the *SSS* are observed to be between 1 and 6 with the high bounds are encountered as **Ω** drops close to 10. This considerable increase is expected as the stick-slip effects become more significant. This effect becomes more significant at the bit end more than at the top end as evident from Fig. 8b.

© 2022 Global Journals

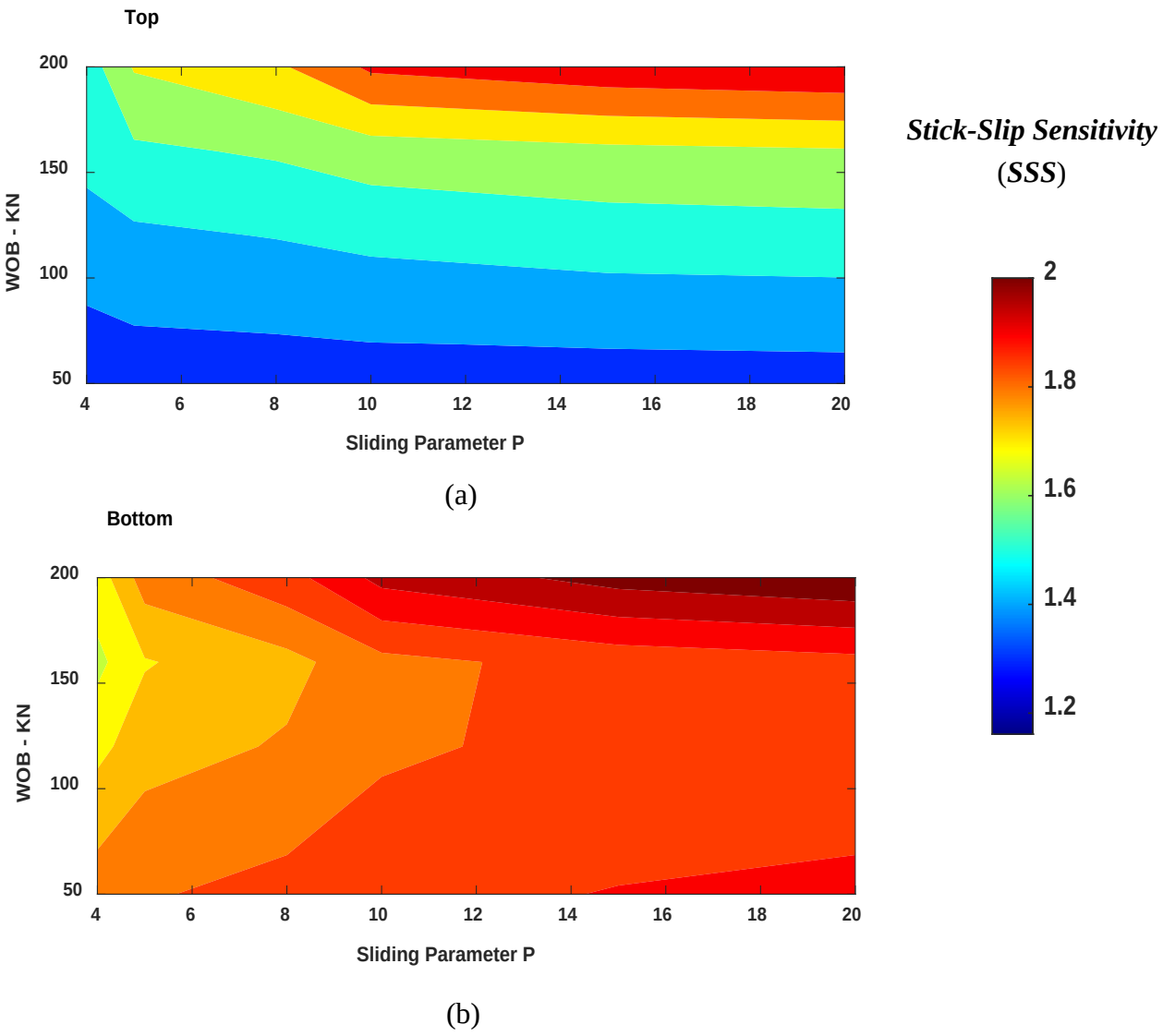

Fig. 7: The Stick-Slip Sensitivities (*SSS*) as function of the WOB and the sliding parameter p for Reference Angular Velocity of $\Omega = 50\ rad/s$

© 2022 Global Journals

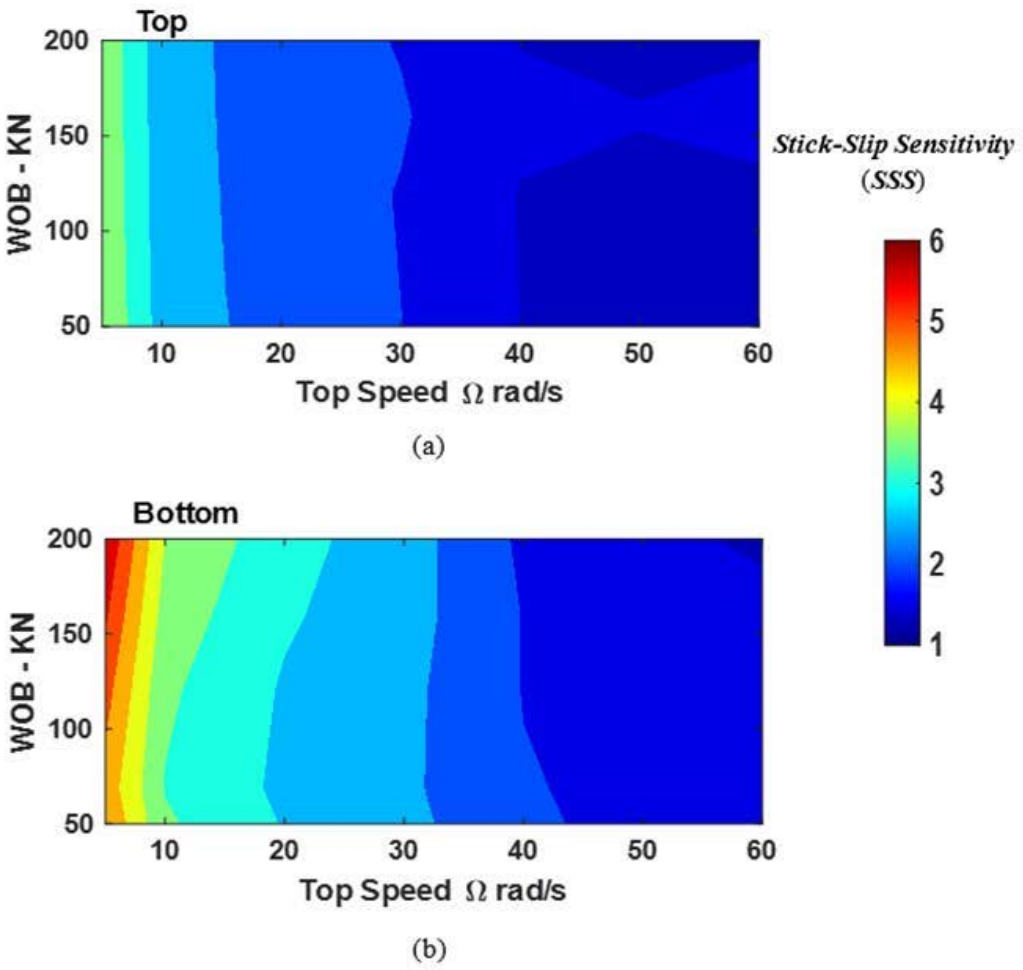

Fig. 8: The Stick-Slip Sensitivities (*SSS*) for Sliding Parameter p=10

VI. Conclusions

This paper has presented a practical, simple, and yet rigorous approach to control the torsional vibrations and angular velocities of drill-strings. The drill-string model considered in here is a two degrees-of-freedom model which is considered as a benchmark model, by many investigators, for studying stick-slip induced torsional vibrations. Such a model is found to be controllable but unobservable. Unlike other investigators who considered this model, the model in its original form is modified here to eliminate its shortcoming by reducing its order in order to render it in a minimum realization form. In that form, the reduced-order model is both controllable and observable while requiring only one pair of collocated actuator and velocity sensor located at the top end. Furthermore, the relationship between the full-order and reduced-order models is established, in the Appendix *A*, in order to extract the entire state-variable of the full-order model from only the measurements of the reduced-order model.

© 2022 Global Journals

The resulting model is integrated, in this study, with a continuous and non-switching robust sliding mode controller (*CSM*). This controller distinguishes our work from all the previous studies that combined the full-order unobservable model of the drill-string with switching sliding mode controllers. The *CSM* controller is developed to simultaneously reject the effect of the interaction between the drill-bit and rock formation which induces non-linear stick-slip friction torque while tracking a desirable constant angular velocity of the drill-string. The controller development included the rigorous establishment of the expressions of the individual components making up the entire control action of the sliding mode controller (*CSM*). These components aim at rejecting the effect of the external disturbance of the stick-slip disturbance and tracking a reference angular velocity of the drill-string. Such development of the control action components is established using Lyapunov stability criterion.

Numerical examples are presented to demonstrate the effectiveness of the *SMC* controller as influenced by the weight-on-bit (*WOB*), the drill-string rotational speed, and the main parameters of the controller. The stick-slip sensitivity (*SSS*) maps are developed to illustrate the performance characteristics of the active system for different operating conditions and important design parameters of the *SMC*. It is established that the harshness of the *SSS* metric occurs when high values of the *WOB* are combined with low operating angular velocities Ω.

The presented active control approach is envisioned to present an invaluable and practical means for effectively mitigating the undesirable effects of stick-slip frictional disturbances on drill-stings.

Appendix A

Parameters of the Full and Reduced-Order Models

A.1. Full- Order Model

a. The triplet (A, B, C) of the full-order system are as follows:

$$\mathbf{A}=\begin{bmatrix} 0 & 0 & 1 & 0 \\ 0 & 0 & 0 & 1 \\ -28.88 & -28.88 & -16.99 & 16.99 \\ 0.772 & -0.722 & 0.425 & -0.425 \end{bmatrix},\ \mathbf{B}=\begin{bmatrix} 0 \\ 0 \\ 0.1044 \\ 0 \end{bmatrix},\ \mathbf{B_d}=\begin{bmatrix} 0 \\ 0 \\ 0 \\ 0.0026 \end{bmatrix},$$

and **C**=[0 0 1 0].

a. Eigenvalues of the open-loop system

These parameters are computed using the *MATLAB* command **eig**(**A**) yielding:

[0 0 -1.9093 -15.5068]

© 2022 Global Journals

b. Controllability Matrix

It is given by: $\mathcal{C} = \begin{bmatrix} \mathbf{B} & \mathbf{AB} & \mathbf{A^2B} & \mathbf{A^3B} \end{bmatrix}$. It has a full rank of 4.

c. Observability Matrix

It is given by: $\mathcal{O} = \begin{bmatrix} \mathbf{C} & \mathbf{CA} & \mathbf{CA^2} & \mathbf{CA^3} \end{bmatrix}^T$. It has a full rank of 3.

d. Markov Parameter

It is given by **CAB** and it is equal to -1.7736.

A.2. Reduced- Order Model

This model is extracted from the full-order model using the *MATLAB* "***mineral***" commands as follows:

$$\begin{bmatrix} \bar{\mathbf{A}}, \bar{\mathbf{B}}, \bar{\mathbf{C}}, \bar{\mathbf{D}} \end{bmatrix} = \mathbf{minreal}(\mathbf{A}, \mathbf{B}, \mathbf{C}, \mathbf{0}) \text{ and}$$

a. The triplet ($\bar{\mathbf{A}}, \bar{\mathbf{B}}, \bar{\mathbf{C}}$) of the reduced-order system are as follows:

$$\bar{\mathbf{A}} = \begin{bmatrix} -17.416 & -40.862 & 16.566 \\ 0.725 & 0.000 & -0.689 \\ 3.72E\text{-}15 & 0.000 & -4.29E\text{-}15 \end{bmatrix}, \bar{\mathbf{B}} = \begin{bmatrix} 0.1044 \\ -0.0000 \\ 0.0026 \end{bmatrix}, \bar{\mathbf{B}}_{\mathbf{d}} = \begin{bmatrix} -0.0001 \\ -0.0000 \\ 0.0026 \end{bmatrix},$$

$$\bar{\mathbf{C}} = [0.999 \;\; 0.000 \;\; 0.025], \text{ and } \bar{\mathbf{D}} = 0$$

e. Eigenvalues of the open-loop system

These parameters are computed using the *MATLAB* command **eig**($\bar{\mathbf{A}}$) yielding:

[0 -1.9093 -15.5068]

f. Controllability Matrix

It is given by: $\bar{\mathcal{C}} = \begin{bmatrix} \bar{\mathbf{B}} & \bar{\mathbf{A}}\bar{\mathbf{B}} & \bar{\mathbf{A}}^2\bar{\mathbf{B}} \end{bmatrix}$. It has a full rank of 3.

g. Observability Matrix

It is given by: $\bar{\mathcal{O}} = \begin{bmatrix} \bar{\mathbf{C}} & \bar{\mathbf{C}}\bar{\mathbf{A}} & \bar{\mathbf{C}}\bar{\mathbf{A}}^2 \end{bmatrix}^T$. It has a full rank of 3.

© 2022 Global Journals

h. Markov Parameter

It is given by $\bar{\mathbf{C}}\bar{\mathbf{A}}\bar{\mathbf{B}}$ and it is also equal to -1.7736.

This indicates that the Markov parameters are maintained unchanged following the model order reduction process.

A.3. Relationship between the Full and Reduced- Order Models

This relationship is established using the transformation matrix T extracted by *MATLAB* "*mineral*" command as follows:

$$T = \begin{bmatrix} -0.0000 & -0.0000 & 0.9997 & -0.0250 \\ 0.7071 & -0.7071 & -0.0000 & -0.0000 \\ 0.0000 & -0.0000 & 0.0250 & 0.9997 \end{bmatrix}$$

This matrix relates the state variables ($\mathbf{X}$, $\bar{\mathbf{X}}$) of the full and reduced-order systems, respectively as follow:

$$\bar{\mathbf{X}} = \mathbf{T}^{\mathbf{T}}\mathbf{X} \qquad \text{(A.1)}$$

Hence, the above equation enables the computation of the reduced-order state variable from the full-order state variable. Conversely, the extraction of the full-order state variable from the reduced order state variable can be carried out using the following expression:

$$\mathbf{X} = \left[\mathbf{T}^{\mathbf{T}}\right]^{\dagger} \bar{\mathbf{X}} \qquad \text{(A.2)}$$

Where $\left[\mathbf{T}^{\mathbf{T}}\right]^{\dagger}$ is the pseudo inverse of the transformation matrix $\mathbf{T}^{\mathbf{T}}$.

Nomenclature

$\mathbf{A}$, $\bar{\mathbf{A}}$	System matrix of the full and reduced order models, respectively.
$b_{0.1,2,3}$	parameters of the drill bit torque model
$\mathbf{B}$, $\bar{\mathbf{B}}$	Input matrix of the control action of the full and reduced order models, respectively
$\mathbf{B_{bit}}$	Input matrix of rock-bit torque
$\mathbf{B_d}$, $\bar{\mathbf{B}}_{\mathbf{d}}$	Input matrix of the external disturbance of the full and reduced order models, respectively
$\mathbf{B_{top}}$	Input matrix of control torque
c_d	the damping parameter

© 2022 Global Journals

$\mathbf{C}$, $\bar{\mathbf{C}}$	Output matrix of the full and reduced order models, respectively
$\mathbf{C_d}$	Damping matrix
$\bar{\mathcal{C}}$	Controllability matrix
d	disturbance
e	tracking error
I_{bit}	the drill-string mass moment of inertia
I_{top}	the top-drive mass moment of inertia,
k	the drill-pipe stiffness
$\mathbf{K}$	Stiffness matrix
$\mathbf{K_{e,y}}$	tracking and output control gain components
$\mathbf{K_G}$	Control gain
$\mathbf{M}$	Mass matrix
$\bar{\mathcal{O}}$	Observability matrix
$\mathbf{p}$	slope of sliding line
T_{bit}	torque at the drill bit end
T_{top}	torque at the top end
u	Control action
$u_{d,\,r}$	Control component to reject the disturbance and track the reference, respectively
V	Lyapunov function
W	Weight on Bit (*WOB*)
$\mathbf{X}$, $\bar{\mathbf{X}}$	state variable of the full and reduced order models, respectively.
y	output

Greek Symbols

β	bound on the external disturbance
$\bar{\beta}$	upper bound of the external disturbance
δ_d	parameter of the sliding controller
λ	parameter of the sliding controller
θ_{bit}	angular displacement at the drill bit end
θ_{top}	angular displacement at the top end
σ	Equation of sliding line
$\mathbf{\Omega}$	desirable reference angular velocity

© 2022 Global Journals

Data Availability

The data that support the findings of this study are available from the corresponding author upon reasonable request.

Funding

The authors received no financial support for the research, authorship, and/or publication of this article.

Declaration of No Conflicts of Interests

The author(s) declare no potential conflicts of interest with respect to the research, authorship, and/or publication of this article.

ORCID

Amr M. Baz @ http://orcid.org/0000-0003-0903-4429

References Références Referencias

1. Y. Alsaffar, S. Sassi, and A. Baz, Band gap characteristics of non-rotating passive periodic drill string. *ASME Journal of Vibration and Acoustics*; 140 (2) (2017): 021004.
2. Y. Alsaffar, S. Sassi, and A. Baz, Band gap characteristics of periodic gyroscopic systems *Journal of Sound and Vibration*. 435 (2018): 301-322.
3. E. M. Navarro-Lopez, and D. Cortes b, Sliding-mode control of a multi-DOF oilwell drill string with stick-slip oscillations, ThC 10.6, August 2007 *Proceedings of the American Control Conference*, New York City, USA, July 11-13, 2007 (2007):3837-3842. DOI: 10.1109/ACC.2007.4282198.
4. V. Vaziri, I. O. Oladunjoye, M. Kapitaniak, S. S. Aphale, and M. Wiercigroch, Parametric analysis of a sliding-mode controller to suppress drill-string stick-slip vibration, *Meccanica* 55 (2020):2475–2492, doi.org/10.1007/s11012-020-01264-5(0123456789().,-volV)(01234567.
5. R. Sadeghimehr, A. Nikoofard, and A. K. Sedigh, Predictive-based sliding mode control for mitigating torsional vibration of drill string in the presence of input delay and external disturbance", *Journal of Vibration and Control*, (2020), DOI: 10.1177/1077546320960995.
6. E. M. Navarro-López, and E. Liceaga-Castro, Non-desired transitions and sliding-mode control of a multi-DOF mechanical system with stick-slip oscillations. *Chaos, Solitons & Fractals* 41(4) (2009): 2035–2044.
7. R. Sadeghimehr, A. Nikoofard, and A. Sedigh, Smith predictor based sliding mode control for torsional vibration control of drill-string with input delay. In: *Proceedings of The 2019th IEEE International Conference on Control, Instrumentation and Automation* (*ICCIA*), Sanandaj, Iran, 30–31 October 2019 (2019).
8. F. Zhou, and D. G. Fisher, Continuous sliding mode control, *International Journal of Control*, 55:2(1992), 313-327. DOI: 10.1080/00207179208934240.
9. T. G. Ritto, and M. Ghandchi-Tehrani, Active control of stick-slip torsional vibrations in drill-strings, *Journal of Vibration and Control*, 25(1) (2019): 194–202.
10. R. L. Williams II, and D. A. Lawrence*, Linear state-space control systems*, John Wiley & Sons, Inc., Hoboken, New Jersey (2007).

© 2022 Global Journals

Global Journal of Science Frontier Research: a
Physics and Space Science
Volume 22 Issue 6 Version 1.0 Year 2022
Type: Double Blind Peer Reviewed International Research Journal
Publisher: Global Journals
Online ISSN: 2249-4626 & Print ISSN: 0975-5896

Explanation of Many Natural Phenomena by One Cause

By Vladimir Igorevich Danilov

Abstract- This article shows how the external gravity force on the core of the planet leads to the appearance of the magnetic field (MF) of the planet. How this force provides acceptable conditions for the existence of life. Natural phenomena, which can easily be explained using the proposed mechanism of interaction of planets, such as earthquakes, mountain formation, ocean currents, tides, time jumps, changes in the duration of the day, periodic Solar activity are considered.

GJSFR-A Classification: *DDC Code: 785.8 LCC Code: M1003*



Strictly as per the compliance and regulations of:

© 2022. Vladimir Igorevich Danilov. This research/review article is distributed under the terms of the Attribution-NonCommercial-NoDerivatives 4.0 International (CC BY-NC-ND 4.0). You must give appropriate credit to authors and reference this article if parts of the article are reproduced in any manner. Applicable licensing terms are at https://creativecommons.org/licenses/by-nc-nd/4.0/.

Explanation of Many Natural Phenomena by One Cause

Vladimir Igorevich Danilov

Abstract- **This article shows how the external gravity force on the core of the planet leads to the appearance of the magnetic field (MF) of the planet. How this force provides acceptable conditions for the existence of life. Natural phenomena, which can easily be explained using the proposed mechanism of interaction of planets, such as earthquakes, mountain formation, ocean currents, tides, time jumps, changes in the duration of the day, periodic Solar activity are considered.**

The proofs are:

- An explicit connection that can be traced in the dependence of the magnetic fields of the planets, their shapes and magnitudes, on the influence of the Sun and satellites on the body of the planet.
- Metric data of the behavior of the magnetic field, gravity, ocean level, under various conditions, as well as processes observed in nature.

Comparison of the measured data leads to a firm conclusion about the influence of the motion of the planetary core on many processes occurring and recorded on the planetary surface.

The proposed model allows us to look at many processes occurring in nature in a different way, taking into account the additional, huge influence of the factor.

The proposed approach makes it possible to combine many disparate natural phenomena into one whole.

Here is a simple example of another approach

We know that if any vessel fill with substances of different specific weights, their separation will occur. The heaviest ones will precipitate out, the lighter ones will be above and the lightest ones at the top. For example, imagine an aquarium. There are rocks and sand at the bottom, then toys, fish, and a feeder at the top in the water. Our planet is the same aquarium for the Sun. And why should it have the heaviest part in the center? The heavy part should be on the sunny side all the time. After all, if we incline the aquarium, will then the stones and sand slide towards the Earth?

“Physics books are full of complex mathematical formulas.

But the rudiment of every physical theory is thoughts and ideas, not formulas."

A. Einstein

Dedicated to the memory of V.A. Morgunov

Author: Schmidt Institute of Physics of the Earth of the Russian Academy of Sciences Ras. e-mail: danvlad@bk.ru

Preface: Dear reader! I have literally two remarks.

1. This article is not a hypothesis, since everything said is confirmed by measured and observed data. This article is not a theory, as no new concepts, laws, patterns are introduced. This article is a description of natural phenomena based on known and proven laws, but taking into account a factor not previously considered.
2. This article is addressed to specialists of different and rather narrow areas - geophysics, oceanics, physics of the Earth's MF, astronomy, etc. And, as a rule, the answers contain the words: "I am not an expert ..." and further by choice. Dear reader, life teaches us to look at questions through a broader lens. Everything is interconnected in nature. And if you really want to be a specialist in your field, then you just need to know as much as possible about the factors affecting the object you are studying. Interest also makes the difference. If you are interested, then you can do a lot, and if you are not, then even receiving a salary for it will not help. And, of course, it`s important to take some time out of your busy life. Having read the article, you may well consider yourself a specialist in the issues under consideration. So, let's start with the MF of the planets.

I. Introduction

A lot has been said about the role of the Magnetic Field (MF) of the planet in the life of humanity and nature, so we will not run past.

One of the most common hypotheses trying to explain the nature of the formation of the field - the theory of the "dynamo effect", suggests that convective and/ or turbulent movements of the conducting fluid in the body of the planet work towards self-excitation, creation and maintenance of the field in a steady state condition.

But in reality, it is not observed that thermal, electrically charged flows float in the same direction all the time - if it is a convective movement, or turbulence arising from rotation, was so constant to maintain the effect of self-excitation, and even in one direction. The nature of turbulence is not clear at all - over time, in the absence of external forces, the internal substance of the Earth will also rotate uniformly together with the shell due to viscosity effect. It also remains unclear where the potentials in these flows come from, why they are not

© 2022 Global Journals

compensated if the substance is electrically conductive. Why does this hypothesis not work on other planets, where the field is different with the same direction of rotation. It also does not explain the inversion of the field. The author of this theory (Braginsky) himself considered it far not proven.

In some hypotheses, "plumes", "jerks", "superchrons" appear, the mythical concept of "frozen-in field lines" that change their configuration in a fantastic way, which leads to the strengthening of the "magnetic embryo", or the rotation of the, for some reason, iron core leads to the appearance of a magnetic field, and it does not matter that it contradicts to the basic laws of physics.

II. The Nature of a Planet's Magnetic Field

Best of all, the Earth's MF, if magnetic anomalies are not taken into account, is interpreted as a magnetic field created by an electric current in a conductor, laid at the latitude of the equator, and located at some depth. At the same time, the current is directed from East to West.

Nature itself has given us the opportunity to find out the sources of the appearance and maintenance of MF of the planets. It placed them in different orbits, made them rotate in different directions, at different speeds, and added, or not, satellites of different sizes and different directions of movement to them. It remains only to analyze these data and, knowing the characteristics of the MF of the planets and assuming that the physics of MF should be the same for all planets, find the forces that create flows of charged particles (electric current), which, in turn, creates MF.

The option of a permanent magnet located in the body of the planet is not considered for known temperature reasons.

Note: It is to be recalled that an electric current is called the directional movement of charged particles. The movement of positive charges is taken as the direction of the current. The direction of the magnetic field lines created by this current is determined by the right-hand Ampere's rule.

a) *The Causes of the Appearance of an Electric-Type Dipole in the Body of the Planet*

According to modern theories of the structure of the Earth (e.g. Korottsev, 2003,) substances below the inner mantle are in liquid form (metallic phase) - high—temperature plasma - consisting of mobile electrons, positively charged ions and nuclei. Sometimes this state is called liquid metallic hydrogen.

The change in the properties of a substance with temperature and pressure increase is specified in the works of D. A. Kirzhnitsa (1971), here is an excerpt from the article:

"With pressure or temperature increase, the substance acquires an increasingly universal structure, and its characteristics become increasingly smooth functions of the composition of the substance. This explicit tendency is due to the fact that because of an increase in the internal energy of a substance, a certain ordering and "simplification" of its structure becomes possible. With pressure or temperature increase molecules or molecular complexes are destroyed and the substance passes into a purely atomic state. The atomic envelopes are rearranged, acquiring more and more regular level occupation. At the same time, there is a separation of external electrons that determine the chemical individuality of the substance. Finally, if a substance remains in a solid state during compression and heating, then its crystal lattice is also ordered. Going through a series of structural transformations, it becomes more and more chemically pure and eventually acquires a single structure (body-centered cubic *) for all substances ".

Here I would like to note that the modern Earth model, with a solid core inside surrounded by a supernatant liquid, is based on the study of the behavior of acoustic (seismic) waves, their ability to travel differently in solid and liquid medium. With pressure and temperature increase, a high-temperature plasma with a close packing of nuclei will conduct seismic waves as well as a solid (crystalline) substance, which does not contradict the measured data, and the accepted boundary of the solid core is the boundary of transition to the "crystalline" plasma state.

Thus, we have a substance in a state of high-temperature plasma (or close to it) inside the planet, characterized by the presence of mobile electrons, ions and nuclei deprived of their atomic envelopes, possessing ideal electrical conductivity, behaving like a liquid, but with acoustic conductivity like a crystal structure has.

b) *The Causes of the Appearance of an Electric Current in the Body of the Planet*

Let's consider the nature of the excitation using the example of the Earth.

If we imagine the Earth as a ball filled with substances of various densities and specific weight, and the Sun as a source of the gravitational force that affects these substances, then it is obvious that heavier structures will "settle" to the closest envelope of the ball and the distribution of density and mass inside the Earth will be uneven not only by depth, but also in the direction of the Sun.

The nuclei and ions of substances are hundreds of times heavier than electrons, and the plasma, under the influence of external gravity forces, will split in density and they, positively charged, will fall into the "deposition". The separation inside the Earth's body will occur not only by mass, but also by electrical potential.

© 2022 Global Journals

The Earth's core will take the form of a dipole with a significantly displaced center of mass, where "+" and the main mass are closer to the Sun.

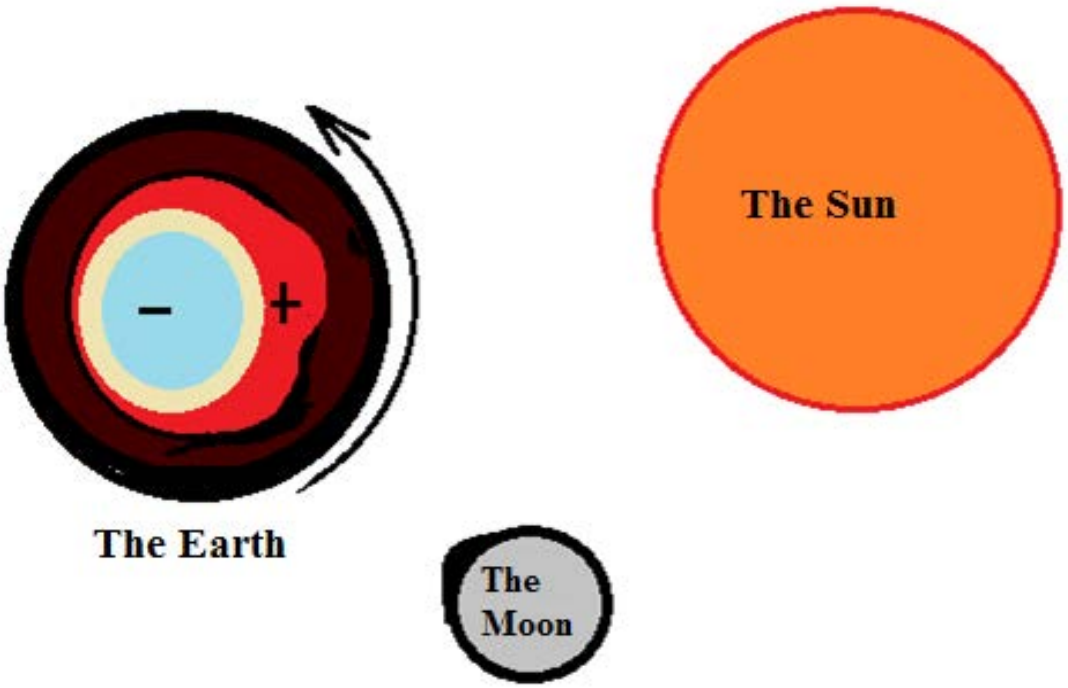

Fig. 1: Distribution of masses and charges under the influence of the Sun and the Moon

The heavy part of the Earth's core follows the Sun when the Earth rotates and thereby creates a directional motion of electrically charged particles and at the same time a circular, cyclic displacement of the center of the Earth mass relative to its envelope. This, of course, does not mean that there is a pure "+" on the one side inside the ball, and "-" on the other, then it would be impossible to have such a magnetic field when rotating dipole due to mutual compensation. The radii of motion are different and, in compliance, the lineal velocities, and, therefore, the potential currents are different too. There is some compensation from the movement of different charges, but "+" prevails.

This moving, polarized nuclei creates an alternating (pulsation) Earth's Magnetic Field.

Generated pulsation (for a point on the surface), with a period of 1 day, the magnetic field is supported by the paramagnetic behavior of the planet body, which smoothes and stabilizes its behavior. In this case, the planet body itself is magnetized.

Thus magnetized, the planetary mass creates the core (main) Earth's Magnetic Field.

It is obvious that the existing MF anomalies were formed at a different direction of movement of charged flows and, perhaps, at different speeds and potentials. The current field is not able to remagnetize them.

The behavior of the Earth's core, apart from the Sun, is also influenced by the Moon.

This mechanism for other planets will naturally be somewhat different due to differences in objects affecting the planet core: somewhere it may be the Sun, somewhere satellites, as well as the properties of the planet itself, but the physics of the phenomenon is the same.

One of the confirmations of this can be daily and annual variations in the direction of the magnetic field density, i.e. the dependence of the field on the position of the Earth relative to other objects of influence, which make adjustments to the separation by mass, charge and trajectory of the core. (There should not be such an influence in the case of the currently accepted hypothesis of a self-excited dynamo effect.)

It is often necessary to answer such a statement - "Coulomb forces are much greater than gravity forces, and they will not allow the latter to separate the element."

Here some confusion arises:

1. In the considered high-temperature plasma, mobile electrons *are already separated* from nuclei and ions due to temperature conditions and pressure.
2. The consideration involves not the gravity forces of two particles, but the huge gravity from the Sun acting on particles of different masses.

© 2022 Global Journals

3. Coulomb forces of gravity assume interaction between differently charged particles, but not between volumes of differently charged particles, where they participate only in the boundary layer. The further away from the contact boundary, the repulsive forces of equally charged particles become more important.

A real-life example is thunderclouds, which have different potentials, and this is proved by lightning, but they do not seek to unite.

There was also such an argument in the discussions - satellites relative to their planets seem to be constantly falling, but they miss. And therefore all parts of the satellite have the same acceleration and cannot separate. If this is an artificial satellite flying in an orbit of about 500 km and it misses a sphere with a diameter of 12,000 km — how can you imagine it? If this is the Earth relative to the Sun and it is in free fall in its field, then where does the tidal gravity come from? And the fact that it presents and is taken from the Sun is a fact, observed and measured. And what is more - neither the satellite, nor the Earth, nor the Moon have increased their speed during their movement, but falling implies constant acceleration.

Sometimes critics claim that there are no such conditions inside the planet to create a "high-temperature plasma". But basically, there is no need to have them for ideal plasma; it is enough to have conditions for the separation of some electrons and the formation of positive ions. It doesn't affect anything.

For example, the cathode temperature in an electric vacuum tube is only about 2000 degrees. And this is enough for the electron emission.

Additionally, for those who like to adjust everything to the formulas, it is necessary to repeat that the main MF is obtained as a manifestation of the magnetization of the Earth's body from the variable and thus it is not possible to find out what value the variable has. Only the main can be measured on the planet surface and it consists of effective, fixed, variable values that have ever been there. The variable field appears only as fluctuations of the main one.

MF has a very complex shape and attempts to fit it to any formula are a waste of time and absolute disregard for the reasons for the appearance of the field.

III. Seasonal Variations of the Trajectory of the Core

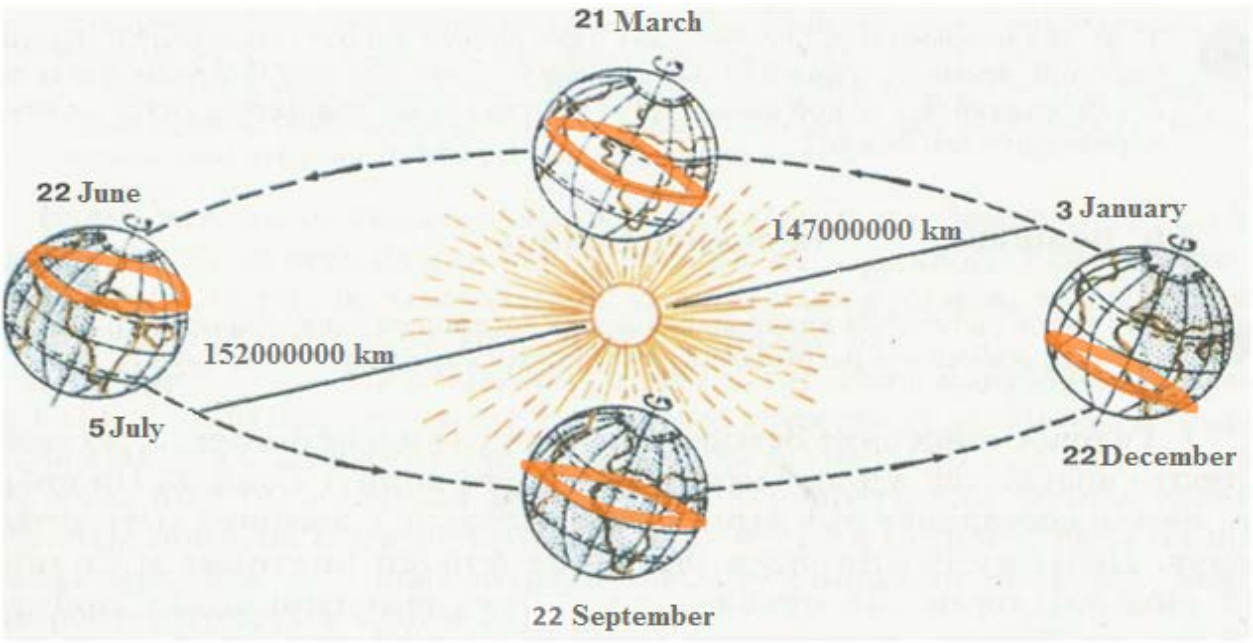

In fact, the heavy part of the core moves from East to West and spirals North-South and back, when the position of the planet relative to the Sun changes (the time of year changes).

Fig. 2: Seasonal shifts of the trajectory of the core

Consider the measurement results confirming this.

1. Very interesting measured data were given by the staff of the "Institute of Monitoring of Climatic and Ecological Systems SB RAS" in the work (Yu.P. Malyshkov, 2009).

Based on long-term studies of the natural pulse electromagnetic fields of the Earth (NPEMFE) in the seismically active areas of the Baikal region, they came to the conclusion about the movement of the planet's core and related natural phenomena - seismic activity,

© 2022 Global Journals

effects on the human body, etc. These are truly remarkable works that continue, already at a more technological level, A. Chizhevsky`s research.

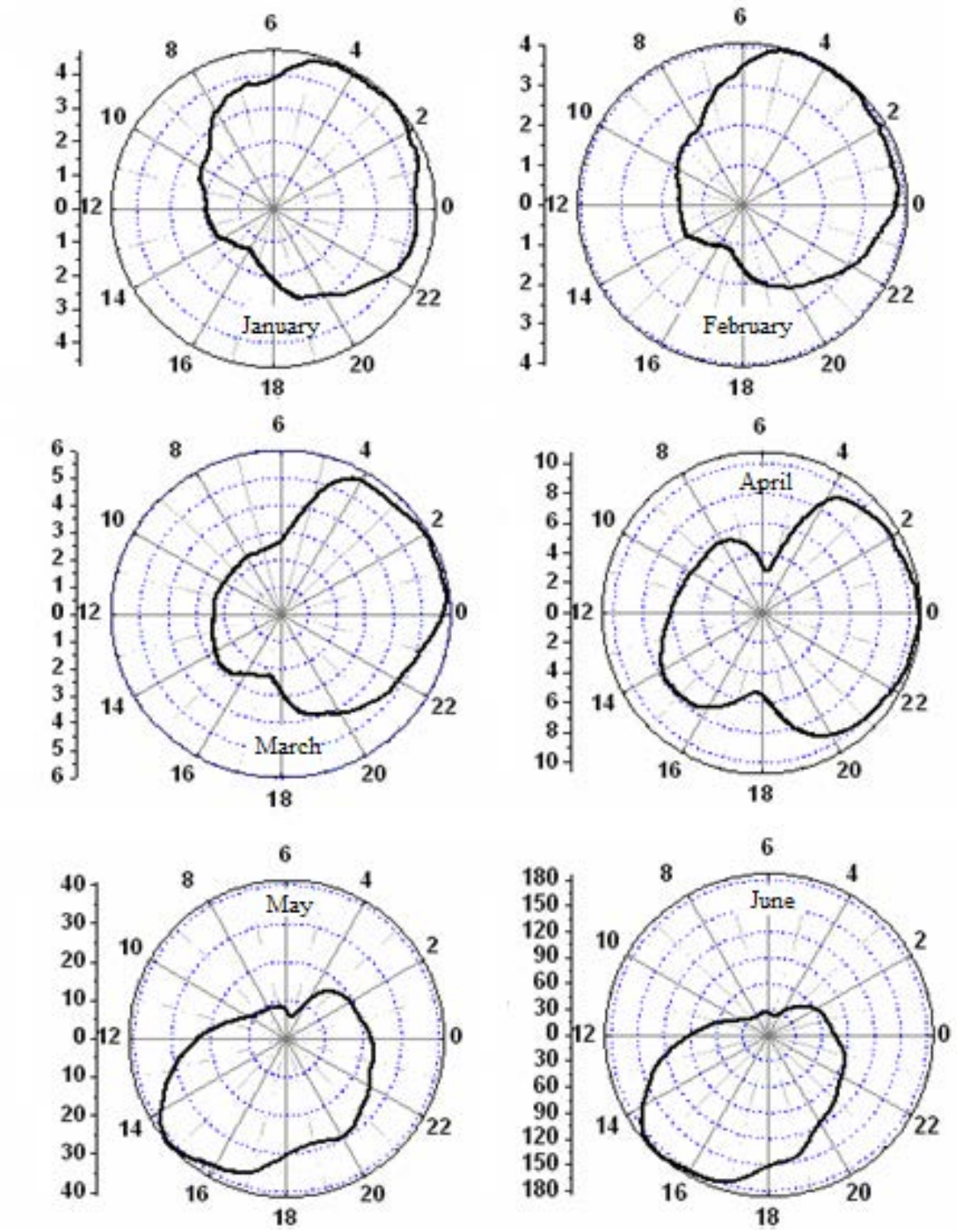

The patterns of the intensity of changes in the NPEMFE at various points in time exactly repeat the movement of the heavy part of the dipole.

© 2022 Global Journals

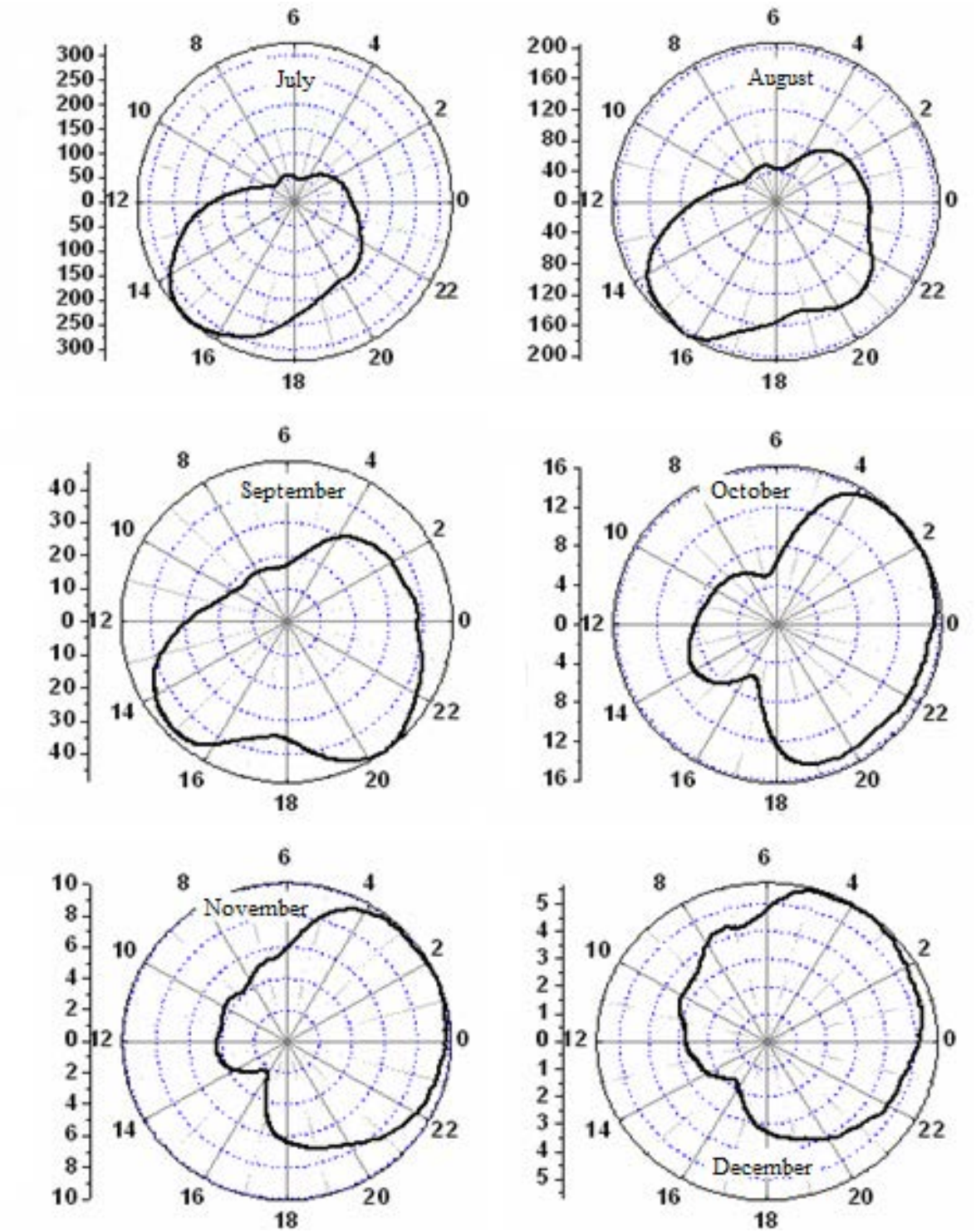

Fig. 3: Averaged for 1997-2004 and smoothed daily variations of NPEMFE in polar coordinates.

These graphs show how the intensity of EM field disturbances changes during the time of day and depending on the season. It can be seen how the intensity decreases significantly during the winter months and the maximum passes into the night, that is, when it is summer in the Southern hemisphere and the heavy part of the core is there, directly opposite the measurement site.

As it`s noted in this work, the area of thunderstorms also migrates during the year after the core of the planet, which can also be explained by the interaction of the charged core and atmospheric electricity, like a huge capacitor. This phenomenon deserves a separate study.

© 2022 Global Journals

2. Consider the data of gravity measurements.

There are four main forces affecting the measuring sensor of the device — the constant one is the gravity of the Earth's body, and the variables: the gravity from the Sun, the Moon and reversed gravity force from the core of the planet, the position and shape of which, in turn, depend on the position of the Sun and the Moon.

Gravity graphs show very well the change in the trajectory of the core. If we imagine that there is no movement of the core, then in winter, when both the Sun and the Moon rise lowest above the horizon, the change in gravity forces should be the smallest in amplitude. But the measured values tell a different story.

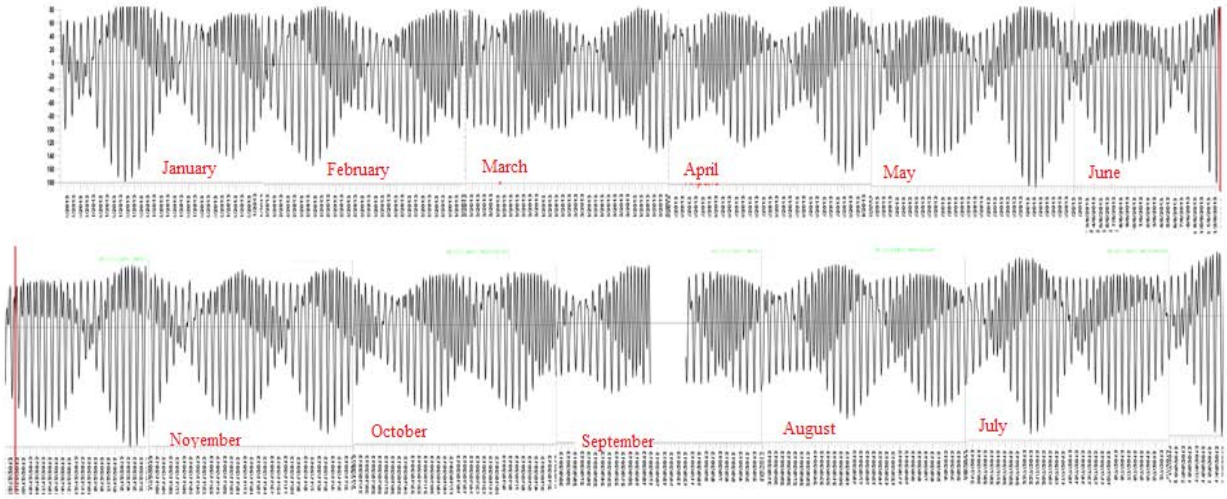

Fig. 4: The behavior of gravity forces before June 22, 2013, and the mirror image after this date, the area of the coast of the Sea of Japan

The almost perfect coincidence of the values before June 22 and the mirror image after, and the decrease in amplitude in the spring and autumn months are very clearly visible.

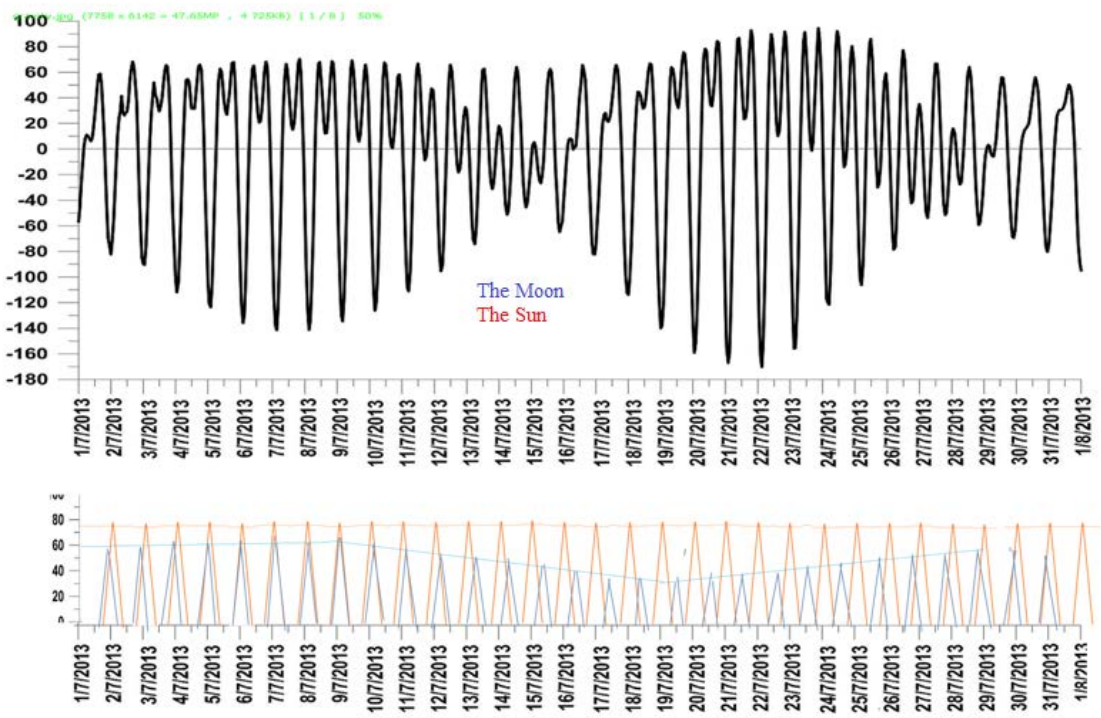

Fig. 5: The behavior of gravity forces in July 2013, near the coast of the Sea of Japan. The lower graph is the position of the Sun and Moon above the horizon

© 2022 Global Journals

Let's see how the behavior of the forces of gravity changes in the summer month on the example of July. At the initial stage, when the phases of the Moon and the Sun coincide, the decrease in the forces of attraction to the Earth should be maximum, especially since the Moon rises high above the horizon and its movement almost coincides with the trajectory of the Sun. But it turns out to be less than with multiphase movement in the 20th of the month. This becomes clear if we imagine that with in-phase motion, they attract a much larger and more concentrated mass of the planet's core, acting on the sensor in the opposite direction.

In the 20th, the Moon "takes away" part of the core during the daytime closer to the opposite part of the Earth, reducing the gravity at the measurement point, and the Sun adds more. As a result, the forces sum, causing the maximum drop in the gravity forces.

In the winter month, the same maximum decrease occurs at nighttime, when both the Sun and the Moon affect the nucleus in phase and it goes not only to the opposite part, but also to the other hemisphere.

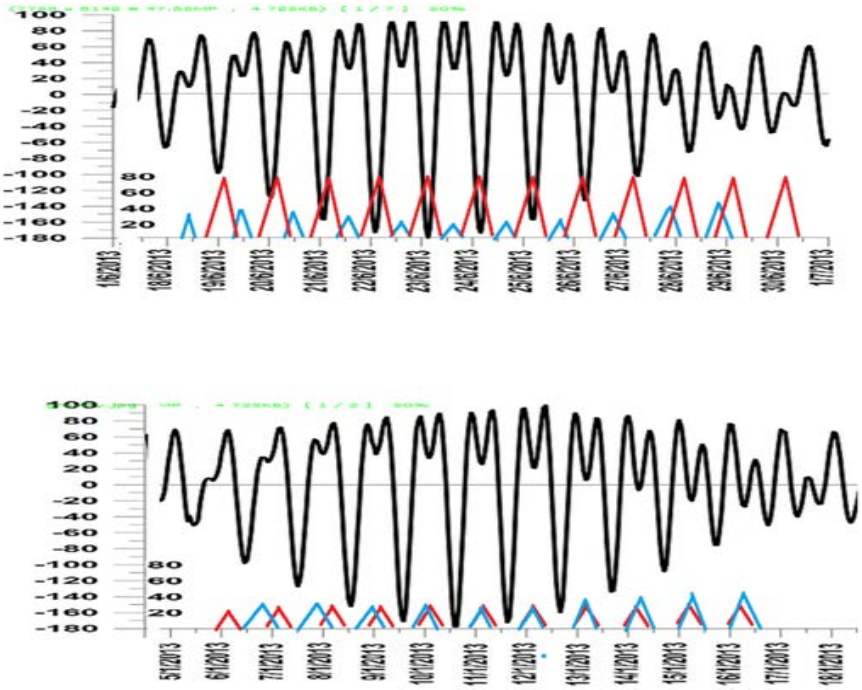

Fig. 6: Comparison of the gravity forces in June and January 2013

IV. Comparison of Magnetic Fields of Planets

Considering the above, the appearance of a magnetic field on other planets, with satellites or dynamic influence of the Sun and without them, becomes clear. For example, Venus does not have a field - there are no satellites and it rotates very slowly, once every 243 earthdays on its own axis and every 225 around the Sun, i.e. if polarization is created inside it, then it is not mobile enough. Or the planet has cooled down and does not have a liquid inner core (the Moon). A change in the polarity of the magnetic field with a changed direction of rotation of the satellite (s) - (Mars) or the presence of a complex field with complex relationships of the planet with satellites - (Uranus, Neptune).

Interestingly, Mercury, which has no satellites, has a field similar that the Earth has, although much smaller, but it is itself a close satellite of the Sun and orbits the Sun quite quickly – in 89 earth days, although it rotates its own axis once every 59 days. Mercury's field is symmetrical and directed along the axis of rotation. The inclination of the equator relative to the orbital plane is only 0.1°. That is, the field appears not only due to its own rotation, like the Earth`s one, but also due to movement around the Sun. The rotation of Uranus is retrograded, as well as the rotation of the satellites. The orbits of the satellites are steeply inclined to the ecliptic plane. The plane of Uranus' equator is inclined to the plane of its orbit at an angle of 97.86° — that is, the planet rotates "lying on its side". If other planets can be compared to spinning tops, then Uranus is more like a rolling ball, Uranus has a very specific magnetic field

© 2022 Global Journals

that is not directed from the geometric center of the planet, and is tilted at 59 degrees relative to the axis of rotation. In fact, the magnetic dipole is shifted from the center of the planet to the southern pole by about 1/3 of the radius of the planet. This unusual geometry leads to a very asymmetric magnetic field. This polarity is opposite to the Earth's one.

A comparison of the fields of Jupiter and Earth can be a good indicator of the influence of motion trajectories on the shape of the field. Jupiter's field is more like a flat disk - most of its satellites rotate in regular circular orbits in the plane of the equator and the axis of rotation of the planet itself is slightly tilted, there is no change of seasons, and the Earth, which has a field shape similar to an apple, due to the changing influence of the Sun at different positions relative to it, caused by the tilt of the axis of rotation. This can be compared to fields from two different electromagnetic coils - wound coil to coil on a "tube", like a tape cassette.

a) Year Period of Solar Activity

Another pattern that was known to the Pulkovo scientist-astronomer Vitinsky Yu.I., but for some reason it was ignored, can be observed - this is the coincidence of the period of rotation of the largest planet in the solar system, Jupiter, with an 11-year period of Solar activity and the influence of this period on the number of formed "Sunspots". Jupiter exceeds the Earth by 1,320 times in volume and 317 times in mass, and its influence on the Sun exceeds the influence of all other planets taken together. It is only 1000 times smaller than the Sun.

Here is what he writes about the history of solar activity research (Yu.I.Vitinsky, 1983):

> "*In the middle of the last century, amateur astronomer G. Schwabe and R. Wolf established the fact of a change in the number of sunspots over time for the first time, and the average period of this change is 11 years... R. Wolf, convinced that solar periodicity is the fruit of the influence of the Solar planets on the Sun, initiated this search himself. ... Finally, one of the "heirs" of Wolf in Zurich, M. Waldmeier, dared to doubt the correctness of his "scientific great-grandfather" and transferred the cause of the 11-year cycle into the Sun itself already in the 40s of this century.*"

And: "*Perhaps the most intriguing of all the questions that arise when studying the Sun can be formulated as follows: "Where does solar activity come from and how does it come down to those features that we talked about in this book?" If any intelligible answer could be given to this question, humanity could rightfully consider itself at least the master of its planet. Unfortunately, a unified theory of solar activity, which could give an answer to the question posed here quite fully and at least without obvious contradictions, has not yet been created. ...At first glance, it may seem that there is nothing to think about here: since the activity is solar, it means that it occurs in the Sun. But this is begun to think so quite recently. And it all started back in the middle of the last century with a hypothesis that was put forward by R. Wolf himself. According to this point of view, solar activity is caused by the Solar planets, more precisely, their tidal effect on the Sun. Such a hypothesis had some ground under it. After all, the period of Jupiter's rotation around the Sun (11.7 years) is incredibly close to the average cycle length of the solar activity (11.1 years), and the length and height of this cycle changes over time hardly chaotically*".

Thus, the original version about an external source of influence on solar activity was changed to an internal one for some reason, but probably in vain.

If we imagine that this "heavy", following Jupiter, the Sun`s center, moves in subsurface space and at the same time it is a charged electrical potential, then this can lead to the appearance of "magnet tubes" on the surface - that is, to the exit points of both poles of local magnetic fields. Everyone probably watched how multidirectional purls are created from the paddle on quiet water.

© 2022 Global Journals

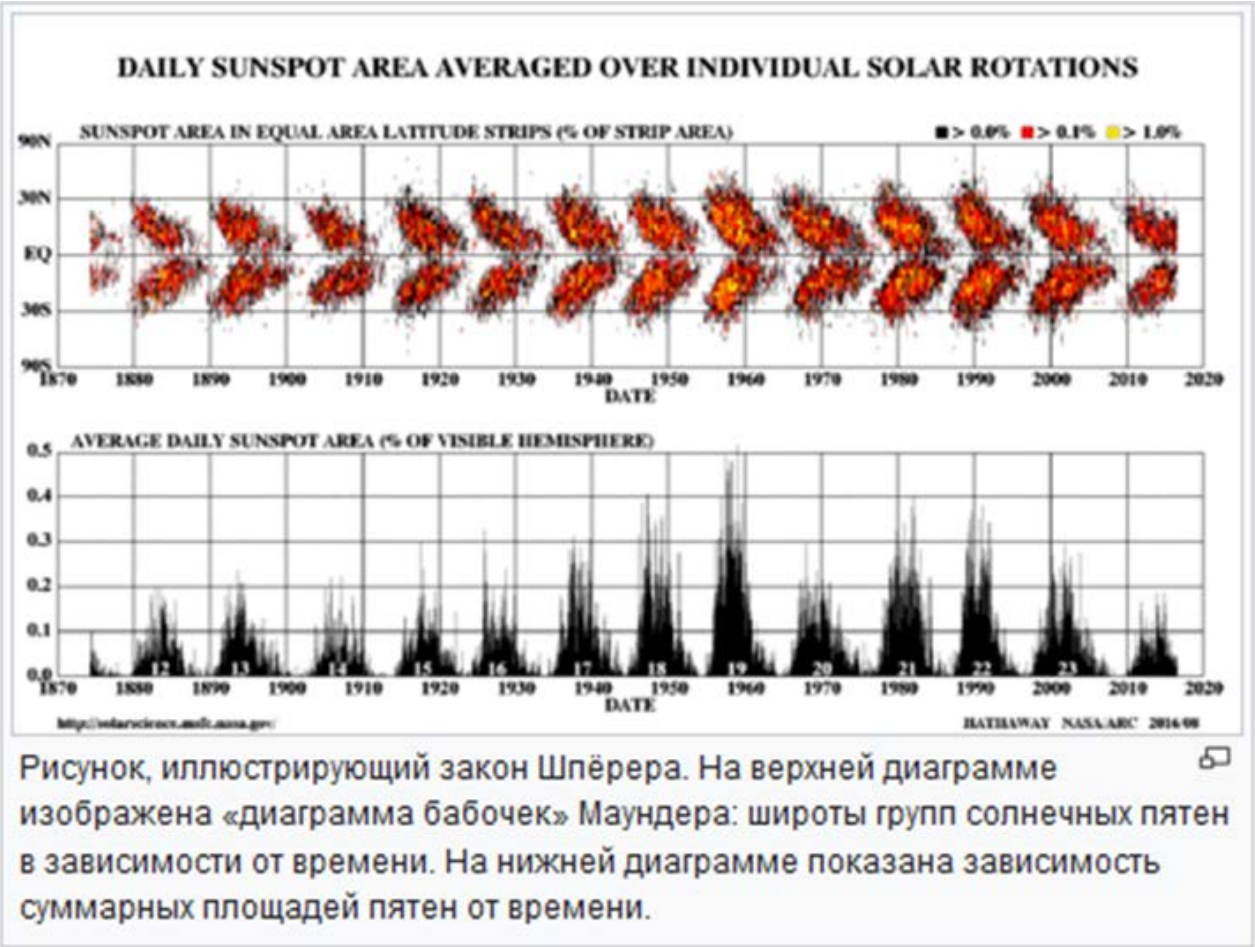

Рисунок, иллюстрирующий закон Шпёрера. На верхней диаграмме изображена «диаграмма бабочек» Маундера: широты групп солнечных пятен в зависимости от времени. На нижней диаграмме показана зависимость суммарных площадей пятен от времени.

Fig. 7: The figure from the Internet

V. The Influence Of Jupiter On The Earth's Biosphere

A.L. Chizhevsky unequivocally showed the direct dependence of the influence of solar activity on the Earth's biosphere in his long-term studies of these processes, suggesting that disturbances observed as "spots on the Sun" cause radiations that affect all living and inanimate, reaching the Earth's surface and penetrating into it (A.L. Chizhevsky, 1976).

Thus, Jupiter causes processes affecting the Earth because of its influence on the Sun. The proposed mechanism can help to explain the appearance of electromagnetic pulse (magnetic storms) in a wide frequency range, which appears as a result of abruptly changing flows of charged solar matter.

The reason for all periodic phenomena occurring on planets is most likely to be sought in their external environment, interaction with other planets - this is, by the way, the basis of astrology.

Any celestial body, being unaffected by other bodies, will strive to adopt such an arrangement of its constituent parts in which the interaction between them is minimal and the temperature is equal to the surrounding, i.e. to minimize entropy.

Even chemical and radioactive processes have an expiration date.

Only external influence can periodically bring the planet out of its steady balanced state.

© 2022 Global Journals

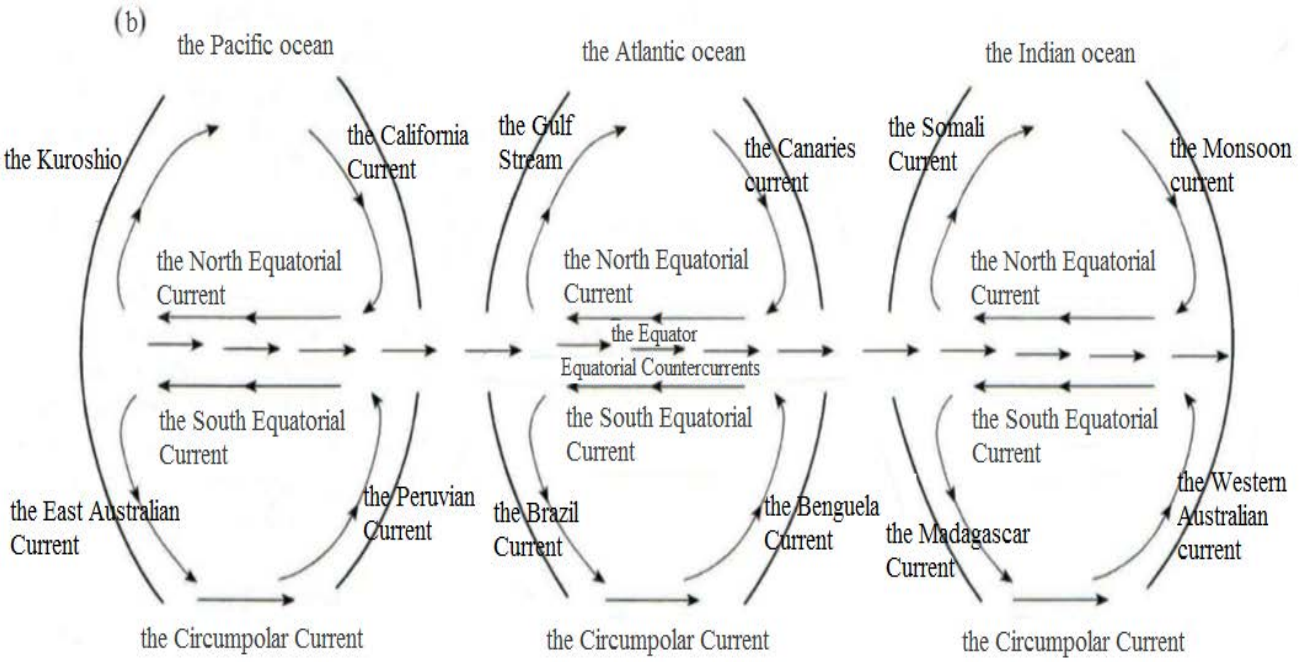

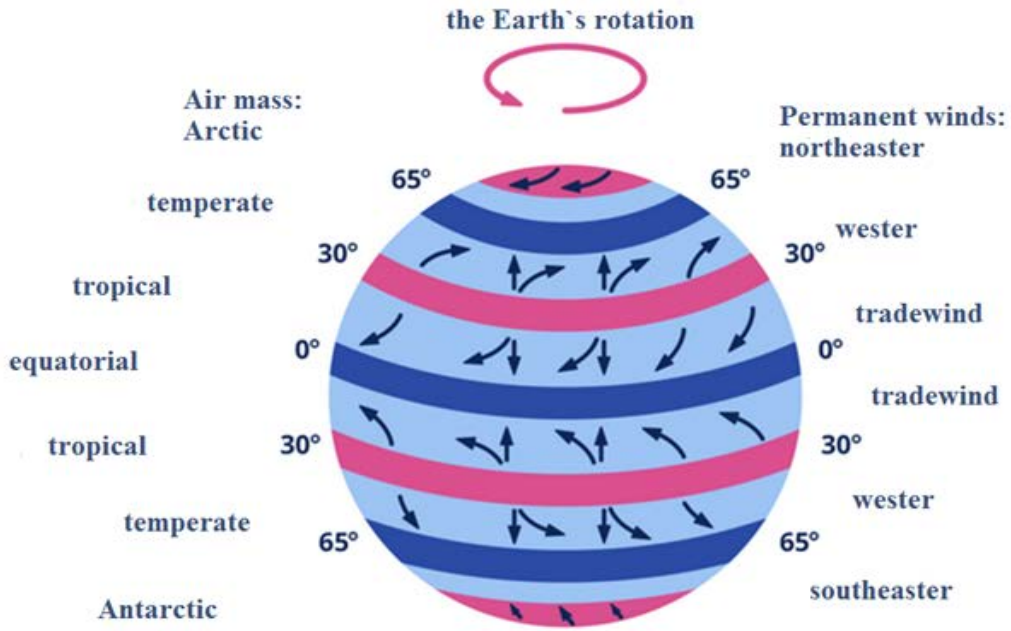

Fig. 8

© 2022 Global Journals

VI. Equatorial Currents and Tides

Fig. 8. A current map and a conditional drawing (Garetsky, 2006) showing the similarity of the structures of large-scale currents of the Pacific, Atlantic and Indian Oceans. Conditional drawing of equatorial winds.

A similar phenomenon can be seen in planets with satellites – their dust rings are located opposite the trajectories of the satellites. If the land of the continents on the Earth`s surface interferes with the flow-through and makes the flows turn in the opposite direction along the peripheral sections, then the flows on other planets are looped. The "Red Spot" on Jupiter is very similar to an obstacle washed by a stream.

a) Modern (scientific) look at the causes of currents and tides

In the scientific literature, it is customary to explain the nature of equatorial currents by winds constantly blowing in the same direction, and the nature of winds by heating the surface and the Earth`s rotation.

Sometimes the formation of currents is attributed to Corioli forces, without taking into account that these forces are not real, but conditional (fictitious), that are used for describing different linear speeds for unequally distant from the centre points at the radius, when the body rotates.

Oceanic tides in modern scientific literature are considered as the rise of water due to attraction from the Sun and Moon, and at the same time there are constant attempts to lead to some kind of mathematics (Melchior, 1968), using correction factors and various models, considering that the Earth is a sort of body with its own oscillation frequency. At the same time, it is forgotten that any oscillations have a dead time, and considering issues last for many centuries. In fact, such a method is not better, but even worse, because of its complexity, than a simple statistical table, that is, a method that has long been successfully used in the practice of sailing, without identifying the main causes of tides.

The difference in the gravity forces in the even several kilometers interval (let's assume that it is the depth of the ocean) at a distance of 380000 km from the Moon, and 150000000 km from the Sun, cannot be so great that it causes the rush and movement of water. And this is under the condition that the entire mass of the Earth is nearby, which is much larger than the same Moon.

The emphasis on tidal forces caused by the influence of the Sun and Moon during the rotation of the Earth is made, for example, in the article (Garetsky, 2006), where it is said that the moving "crest" of the mantle causes the movement of water (Discrete wave motion). But it is not taken into account that the crest moves at a depth, and the main flows of the current do not fall below 200 meters (Stockman, 1948), thus such a mechanism cannot work.

The affect of tidal forces directly on the ocean waters also cannot cause such a current for the reason that these forces affect the masses of water first from the East, and then just the same from the West. Even if they shift the mass of water first to one side, which is not possible, then they will return it back by as many.

b) The real causes of currents, tides and winds

But there are also quite significant currents — movement speeds are measured from 30 to 150 cm / sec. (Shtokman, 1948), which means that there is also a force that causes them. Moreover, this force is centuries-old, of constant direction.

There are no external, observable forces. So there are internal ones.

It should be noted at once that there are two types of manifestation of these forces-

The tide (rise) of the mainland of the planet - this tide is difficult to notice without instruments.

The tide of water in the ocean - is well observed on the coast.

Let's imagine the Earth as a kind of ball, with a rather thin, relative to the total volume, shell (mantle), which can deform from the movement of the inner mass if it is attracted to the outer mass (the Sun, the Moon). Globally speaking, it can be compared with an air, inflated and, what is more, poured with water balloon. Water will cause deformation of the shell due to gravity, and this deformation will move around the circumference when the balloon rotates, - this is the analogue of the tide of the Earth`s solid part. *But this is not the tide on the ocean*!!. *The tide at the shore on the water will be caused by water discharge from the point of maximum mantle rise to the shores.* If, for example, you pour water into a plastic plate and press from below, then the water will overflow to the edges, shores. This fact is very clearly visible in figure 9, when superposition graphs of the measured behavior of gravity forces, a graph of the water level and the positions of the Sun and Moon at one measurement point. And also in Fig.10, where the maximum tide rise just on ocean shores, is clearly visible.

© 2022 Global Journals

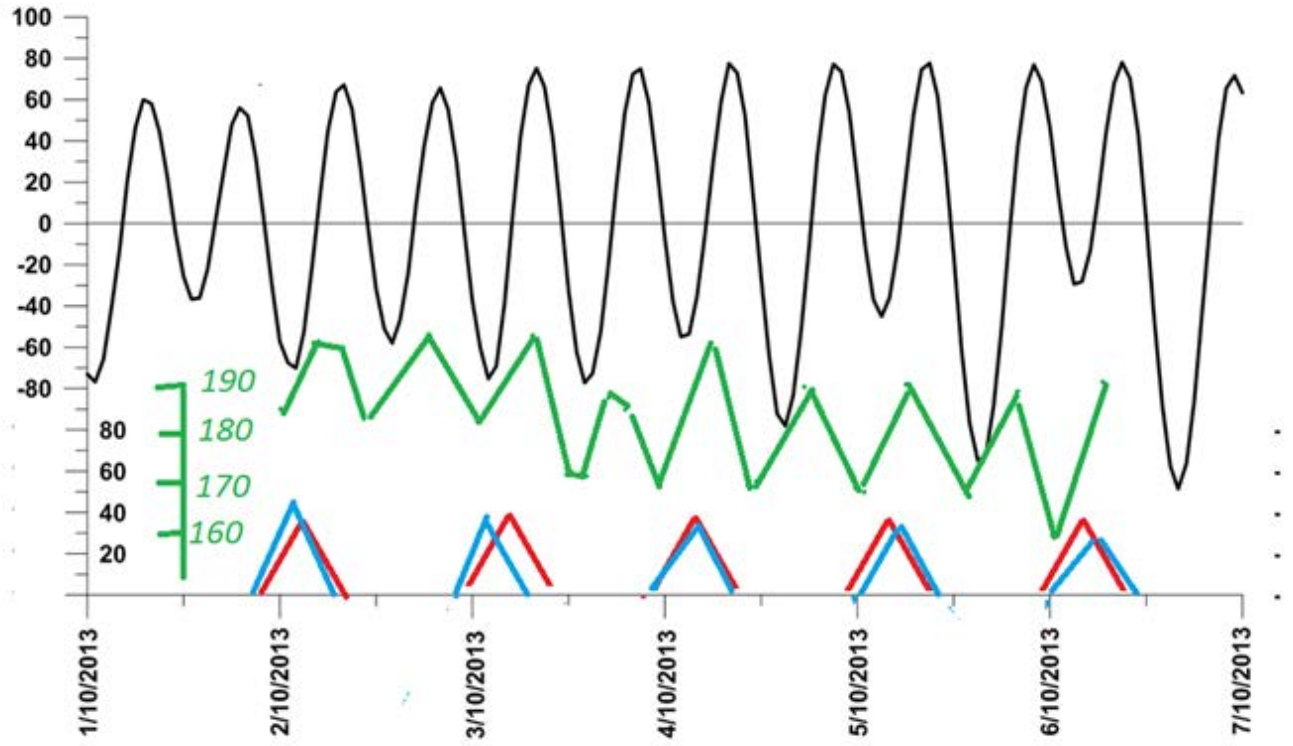

Fig. 9: Measurement data. The station "Poset" of the Pacific coast

On the horizontal axis, Time is Universal.

The black line is the measured force of gravity. mcGal.

The red one is the position of the Sun above the horizon in degrees (time of sunrise, maximum position, sunset).

The blue line is the position of the Moon above the horizon in degrees (time of sunrise, maximum position, sunset)

The green line shows ocean water level in cm.

Time interval when the Sun and Moon are in the sky side by side and simultaneously affect the core of the Earth was specially selected.

Gravity forces measurement data were provided by employees of the gravimetry laboratory of the POI FEB RAS.

Ocean level measurement data made at the Poset station were kindly provided by the staff.

The data of sunrise times, maximum position, sunset and ascending angle of the Sun and Moon are taken from the StarCalc program with reference to the station location.

It can be seen how a low tide and at the same time a decrease in the gravity force, i.e. the high tide of the solid part of the planet appears a couple of hours before the zenith point passing by the Sun and Moon. The outflow of water is also visible at night, when there is a mantle tide from the departure of the planet's core to the opposite part of the Earth.

It is this fact that explains not the coincidence of the high tides, but the coincidence of the low tides on the water, with the positions of the Sun and Moon at the zenith.

The "crest" on the mantle will change its position and size depending on:

- Time of year (tilt of the axis);
- The distance of the Moon and the Sun from the Earth;
- "Outpahse", i.e. different positions of the Moon and the Sun between each other;

And the tide near the shore will not be constant, but will depend on these factors and the bottom relief.

Now let`s talk about the rise (tide) of the mantle on the opposite side of the globe.

Unfortunately, it is difficult to reveal this, as in the first case, but even here everything is quite simple. The mass of the planet's core shifted towards the Sun and Moon will weaken the gravity force on the opposite side of the ball in proportional to the square distance of the displacement. In the graph below, these will be the failures of gravity forces (black) during periods when there is neither the Sun nor the Moon above the measurement point. It is impossible to explain such a decrease in the gravity forces in any other way, since the gravimeter reacts only to the gravity force (mass).

When the Earth rotates, the "crest" will describe cyclic circular trajectories - this is the only observed

© 2022 Global Journals

movement in one direction, coinciding with the direction of movement of the main ocean current. (Garetsky, 2006)

The gravity force of the close to the water mass of the moving inner core of the planet will make the mass of water move in the same direction.

This is the reason for the main ocean current.

These same forces move the air masses, creating constant etesian winds.

Unlike currents, these winds pass over the continents unhindered and close in a ring. Moreover, they reach the heights of the stratosphere, where there are no temperature differences from heating the surface. Only the gravity forces of the chains: the planet's core-the Sun and the core-the Moon.

Since the bulk of the core moves in the equatorial region, the waters near the equator are also set in motion.

Note: The cause of the backflow is not considered in this article due to the lack of measured data, and it is better not to give untested hypotheses.

Encountering continents in its path, this current diverges away from the equator and, since the basins of the oceans are practically closed, the water mostly moves about a closed path. Figure 8.

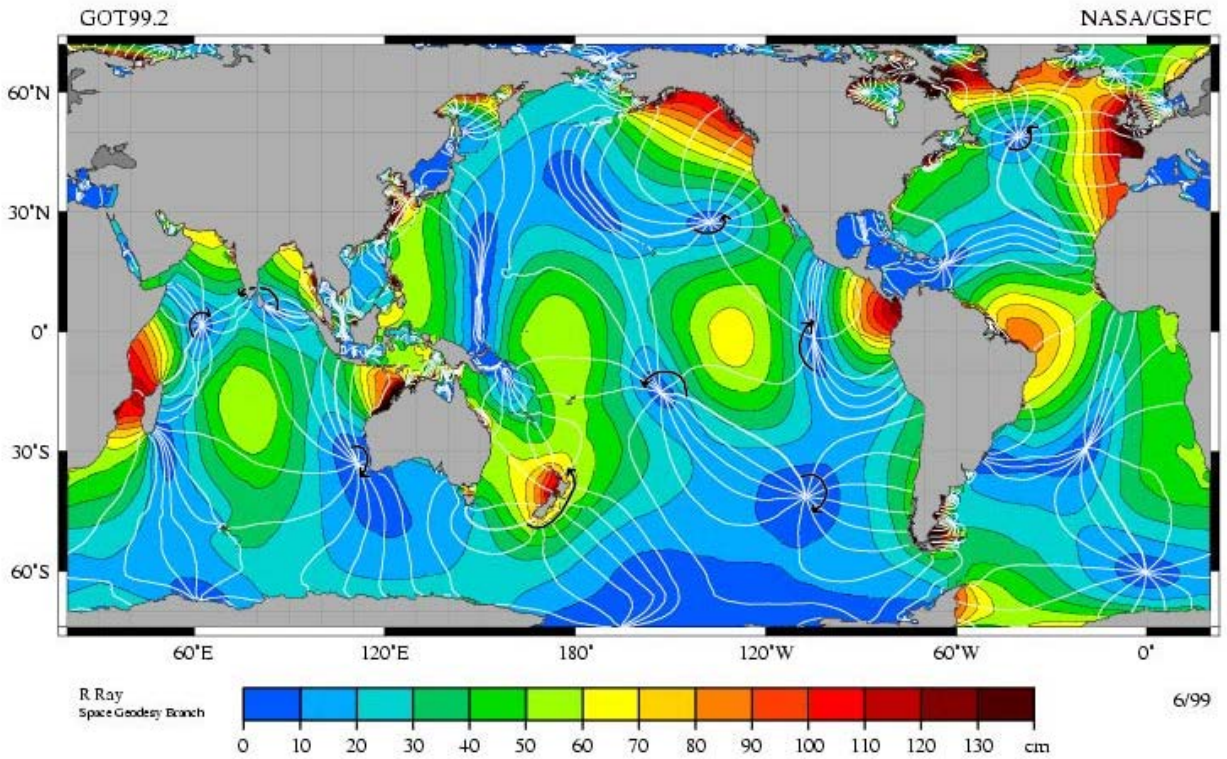

Fig. 10: Cotidal lines

The change in the water level of the seas and oceans is only a manifestation of the change in the level of the solid surface of the planet. Water changes its level depending on the relief of the bottom and shore due to the flow properties. At the same time, the values of changes in the solid shell of the Earth depend on its structure and thickness. Mountain and mainland massifs with large deep parts will naturally be less affected than low, thinner, underwater areas. That is why the waters of the lakes practically do not change their level, because they are located on the body of massive continents and at the same time the bottom level of the entire reservoir changes slightly. There are amphidromic points (with no tides) and cotidal lines (lines on the map connecting all points where the crest of a tidal wave appears simultaneously, i.e. points where high water comes at the same time) on the plain of the oceans. If the tide had arisen only from the impact on the water, this could not have happened.

© 2022 Global Journals

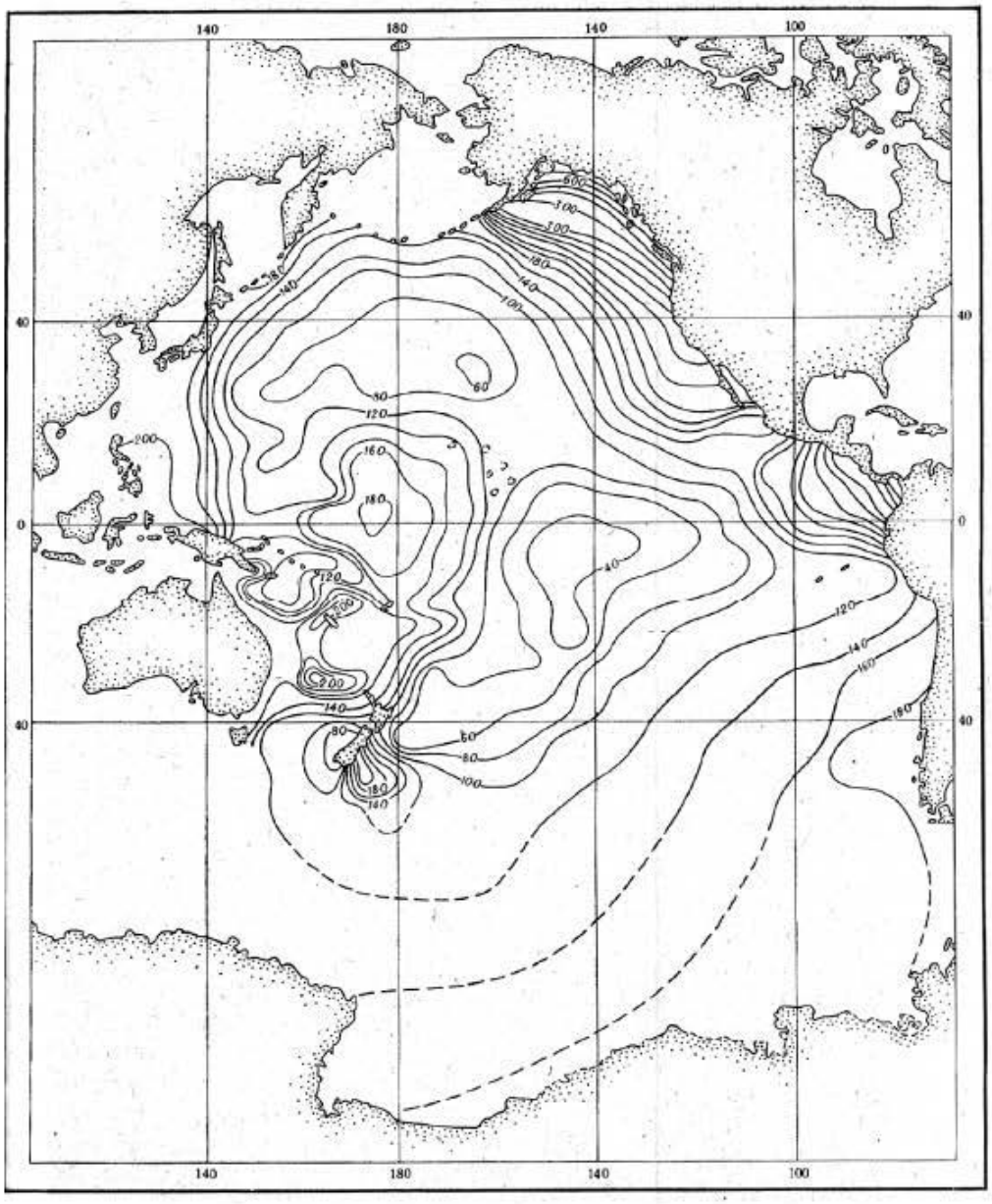

Рис. 3. Максимально возможная величина прилива (в сантиметрах) на акватории Тихого океана

В последние годы с помощью современных цифровых гравиметров проводится мониторинг поля силы тяжести на станции мыс Шульца (полуостров Гамова, юг Приморья, ТОИ РАН, 42.58°N, 131.16°E, 150 м от берега Японско-

Fig. 11

© 2022 Global Journals

This is very clearly seen in the figure from the article (16) above (unfortunately, the original source of the data could not be found) It is noticeable that in the zone where, according to modern theories, there should be a maximum influence (the equator zone), the level of oceanic tides, on the contrary, is minimal.

VII. Why Does the Moon Come to us with One Side

There is usually the following answer to this question - it makes one revolution around itself during the flyby around the Earth. But what makes it behave like this?

Its former rotation is indicated by the presence of meteorite craters on the entire surface, but not only on the side facing the cosmos.

This is also confirmed by the fact that previously it had an intense magnetic field, and now only a remanent one.

In the process of cooling, the heavy masses of internal substance were grouped mainly in the Earth-facing side, thus turning the Moon into a kind of "Roly-Poly", making it turn to us with one and the same heavy side.

Thus, the mutual gravity force not only keeps the Moon in the orbit of the satellite, but also makes it constantly rotate, that contributes to the waste of energy.

The fact that most of the satellites rotate around their planets with one side facing them, and the rotation of planets such as Venus and Mercury is synchronized with the movement of the Earth (these two planets turn to it with one hemisphere when approaching the Earth), suggests that the planets interact with each other as bodies with displaced centers of mass. At the same time, in the case of a liquid core, this center can move inside the solid envelope of the planet.

The same mechanism can explain the reasons for the appearance of a dip in the graph of gravity when the Sun and Moon pass through the sky.

According to the measurement data (8), the presence of a third mass can be seen, affecting the instrument readings. I'll try to explain it.

Let's imagine that only the Sun and Moon affect the tide on the mantle. If the motion trajectory of these two bodies coincided (Fig. 12), for example, the section from 5.05.2013 to 13.05.2013, the readings at the measurement point would be uniformly transitioning from the minimum, at the time of the location of the Sun and Moon at the zenith, to the maximum, when they are above the opposite side of the Globe. Now let's look at the measured data.

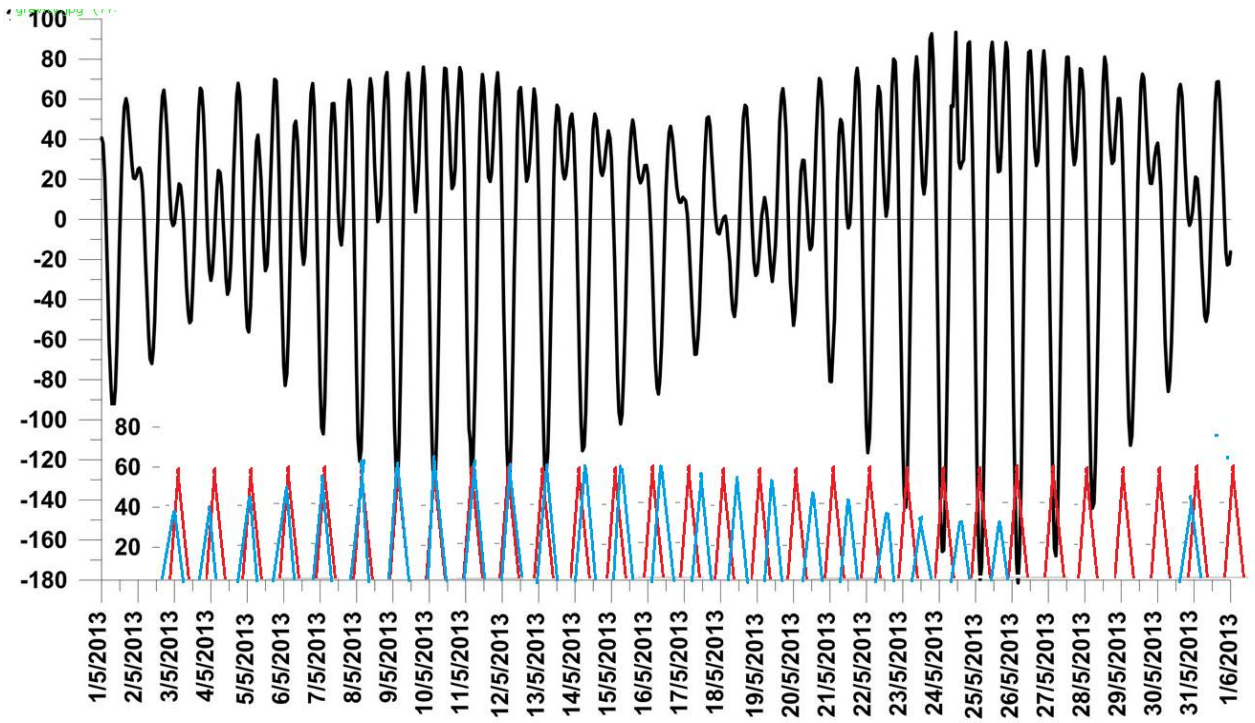

Fig. 12: The behavior of gravity forces during May, 2013

Red color shows the conditional position of the Sun in degrees above the horizon, blue one - of the Moon.

Conspicuously, in addition to a smooth and harmonious change, there are also significant dips in the instrument readings at night, when both the Sun and

© 2022 Global Journals

the Moon, being on the opposite side, should increase the gravity to the Earth. In fact, there is a decrease in the gravity forces. Such indications cannot be explained in any other way, except by the influence of the third mass. And this mass, moving after the external gravity forces, is the heavy part of the Earth's core. The gravity force decreases proportional to the square of the distance to the center of nuclear mass, moving away from the measurement point.

As a comparison, you can look at the section of the graph from 20.05 to 26.05 (when the Sun and Moon are in opposite phase); it is clear that the gravity at the measurement point exactly depends on the position of the Sun and the Moon.

In addition to the location of the core, these forces affect its shape- grouping or smearing it on the internal volume of the planet.

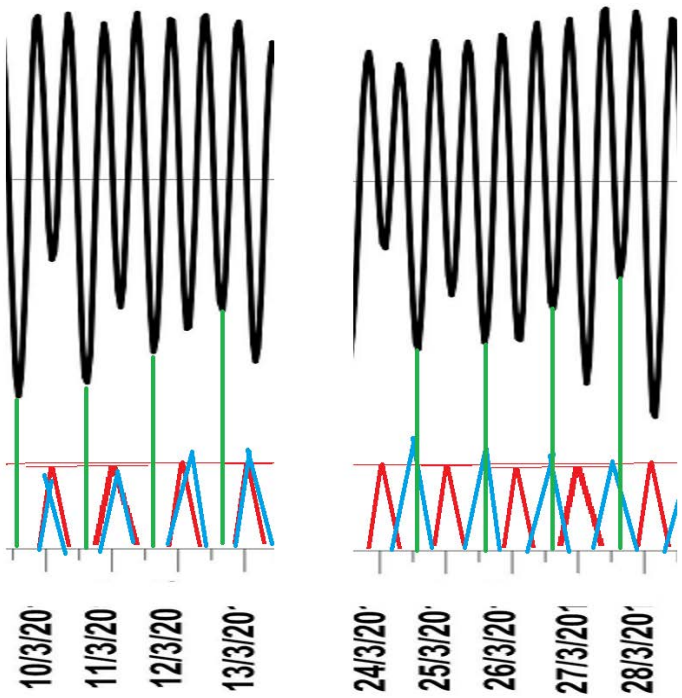

Fig. 13: The behavior of gravity forces in March, 2013

This graph shows how the almost identical behavior of the instrument readings is caused by completely different positions of the Sun and Moon.

This can be demonstrated very easy, without any mathematical models, by pouring iron balls into a glass jar and turning it, having the Earth as one gravity force, and the other one simulate with a magnet. It can be seen that the core can even split into two, depending on the location and magnitude of the applied forces.

The movement of the Earth's core leads to the heating of the internal structures of the planet, which, together with solar exposure, allows you to maintain a temperature range on the planetary surface suitable for the existence of known life forms.

VIII. Changes in the Earth-Rotation Period (Duration of the Day) — Seasonal and Half-Monthly

This portion of the paper is based on the data given in the excellent monograph by V.M. Kiselev, Ph.D. (Siberian Federal University) (13) "The rotation of the Earth from the Archean up to now", that is why it will mainly consist of quotations.

"The basis for instrumental measurements of the features of the Earth's rotation around its axis are astronomical definitions of the time intervals between two consecutive similarly-named culminations on the same geographical meridian of some luminary or a conditional point of the coelosphere. Stars and the Sun are used as such luminaries, and the vernal equinox (Aries point) and the mean equatorial Sun are used as conditional points on the coelosphere".

"The local solar time on the meridian of Greenwich, counted from midnight, is called Universal Time UT0. Thus, the universal time scale obtained as a result of astronomical observations of the luminaries is a scale determined by the Earth`s rotation around its axis"

Whereas:

"... since 1955, atomic and molecular systems for reproducing frequency and time reference have been

© 2022 Global Journals

used, on the basis of which the Atomic time scale TA1 was created".
Currently, this accuracy has increased to 0.001ms.

IERS Service (International Earth Rotation and Reference Systems Service) posts information about changing the rotation time on the site: https://datacenter.iers.org/data/latestVersion/224_EOP_C04_14.62-NOW.IAU2000A224.txt

Let's use the graph constructed by the author of the monograph, based on these data.

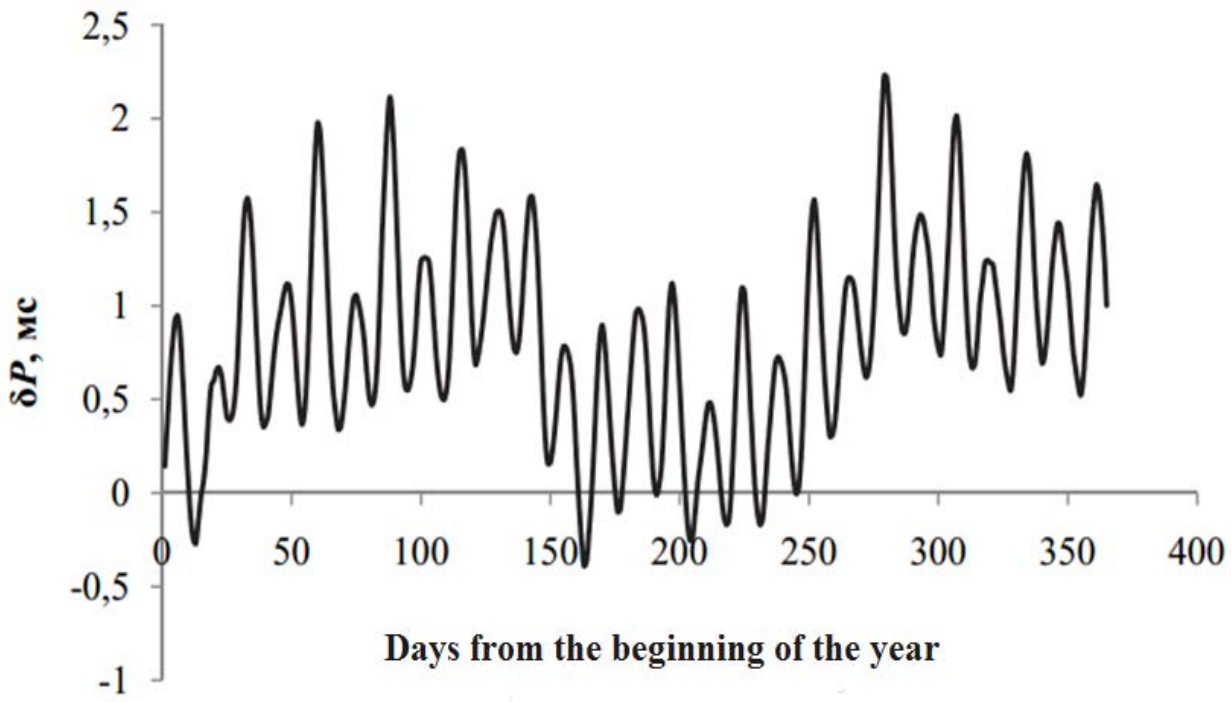

Fig. 14: Change of the duration of the day in 2006

The graph shows periodic changes in turnover time - semi-monthly and during the year.
Let's try to explain these fluctuations.

As it was mentioned earlier, the core of the planet moves not only in a circular motion, but also from one hemisphere to another and back, depending on the time of year. Such a change in the place of movement leads to the fact that the path of the core motion changes from the minimum at the poles (winter, summer) to the maximum at the equator (autumn, spring) (see Fig. 2). It is clear that a longer path of motion in the equatorial region causes greater resistance to the rotational motion of the planet, thereby increasing the rotation time (days).

Half-monthly fluctuations are explained by the separation or vice versa grouping of the mass of the planet's core under the influence of solar and lunar gravity, depending on the location of the Sun and Moon relative to the Earth. A more detailed study of this influence has yet to be carried out.

Based on these data, with a competent mathematical approach, it is probably possible to estimate the weight value of the moving part of the planet's core.

IX. Earthquakes, Mountain Formation and Continental Migration

The mass of the planet's core, influenced by various, then folding, then subtrahend gravity forces from the Sun and Moon, moves along the "inner" surface of the Earth, constantly mixes, bumps into irregularities, making a new passage for itself every day. At the same time, the inner part of the Earth crust is constantly under the influence, which is transmitted to the tectonic plates, making them gradually move, thereby moving the continents. And they really move transversally (East-West) and do not move in the longitudinal direction (South-North). Sometimes, in literature, movement is associated with tidal forces. As we can see, this is partly true, but tidal forces alone cannot create movement, because they are directed first to the East, and then during exactly the same time to the West. And only the moving core is directed from East to West.

The exposure on the inner surface of the mantle will naturally be ununiform, due to its heterogeneity.

© 2022 Global Journals

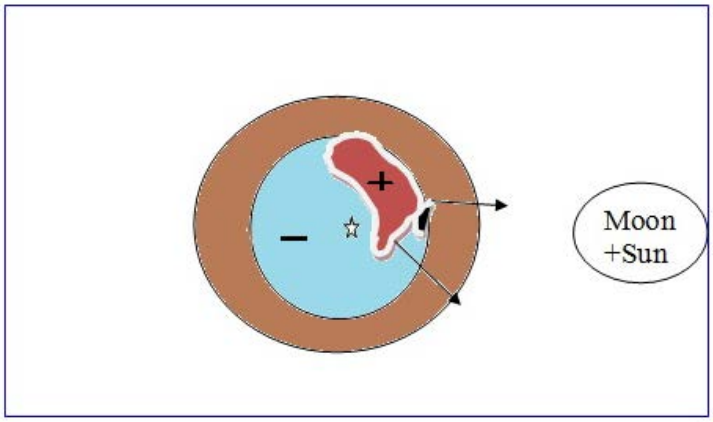

When the flow is moving, a wave with a crest may appear when crawling onto an internal irregularity and further collapse can cause an earthquake. Fig 15. Collapse of a part of the core

Confirmation of this mechanism of earthquakes occurrence is that most seismic origins are located on the boundaries of lithospheric plates, in other words, on the place of geological irregularities.

This phenomenon may be the cause of movements in the surface layers of the mantle, leading to the appearance of additional seismic origins and aftershocks.

It should also be noted that magnetic storms on Earth are accompanied by low-frequency vibrations of the Earth's body and, conversely, earthquakes are accompanied by electromagnetic radiation, i.e. these two phenomena are interrelated, that can also serve as confirmation because there are jumps in electric charge (stream of the charged substance), and the transition process, as known, has a wider spectrum than direct current.

One more thing, – the "lull" effect of seismic activity and electro-magnetic background radiation before major earthquakes is known. This is how it is described in the works of the Malyshkovs (2009): "*... on the eve of many earthquakes, we found not an increase, but a decrease in the intensity of the fields. Depending on the energy of the upcoming earthquake, the reduced pulse count lasted from several hours to several days and was observed at night and in the afternoon, in the summer and winter months. If the fields were increasing, it would be possible to talk about the inclusion of additional sources arising in the focus of the rock mass damage that has begun. The decrease in the pulse flow was puzzling*".

Such an "accumulation" of the mass of the charged substance of the nucleus, causing a lull and leading to a subsequent damage, as we see, is quite understandable.

And one more thing, - according to eye-witnesses, a loud roar is heard during large earthquakes, as if it is a huge avalanching, i.e. there are mass movements over long distances.

The assumption of damage is also supported by the fact that, according to acoustic studies, an earthquake occurs almost simultaneously over a large extent of the Earth's surface (up to 1000 km). Naturally, the damage itself is much smaller, and there is the expansion of the sphere and the multidirectional nature of the seismic wave causes increasing the area.

Such a mechanism of internal dynamics can also help in understanding the process of mountain formation. There are not just some incomprehensible forces of tension in Earth crust, but concrete ones with known directions and causes. If you look at the physical map of the world, you can see that most of the mountain ranges stretch in the south-north direction, and this reminds everyone of the familiar formation of glacial hummocks during ice motion. The mechanism is very similar- both there and there is a stream and ice or Earth crust above it.

X. Time Jumps and "Killer Waves"

With the advent of new, more precise time measuring means, it was noticed that sometimes the course of celestial (stellar) time changes relative to the reference atomic ones in jumps, as a rule, during large earthquakes. How can this be explained but through the Earth being exposed of forces, turning it at a certain angle? But we observe no external forces of such a power, so we have internal ones left.

It is quite possible that, when the core affects an internal "roughness", the core "pushes" the main body of the planet, altering the astronomical time relative to the stable reference one.

Marines know such a natural phenomenon known as a "killer wave" (periodic waves, monster waves, rogue wave, freak wave, onde scelerate, galejade).

Just a while ago, scientists considered the sailors` stories about gigantic killer waves that emerged

© 2022 Global Journals

from nowhere and took down ships to be just maritime folklore.

The existence of sea waves 20-30 meters high contradicted the laws of physics and did not fit into any mathematical model of formation of waves. It should be noted that these waves appear on relatively calm water surface. They can be a crest or a trough, single one or coming in a set.

The proposed hypothesis can quite logically explain the mechanism of occurrence through the same interactions between the moving core and the internal irregularities of the planet's body, which are carried over the ocean surface.

XI. The Motion of the Magnetic Poles

Thus it turns out that the outer shell of the Earth is weakly related to the processes taking place between the planets, and therefore is “free” to move relative to the center of mass (it is similar to rotation of the outer rim of a bearing with internal one being fixed), while changing the position of the magnetic poles on the surface of the Earth, but without changing the position in space. A shift occurs before the mantle comes into one of the local stability points. It does not have to be a complete polarity reversal. Although inversion is more likely than just some kind of a lope, for the reason that for many millennia, the core has "washed out" a certain moving direction, gave the planet a known shape (geoid) and if the shell is tilted in some way, it will be more difficult for the flows to make new directions than just to return to the old ones, but flow into the opposite side.

XII. On the Question of Gravitational Waves

Changes in the values of Newton's gravitational constant G, measured at different times, led scientists to think about the influence of external gravitational forces, called gravitational waves. The search for these waves engages many scientific organizations in, and significant funds are being invested in the creation of installations. The history of this study of these phenomena and emerging in the process problems are considered in detail in the work of Vikulin A.V. (15). For example, he says:

"The conclusion about the existence of a relationship between geodynamic processes and phenomena in Space is in full accordance with Mach's principle of the universal coherence of all processes occurring in the Universe. Only gravity, which unites all parts of the universe into a single whole, can become the connecting "cosmic" link of such a relationship. The connecting "earth" link of the relationship between geodynamic processes and phenomena occurring in Space can be rotary geodynamic waves, which are as distinctive for an orbiting geological environment (geo-environment) as for bodily seismic (elastic) waves for an "ordinary" solid. The existence of a relationship between cosmic (gravitational) phenomena and geodynamic processes is almost obvious. The possibility of such an approach to the problem has been discussed in various papers".

As we can see, the author has almost approached understanding the ongoing processes, and if we change the newly introduced definition of "rotary geodynamic waves" to a simple one - the mass motion of the core, then all will make sense, and the problem of gravitational waves will be solved. In other words, we can say that sound waves are created by an oscillating diffuser, electromagnetic waves create alternating current, and gravitational waves create a change in the distance from the main mass of the planet to the recording device, and they should be searched not in space, but "underfoot". Perhaps these values of G, measured at different moments, will allow us to estimate the mass of the moving core.

© 2022 Global Journals

XIII. Why are the Trajectories of the Planets of the Solar System (SS) Located in the Same Plane?

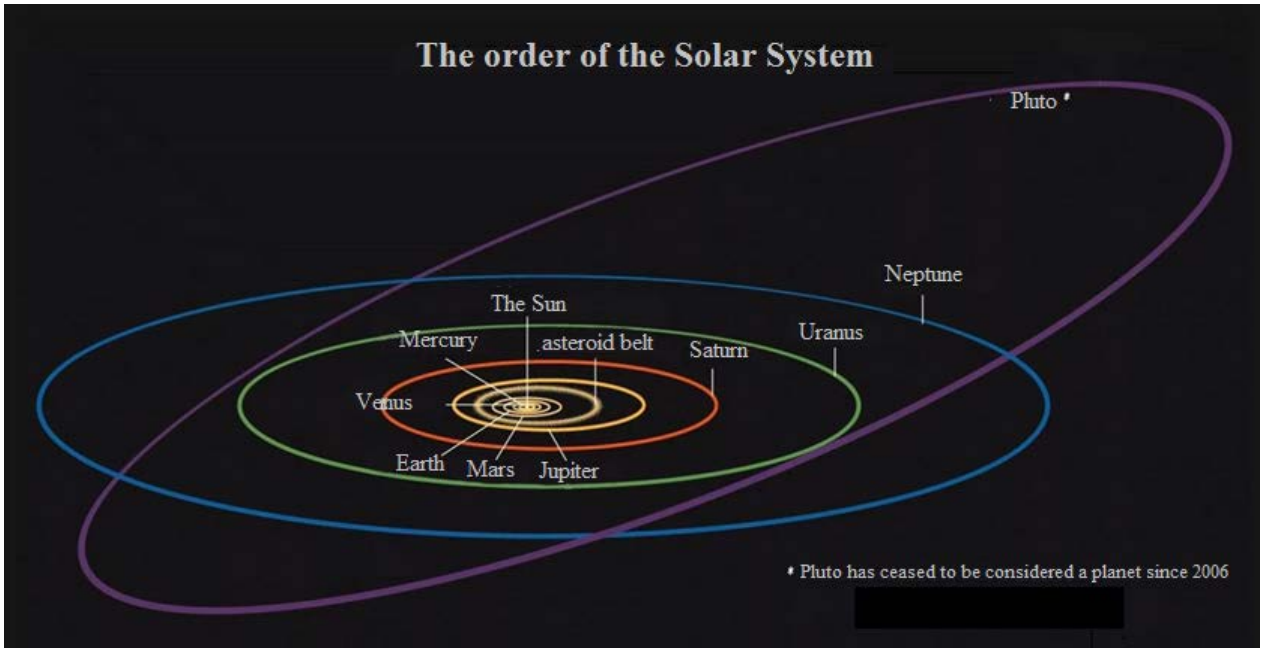

Fig. 16: Drawing from the Internet

And really, why?

(The angle between the ecliptic plane and the orbit plane is called the inclination (declination). Pluto was the planet with the largest inclination of 17° until it was demoted its planetary status. Mercury is the only planet with a significant inclination of 7°.)

If we exclude some external, reasonable influence (Supreme Intelligence), which not only once determined such an order of motion, but also constantly maintains this order, then it would be quite logical to consider this a property of the system itself. In other words, the components of this system are endowed with such characteristics that together they are located in order, or they at least try to.

Currently, gravity forces are considered to be the main power of influence of cosmic bodies on each other.

Let's imagine that one of the planets went wrong of the general system and began to move out of the plane. Then, when passing by the "neighboring" planets, forces, making it get into line, will immediately appear. Otherwise, apart from centrifugal and centripetal forces, a force vector perpendicular to the trajectory will appear. As a result, it will bring the planet to return to its place.

Apparently, the planets, that currently have a declination other than zero, have not yet fully established their orbits. Most likely, the planet determining the location of the ecliptic SS is Jupiter, as the largest and most massive planet. All the other planets "adjusts" to its influence.

The angle of inclination of the Earth's orbit is traditionally taken as the zero angle of inclination, and all other angles look like this:

Mercury – 7.005

Venus – 3.395

Earth– 0

Mars – 1.850

Jupiter – 1.303

Saturn – 2.489

Uranium – 0.773

Neptune – 1.770

And if we take the orbit of Jupiter as a zero angle of inclination, then the spread will noticeably decrease and will be like this:

Mercury – 5.702

Venus – 2.092

Earth – 1.303

Mars – 0.547

Jupiter – 0

Saturn – 1.186

Uranium – 0.53

Neptune – 0.467

And the "width" of the plane of motion will narrow its boundaries.

In addition to planets, the trajectories of most satellites also do not go far from the general plane.

© 2022 Global Journals

Everything seems to be simple, but I have not found an explanation of this behavior of planets for some reason, that's why I decided to write.

XIV. Conclusion

The presented mechanism of planets interaction and the physics of MP is confirmed by the properties of the fields of all terrestrial planets of the Solar System without exception.

The proposed approach opens up new opportunities in the study of phenomena occurring on and inside planets. Though cyclical processes are complex, but they are explicable and much easier to predict and interpret.

A lot of literature related to this topic was studied while preparing materials for this article (the list would take at least 2 pages), and the fact of the huge presence of mathematics along with the complete absence of a clear description of the physics of the ongoing processes was always striking. Moreover, Newton's approach was completely ignored – "I frame no hypotheses. For whatever is not deduced from the phenomena must be called a hypothesis; and hypotheses, whether metaphysical or physical, or based on occult qualities, or mechanical, have no place in experimental philosophy".

Let`s do a small digression from the topic.

Mathematics is a very useful tool for description and prediction, but it works on a certain, limited range of input parameters. At the same time, it is necessary to know the full set of these parameters, and also take into account that going beyond the known ranges can lead to qualitative changes in the properties of matter.

The use of mathematics without taking into account physics leads to a significant distorted view of the idea of reality. Overuse of substituting the properties of nature with models is like going into a virtual world that has little in common with reality. Nature did not know mathematics, creating this world; it was invented by people for their convenience. Most of the basic, practically used laws are empirical.

Naturally, further work is required to confirm and expand the understanding of the ongoing processes, as well as the development of mathematical methods, that will take into account many parameters that affect the behavior of planets, many of which are unknown up until now.

I hope that anyone who has read up to this point will take into account such a statement:

"We are much more diligent in noticing contradictions, often imaginary, and other mistakes in the writer rather than we benefit from his judgments, both correct and faulty".

Luc de Vauvenargues

I wish you all success in your endeavors.

References Références Referencias

1. O.N. Korotrsev. Astronomy. - St. Petersburg: ABC classics. 2003-736 P. ISBN 5-352-00496-8 (in Russian)
2. D.A. Kirzhnits "Extreme states of matter (ultrahigh pressures and temperatures)" Successes of physical sciences, Physics of our days. v. 104 489-508 (1971) (in Russian)
3. I. L. Iosilevsky, "Plasma polarization in massive astrophysical objects", TVT, 48:6 (2010), 804-809
4. A.L. Chizhevsky "The earthly echo of solar storms" Moscow, "Thought", 1976,367 p. (in Russian)
5. Yu.P. Malyshkov, C.Yu. Malyshkov "Periodic Variations of Geophysical Fields and Seismicity, Their Possible Connection With the Motion of the Earth's Core" // Geology and Geophysics,- 2009- v. 50- No. 2- pp. 152-172 (in Russian)
6. Tkalˇci´c H., Young M.K., Bodin T., Ngo S., and Sambridge M., The shuffling rotation of the Earth's inner core. Nature Geoscience, 2013, v. 6, 497-502.
7. Yu. I. Vitinsky "SOLAR ACTIVITY"

Second edition, revised and supplemented

Moscow "NAUKA" Main Editorial Office of Physics and Mathematics Literature 1983. (in Russian)

8. Bulletin of Kraunts. Earth Sciences. 2015. No. 3. Issue No. 27
   Z. N. Proshkina, M. G. Valitov, R. G. Kulinich, T. N. Kolpashchikova.
   Study of Tidal Variations of Gravity in the Transition Zone from the Continent to the Sea of Japan (In Russian)
9. G. P. Arnautov, E. N. Kalish, Yu. F. Stus, M. G. Smirnov, I. A. Bunin, D. A. Nosov IAE SB RAS, Novosibirsk Measurement Of Gravity Variations During Solar Eclipses On July 31, 1981 And August 1, 2008. According To The Results Of Gravimetric Observations In The Novosibirsk Region (in Russian)
10. Avsyuk Yu.N., Adushkin V.V., Ovchinnikov V.M. Complex study of the mobility of the inner core of the Earth // Physics of the Earth, 2001, No. 8. pp. 64-75. (in Russian).
11. Ovchinnikov V.M. Complex investigation of the mobility of the inner core of the Earth // Physics of the Earth, 2001, No. 8. pp. 64-75. (in Russian).
12. Sidorenkov N.S. Physics of instability of the rotation of the Earth. M., Nauka. Fizmatlit, 2002, 384 p (in Russian).
13. Kiselev, V.M. K44 Rotation of the Earth from the Archean to the present day: monograph / V.M. Kiselev. – Krasnoyarsk: Sib. feder. un-t, 2015. – 262 p. ISBN 978-5-7638-3199-3 (in Russian).
14. Melchior P. Earth tides. From the "WORLD" Moscow 1968. (in Russian)

© 2022 Global Journals

15. Vikulin, A.V. On geodynamic detector of gravitational waves / A.V. Vikulin // Space and Time. — 2014. — № 1(15). — Pp. 196-207. Fixed network address: 2226-7271provr_st1-15.2014.71 (in Russian)
16. Dehant V. Tidal parameters for Earth // Ph. Earth and Pl. Int. –1993. – vol. 76. –p. 259-315.
17. Melchior P. "Earth tides." Publisher "WORLD" Moscow 1968. (in Russian)
18. Shtokman V.B. "Equatorial counterflow in the oceans" Leningrad 1948. (in Russian)
19. Garetsky R.G. Dobrolyubov A.I. "Tidal discrete wave movements and continental drift". Geotectonics 2006, N1, pp. 3-13 (in Russian).

© 2022 Global Journals

This page is intentionally left blank

© 2022 Global Journals

Global Journal of Science Frontier Research: a Physics and Space Science
Volume 22 Issue 6 Version 1.0 Year 2022
Type: Double Blind Peer Reviewed International Research Journal
Publisher: Global Journals
Online ISSN: 2249-4626 & Print ISSN: 0975-5896

Elivination of the Contradiction between Thermodynamics and Evolution

By Etkin V. A.
Togliatti State University

Abstract- The article proves the dialectical unity of the processes of evolution and involution in biological systems, due to the simultaneous flow of which the process of their "aging" slows down, and the duration of the reproductive period increases. The strengthening of the role of such "opposite" processes as the systems become more complex is the essence of the basic law of their evolution, which eliminates "the glaring contradiction of thermodynamics with biological evolution." A more general energy-dynamic theory of biosystems is presented, which takes into account their heterogeneity with the help of additional parameters of their non-equilibrium. The theory returns to thermodynamics the concepts of force, speed and power of real processes and supplements the theory of irreversible processes by taking into account the reversible component of real processes. The unity of energy conversion processes in technical and biological systems is proved. Simpler non-entropy criteria for the evolution and involution of biosystems are proposed for each degree of freedom inherent in it. It is shown that relaxation processes in some degrees of freedom of biosystems are accompanied by the performance of work "against equilibrium" in other degrees of freedom, which is the essence of the Darwinian "struggle for existence".

Keywords: thermodynamics of biosystems, evolution and involution, processes of relaxation and metabolism, bioenergetics and survival.

GJSFR-A Classification: DDC Code: 536.7 LCC Code: QD504



Strictly as per the compliance and regulations of:



© 2022. Etkin V. A. This research/review article is distributed under the terms of the Attribution-NonCommercial-NoDerivatives 4.0 International (CC BY-NC-ND 4.0). You must give appropriate credit to authors and reference this article if parts of the article are reproduced in any manner. Applicable licensing terms are at https://creativecommons.org/licenses/by-nc-nd/4.0/.

Elivination of the Contradiction between Thermodynamics and Evolution

Etkin V. A.

Abstract- The article proves the dialectical unity of the processes of evolution and involution in biological systems, due to the simultaneous flow of which the process of their "aging" slows down, and the duration of the reproductive period increases. The strengthening of the role of such "opposite" processes as the systems become more complex is the essence of the basic law of their evolution, which eliminates "the glaring contradiction of thermodynamics with biological evolution." A more general energy-dynamic theory of biosystems is presented, which takes into account their heterogeneity with the help of additional parameters of their non-equilibrium. The theory returns to thermodynamics the concepts of force, speed and power of real processes and supplements the theory of irreversible processes by taking into account the reversible component of real processes. The unity of energy conversion processes in technical and biological systems is proved. Simpler non-entropy criteria for the evolution and involution of biosystems are proposed for each degree of freedom inherent in it. It is shown that relaxation processes in some degrees of freedom of biosystems are accompanied by the performance of work "against equilibrium" in other degrees of freedom, which is the essence of the Darwinian "struggle for existence". The connection of the mentioned law of evolution with other theories of evolution is discussed and a conclusion is made about its correctness.

Keywords: thermodynamics of biosystems, evolution and involution, processes of relaxation and metabolism, bioenergetics and survival.

I. Introduction

Despite certain successes in studying the processes of evolution of living and non-living nature from the standpoint of nonequilibrium thermodynamics [1-9], bioenergetics [10-15] and synergetics [16-20], an obvious contradiction of not only classical, but also nonequilibrium thermodynamics the nature of biological evolution ”is preserved. Interpretation of the second principle as a principle of increasing entropy imposes “thermal death” on the Universe, and degradation on any of its closed parts [21]. Attempts to consider evolution as a random process [22], the result of the emergence of “order” from “chaos” [19] and even more so “consumption of negentropy” [11] did not give satisfactory results. The very concept of “self-organization” of systems, understood as a spontaneous (not imposed from the outside) ordering of the system [21], is in “blatant” contradiction with the principle of “self-infringement of equilibrium” of classical thermodynamics. Attempts to "explain" the emergence of anti-dissipative thermo-mechanical, thermochemical, thermoelectric, thermo-magnetic, thermo-galvanomagnetic, etc. effects as manifestations of "synergetism" - the superposition of dissipative processes [2, 3].

A way out can be found from the standpoint of a more general theory of transfer and transformation processes of any forms of energy [23], developed and supplemented later in the monographs "Thermokinetics" [24] and "Energodynamics" [25]. Unlike W. Thomson's "pseudothermodynamics" [25] or L. Onsager's "quasithermodynamics" [26], this theory does not exclude from consideration any (irreversible or reversible) part of the phenomenon under study and covers the entire range of real processes - from quasireversible to extremely irreversible. This is achieved by finding the driving forces of these processes Xi and their speeds (flows Ji), directly on the basis of the law of conservation of energy, generalized to systems that are far from equilibrium. This opens up new possibilities for the application of thermodynamics to the study of biosystems and eliminates its contradictions with the laws of biological evolution.

II. Methodological Features of Energodynamics

The fundamental difference between energo-dynamics and thermodynamics of the irreversible processes (TIP) and other fundamental disciplines is its ability to consider nonequilibrium systems as a whole, without dividing them into an infinite number of elementary volumes *dV*, assumed to be homogeneous. This allows you to preserve the so-called system-forming connections inherent in the biosystem as a whole but absent in its individual parts. It is these properties that distinguish a living organism from a simple set of organs (subsystems) or mass elements that are formed during such fragmentation. In view of the inevitable disruption of the functions of individual organs when the organism is divided into volume elements, attempts to restore the system-forming properties lost at the same time by finding "suitable integrals" are doomed to failure. The realization of this circumstance was, according to A. Poincaré, “the greatest shock that physics experienced since the time of I. Newton” [28].

Author: Prof., Doctor of Technical Sciences, Togliatti State University (Russian Federation). e-mail: v_a_etkin@bezeqint.net

© 2022 Global Journals

Another methodological feature of energy dynamics is taking into account the opposite direction of processes in different parts (areas, phases, components) of a nonequilibrium system, which makes such processes irreversible even when they are quasi-static (infinitely slow). This can be verified by selecting subsystems with volumes V' and V'' in a non-uniform object of study, within which the density $\rho_i=d\Theta_i/dV$ of any extensive parameter of the system Θ_i (its mass M, number of moles k-th substances or phases N_k, entropy S, charge Θ_e, components of momentum P and its moment L, etc.) is greater or less than their average value $\overline{\rho}_i=V^{-1}\int\rho_i dV=\Theta_i/V$. Then, by virtue of the obvious equality $\Theta_i=\int\rho_i dV=\int\rho_i' dV'+\int\rho_i'' V''=\int\overline{\rho}_i dV$ we have:

$$\int(\rho_i'-\overline{\rho}_i)\,dV'+\int(\rho_i''-\overline{\rho}_i)\,dV''=0. \qquad (1)$$

Hence it follows that in a non-uniform system there are always subsystems (areas, phases, components) in which this deviation of $(\rho_i'-\overline{\rho}_i)$ and $(\rho_i''-\overline{\rho}_i)$ has the opposite sign. the law of "unity and struggle of opposites."

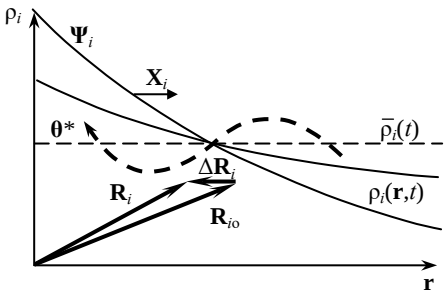

Figure 1: To the formation of the distributionmoment

Another methodological feature of energy dynamics is the refusal to use in the foundations of the theory of hypotheses, postulates, model representations and considerations of the molecular-kinetic and statistical-mechanical theory, including the hypothesis of local equilibrium by I. Prigogine, which lies at the basis of the TIP. According to this hypothesis, the volume elements of a non-equilibrium system as a whole are in local equilibrium (despite the occurrence of dissipative processes in them), so that their state can be described by the same number of variables as in equilibrium (despite the appearance of local "thermodynamic forces" X_i), and all equations of classical thermodynamics are applicable to them (despite their inevitable transition into inequalities). Contrary to this hypothesis, additional parameters of nonequilibrium of the systems under study are introduced in energy dynamics. The necessity of their introduction is proved by the "principle of definiteness", according to which the number of independent arguments Θ_i of the internal energy U as a function of the state of the system is equal to the number of independent processes occurring in it. This principle, which is proved in energy dynamics "by contradiction", requires the introduction of additional coordinates of vector relaxation processes that cause a "redistribution" of extensive parameters Θ_i over the volume of the system. To find these coordinates, consider an arbitrary system with an inhomogeneous density $\rho_i(r) = \partial\Theta_i/\partial V$ of any extensive parameter Θ_i, considered as a quantitative measure of the i-th energy carrier (Fig. 1). As follows from the figure, when ρi deviates from the average value, a certain amount Θ_i^* of the energy carrier Θ_i is transferred from one part of the system to another in the direction indicated by the dotted arrow. Such "redistribution" of the extensive value Θ_i causes a shift in the center of its value from the initial position $R_{io}=\Theta_i^{-1}\int\overline{\rho}_i r dV=0$ to the current one $R_i=\Theta_i^{-1}\int\rho_i r dV$. In this case, a certain "moment of distribution" Z_i arises:

$$Z_i=\Theta_i\Delta R_i=\int_V\left[\rho_i(\boldsymbol{r},t)-\overline{\rho}_i(t)\right]\boldsymbol{r}dV. \qquad (2)$$

with a shoulder $\Delta R_i=R_i-R_{io}$, called in energy dynamics "displacement vector" [25].

Since $\Delta R_i=0$ in a homogeneous state, the state of the nonequilibrium system as a whole is characterized in the first approximation by a doubled number of state variables Θ_i and R_i, i.e., $U=\Sigma_i U_i(\Theta_i,R_i)$. In this case, its total differential can be represented as an identity [25]:

$$dU\equiv\Sigma_i\Psi_i d\Theta_i-\Sigma_i F_i\cdot dR_i, \qquad (3)$$

where $\Psi_i\equiv(\partial U/\partial\Theta_i)_R$ is the average value of the generalized potential (absolute temperature T and pressure p, chemical μ_k, electric φ, gravitational ψ_g and other potentials); $F_i\equiv-(\partial U/\partial R_i)_\Theta$ is the forces in their general physical understanding as a gradient of the i-th form of energy with the opposite sign, the specific value of which $X_i=F_i/\Theta_i$ corresponds to the concept of thermodynamic force X_i in its "energy" representation [29].

The members of the 1st sum in expression (3) are in conditions of constancy of ΔR_i, that is, in the absence of redistribution processes. This means that the local potentials ψi in such processes change to the same extent in all parts of the system (as well as in homogeneous systems). This kind of change in state is reminiscent of a uniform fall of precipitation on an uneven surface. Their particular case is the equilibrium (reversible) processes of heat and mass transfer of the system, the work of introducing k-th substances or charge into the system, its all-round compression or expansion, etc. do not determine the heat or work of the process, as was the case in the case of reversible

© 2022 Global Journals

processes. On the contrary, from the very beginning it is recognized that the variables ψ_i are emergent quantities, that is, they can change in the general case both due to external energy exchange and due to internal sources during the course of internal spontaneous processes. This is reflected in the equations of the balance of these quantities, which are similar in meaning to the equations of the balance of entropy. This approach means refusal to calculate the external energy exchange of the system by changing the parameters Θ_i, R_i, and the transition to direct measurement of energy carrier fluxes through the boundaries of the system $J_i = \Theta_i \upsilon_i$, where $\upsilon_i = dR_i/dt$.

The second sum of identity (3), on the contrary, owes its origin to the spatial heterogeneity of the systems under study. Its terms also characterize the elementary work of the same kind as in mechanics, which is determined by the product of the resulting force of the i-th kind F_i by the displacement dR_i caused by it of the object of its application (in this case, the value Θ_i). This work is different from those included in the first sum (3). Since the forces in (3) are under the conditions of constant parameters Θ_i, then $F_i \equiv -\partial U/\partial R_i = \Theta_i X_i$, where $X_i = -\partial U/\partial Z_i$. The work $dW_i = F_i \cdot dR_i = X_i \cdot dZ_i$ performed by the forces F_i or X_i consists in the redistribution of the energy carrier Θ_i over the volume of the system. Thus, energy dynamics introduces into consideration a new class of transfer processes that have a vector (directed, ordered) character.

In the particular case of homogeneous systems ($\Delta R_i = 0$), expression (3) turns into the combined equation of the 1st and 2nd principles of classical thermodynamics of open systems in the form of the Gibbs relation [21]:

$$dU = \Sigma_i \Psi_i d\Theta_i, \tag{4}$$

where $i = 1,2,\ldots, n$ is the number of independent energy carriers of the system.

At the same time, a unique feature of energy dynamics consists in obtaining many non-trivial consequences even before its application to specific systems. The latter, as is known, requires the use of uniqueness conditions, in that knowledge of the thermophysical properties of the object, its equations of state and transfer, boundary conditions, etc. Therefore, the consequences obtained directly from identity (4), before using the uniqueness conditions, acquire the status immutable truths.

III. Finding Driving Forces and Generalized Speeds of Biological Processes in Energodynamics

In contrast to the existing linear TIP, energy dynamics introduces thermodynamic forces X_i and flows of energy carrier J_i on a more general basis of the law of conservation of energy, and not the principle of increasing entropy. In L. Onsager's "quasithermodynamics" [27] dealing with relaxation processes, their scalar analogs X_i^* and J_i^* are found from the expression for the rate of entropy increase in an adiabatically isolated system dS/dt:

$$dS/dt = \Sigma_i X_i^* J_i^*, \tag{5}$$

where $X_i \equiv \partial S/\partial \alpha_i$ is "thermodynamic force" as a measure of the deviation of some i-th parameter of the system α_i from its equilibrium value α_{io}; $J_i \equiv d\alpha_i/dt$ is the generalized rate of the i-th relaxation process.

However, since the parameters α_i are obviously absent in equilibrium thermodynamics, Onsager's theory was a kind of formalism that has nothing to do with reality. The situation changed when I. Prigogine proposed to move on to the study of the so-called "stationary irreversible processes", in which the parameters X_i and J_i acquire a vector nature and are maintained unchanged by means of "external compulsion", that is, performing work on the system dW_i" against equilibrium". In this case, the parameters X_i and J_i can be found from disciplines operating with the concept of work, by separating from dS/dt that part of it d_iS/dtthat is responsible for the "production of entropy" and is numerically equal to the work done on the system dW_i/dt. However, this required the compilation of cumbersome equations for the balance of energy, mass, charge, momentum, entropy, etc. in order to isolate from them the irreversible part of the process associated with the production of entropy d_iS/dt. This most time-consuming part of the TIP application required from the user not only an outstanding knowledge of the relevant fundamental disciplines, but also the application of a number of hypotheses, since these disciplines were deliberately limited to the consideration of conservative (nondissipative) systems and did not contain dissipative terms. This was the main reason why teaching consumer goods in higher education turned out to be unrealistic.

The situation is completely different in energy dynamics, where the sought forces X_i and fluxes J_i are already contained in its basic identity (3). At the same time, the arbitrariness inherent in TIP in the choice of driving forces and generalized speeds of transfer processes is eliminated, and the concept of force and generalized speed of the process becomes the same for all disciplines. So, if the first sum (3) includes the term TdS, which characterizes reversible heat transfer in the combined equation of the 1st and 2nd principles of classical thermodynamics, then the term $X_s \cdot J_s$, will appear in the 2nd sum (3), where $X_s = -\text{grad}\, T$ is the specific "thermomotive" force, $J_s = S\upsilon_s$ is the entropy flux. Similarly, if the first sum (3) includes the term pdV, which characterizes the reversible work of expansion, then in the second sum (3) there will appear an additional term $X_v \cdot J_v$, which characterizes the process of contraction of

© 2022 Global Journals

some and expansion of other parts systems, for example, the ventricle and atrium (X_v = –grad p,J_v is volumetric flow). In the same way, if the first sum (3) includes the term $M_k dN_k$, which characterizes the reversible transfer of the k-th substance through the boundaries of the system, then in the second sum (3) there will appear a term $X_k \cdot J_k$, which characterizes the work separation of this substance in the cell membrane or in the dialyzer (X_k = -grad M_k, $J_k = N_k v_k$ is the flow of the kth substance). Similarly, driving forces can be found in so-called "complex" systems that perform other types of work besides expansion work. So, if the term $\varphi d\Theta_e$ is included in the 1st sum (3), which characterizes the reversible work of introducing an electric charge Θ_e into the region with an average electric potential φ, then in the second sum (3) the term $X_e \cdot J_e$, creating the elementary work of separating charges in the cell membrane or in a galvanic cell ($X_e \equiv E$ = –grad$\varphi$is electric field strength, J_e - electric current).

It is easy to see that the terms of the second sum (3) can have different signs depending on whether the system is doing work or work is being done on the system. This is the fundamental difference between the proposed method and TIP, in which the $X_i \cdot J_i$terms are always positive (as well as "entropy production"). Meanwhile, in biosystems that consume free energy from the environment, $X_i \cdot J_i < 0$, which contradicts (5) and leads to absurdities such as “negentropy production”. In addition to eliminating it, this approach allows energy dynamics to study real processes, not excluding from consideration any (reversible or irreversible) component.

A significant advantage of this approach is also that it eliminates the need to draw up cumbersome equations for the balance of energy, mass, charge, momentum, entropy, etc. It is also important that energy dynamics acquires the ability to reflect on a quantitative and qualitative level the emergence of new (emergent) properties in the system. Indeed, the parameters Z_i are absent in equilibrium systems ($\Delta R_i = 0$) and their elements, and arise only when they deviate from a uniform state. Thus, energy dynamics is distinguished by taking into account not only the local nonequilibrium of the studied systems ($\nabla\psi_i \neq 0$), but also the ability to reflect the evolution of biosystems, which consists in the appearance of new properties in them. In the future, this also makes it possible to substantiate the dialectical unity of the processes of evolution and involution [30]. In addition, the unity of the dimensions of forces of various natures F_i opens up the possibility of finding their resultant $F = \Sigma F_i$, which subsequently makes it possible to significantly simplify the transport equations.

IV. Correction of the Equations of "Passive Transport" in Biosystems

In L. Onsager's “quasi-thermodynamics” [27], it is postulated that each of the fluxes J_i linearly depends on all thermodynamic acting in the system forces$X_j (j = 1,2,\ldots,n)$. The corresponding equations are called the "phenomenological laws of Onsager":

$$J_i = \Sigma_j L_{ij} X_j. \qquad (6)$$

Here L_{ij} is constant (independent of X_j) kinetic coefficients, called phenomenological and obeying the so-called "reciprocity relations" Onsager $L_{ij} = L_{ji}$. These ratios reflect, in his opinion, the interconnection of the J_i flows, which is the reason for the appearance of the aforementioned “side” effects of their “overlap”.

According to (6), the terms $J_{ij} = L_{ij} X_j$ of the flow $J_i = \Sigma_j J_{ij}$ have the same sign This is natural for the case of purely dissipative processes, when the total rate of approach of the system to equilibrium is the sum of the rates of individual relaxation processes. Meanwhile, a class of so-called "conjugate" processes is known, when some of them proceed in the direction of equilibrium, while others, on the contrary, remove it from equilibrium. Such, for example, are the Belousov-Zhabotinsky cyclic reactions called "chemical clocks" [31], "active transport" in biosystems (transfer of substances to the region of increased reaction affinity) [32], "ascending diffusion" in metals and alloys [33], the processes of concentration of matter in the Universe [30], etc. This means that at least some of the forces and flows have the opposite sign, that is, when some i-th relaxation process occurs, the system moves away from equilibrium on other, j-th degrees of freedom. In other words, along with dissipative phenomena in such systems, processes of opposite direction are observed. These include, in particular, the transfer of a substance to an area with its increased concentration (the so-called "ascending diffusion"), the phenomenon of "self-organization" of biosystems, processes of structure formation in solutions and melts. the state of equilibrium is possible only by performing useful work on it, we have to admit that in biosystems, along with external work, internal work is performed against some of the forces X_j, which is not associated with the production of entropy. Equations (6) do not take into account this specificity of systems performing useful work. This makes TIP inapplicable to biosystems.

The interpretation of the effects of superposition of heterogeneous processes in consumer goods is also erroneous. Indeed, if the flows J_i in the consumer goods are found as time t derivatives of the independent parameters α_i, then they are also independent of each other and therefore cannot interact (overlap). This is especially obvious for stationary states, when part of the "superimposed" flows simply disappears, and the effects of "superimposition" nevertheless take on a maximum value. This means that the explanation of various (thermomechanical, thermoelectric, thermochemical, electromagnetic, etc. effects) in consumer goods as a consequence of the interaction of dissimilar flows, and

© 2022 Global Journals

not the summation of forces, does not correspond to the essence of the matter.

The transfer equations from the standpoint of energy dynamics appear in a completely different light. Like classical thermodynamics, it involves any equations (state or transfer) from the outside as a kind of uniqueness condition describing the properties of specific systems. At the same time, the mathematical apparatus of thermodynamics and energy dynamics, based on the properties of the total differential of a number of state functions, does not depend on these equations. As is known from mechanics, for each independent transfer process there is a unique (resultant) force F_i, which generates this process and disappears when it stops [25]. The components of this force F_{ij} differ in their physical nature, however, unlike X_i, they have the same dimension [N]. If such (resulting) force is found, $L_{ji}X_i = 0$and laws (6) take the so-called "diagonal" form, similar to the equations of heat conduction, electrical conductivity, diffusion, etc. and does not contain cross terms with $i \neq j$ [34]:

$$J_i = L_{ii}F_i = L_{ii}\Sigma_j F_{ij}. \quad (7)$$

In this case, Onsager's reciprocity relations are fulfilled trivially ($L_{ij} = L_{ji} = 0$) and become redundant, and with them the requirement of linearity of laws (6), which is necessary for their fulfillment. This means that the phenomenological coefficients L_{ii} in (7) can be arbitrary functions of the variables Θ_i and the forces F_{ij}, while laws (6) in the general case can be nonlinear. In particular, as shown in [24], the laws of passive transport of k-th substances take the form:

$$J_\kappa = L_k X_\kappa = -L_k \nabla\mu_k, \quad (8)$$

where L_k are the coefficients of osmotic diffusion of the kth substance, depending on the fields of temperature, pressure and concentration of all independent components of the system; $\nabla\mu_k$is drop in the chemical potential on the membrane. Meanwhile, in the diffusion laws proposed by Osager himself, the sum $\nabla\mu_k$ appears, as in (5) [27]. In the diagonal form of laws (7.8), their nonlinearity, associated with the variability of the coefficients L_k, no longer interferes with the finding of superposition effects. Let us show this by the example of a biological membrane permeable to the k-th substance. Expanding the expression for the total differential of the chemical potential μ as a function of temperature, pressure and concentrations of all j-th independent components of the system (j = 2,3, ..., K), we have:

$$d\mu_k = (\partial\mu_k/\partial T)\, dT + (\partial\mu_k/\partial p)\, dp + \Sigma_j(\partial\mu_k/\partial c_j)\, dc_j. \quad (9)$$

This means that the transfer equation (6) for discontinuous media in their expanded form has the form:

$$J_\kappa = -L_k[(\partial\mu_k/\partial T)\,\Delta T + (\partial\mu_k/\partial p)\,\Delta p + \Sigma_j(\partial\mu_k/\partial c_j)\,\Delta c_j], \quad (10)$$

where ΔT, Δp, Δc_j are temperature, pressure and concentration drops of j-th substances on the membrane. The terms of this expression are the components of the resulting force $X_\kappa = -\Delta\mu_k$, the first of which is responsible for the phenomenon of thermal diffusion (transfer of matter due to temperature difference), the second - for the phenomenon of barodiffusion (transfer of matter due to pressure difference) , and the third - for the phenomenon of ordinary (concentration) diffusion. The mutual compensation of these components of the resulting force ($X_\kappa = 0$) is the reason for the onset of a stationary state, which would be more correctly called the state of "partial equilibrium". In this case, the very stationary effects such as $\Delta T/\Delta p, \Delta T/\Delta c_j$ и $\Delta p/\Delta c_j$ are obtained in energy dynamics as a result of the "superposition" of dissimilar forces, not flows.

In particular, from (10) at $J_k = 0$, regardless of the value of L_k, the well-known expression for the stationary effect of the appearance of the so-called osmotic pressure Δp in a binary isothermal system (the first component is a solvent) follows directly:

$$(\Delta p/\Delta c_2)_{st} = -(\partial\mu_1/\partial c_2)/(\partial\mu_1/\partial p), \quad (11)$$

Here Δc_2 is the stationary difference in the concentration of the solute on both sides of the biological membrane.

This made it possible to propose a method for studying superposition effects in nonlinear systems [23], which opens up the possibility of studying the kinetics of processes in biosystems that are far from equilibrium.

V. Establishing the Relationship of Chemical Reactions with Metabolic Processes

When applying the TIP to phenomena of different tensor rank and type, it turned out that, in accordance with the Curie principle (which establishes the conditions for the preservation of bonds during coordinate transformations), the generalized rate of a process in equations of the type (1) can depend only on thermodynamic forces of the same (or even) of tensor rank [1,2]. This meant that the chemical reactions described in TIP by the terms $\Sigma_r A_r d\xi_r$ (where A_r is the standard chemical affinity of the rth chemical reaction, ξ_r is the degree of its completeness), i.e., as scalar processes, cannot interact with the processes of metabolism (exchange substances) having a vector nature. There was an obvious contradiction between TIP

© 2022 Global Journals

and biology, for which it is precisely this interaction that plays a decisive role in the life processes of biosystems. To resolve this contradiction, I. Prigogine put forward the theory of "stationary conjugation", in which the fact of the presence of active transport of substances through biological membranes due to the occurrence of chemical reactions on them was explained by the specificity of stationary states with their inherent ratios between the costs of individual reagents. However, it remained unclear why the aforementioned relationship of chemical reactions with metabolic processes persisted in non-stationary regimes. The answer to this question is given by the basic identity of energy dynamics in the form (4). If the term $\Sigma_r A_r d\xi_r$ appears in its first sum, describing the r-th scalar chemical reactions in homogeneous media, then in the second sum (4) additional terms of the vector nature $\Sigma_r \boldsymbol{X}_r \cdot J_r$, reactors, Van't Hoff boxes, cell reactors, etc.), where $\boldsymbol{X}_r = -\text{grad}(A_r\xi_r)$; $A_r\xi_r$ is the local value of the chemical affinity of the r-th chemical reaction in a given cross-section of the flow reactor; J_r is the flow of reagents participating in it. Indeed, for steady-state reactions, the term $\Sigma_r A_r d\xi_r$ can be represented as $\Sigma_r[\partial(A_r\xi_r)/\partial R_m]\, dR_m = \Sigma_r F_r \cdot dR_m$, where $F_r = grad(A_r\xi_r)$ is the local value of the driving force of the r-th flow chemical reaction; R_m is the coordinate of the "reaction front" in the flow reactor. In this case, the laws of active transport of substances in membranes take the form:

$$J_m = -L_m \Sigma_r \nabla(A_r\xi_r), \qquad (12)$$

where $J_m = \Sigma_k N_k dR_m/dt$ is the flow of chemically reacting substances through the biological membrane. Thus, under conditions of spatial separation of reagents (as in a Van't Hoff box), chemical reactions acquire a directional (vector) character, which determines their interaction with metabolic processes in full accordance with the Curie principle. In the absence of the transfer of reagents in the field of intermolecular forces, chemical reactions inevitably acquire a dissipative character, which is taken into account in TIP by assigning the term $\Sigma_r A_r d\xi_r$ entirely to heat sources. This removes one of the main contradictions between consumer goods and bioenergetics [24].

VI. Criteria for the Evolution and Involution of Biological Systems

In classical and nonequilibrium thermodynamics, there are no parameters or state functions that could be quite general and strict criteria for the development (ontogenesis) and evolution (phylogenesis) of biosystems. Entropy S is not applicable for this purpose, since in biosystems exchanging energy and matter with the environment, it can change due to heat transfer or mass transfer and, on the contrary, remain unchanged if the system moves away from equilibrium or approaches it due to the performance of useful work.

As for the well-known thermodynamic potentials such as the Gibbs free energy G or Helmholtz F, they are defined, strictly speaking, only for closed homogeneous systems and are not applicable in the boundary conditions specified by the flows of matter [27]. It cannot serve as a measure of the ordering of a biosystem and its exergy (technical performance) of extended systems [35], since it depends on the energy supplied from the outside in the process of performing work, as well as on environmental parameters, and is not a function of the state of such systems.

The so-called "production" of entropy dS/dt (the rate of its increase due to irreversibility) also does not meet these requirements, since this indicator has a minimum only for stationary states of linear systems, and then only near equilibrium [36]. The way out of the situation is again prompted by energodynamics.

Let us pay attention to the second term (3), which determines the algebraic sum of all types of work (external and internal, useful and dissipative, mechanical and non-mechanical) that can be performed by the open system under study with an arbitrary number of nonequilibrium degrees of freedom $i = 1.2, \ldots n$. This sum characterizes the transformed (non-equilibrium) part of the internal energy of a spatially heterogeneous system, which we called "*inergy*" I (as opposed to the equilibrium, non-workable part of the energy $U - I$, which we named after Z. Rant (1955) "*anergy*"). Inergy I as a non-equilibrium (ordered) part of the internal energy U is a function exclusively of the parameters of the spatial inhomogeneity Z_i or ΔR_i. According to (3), a homogeneous system ($R_i = 0$) cannot perform either external or internal work, since $dW = \Sigma_i F_i \cdot dR_i = 0$. This means that the measure of the efficiency of the system is precisely the energy as an ordered part of the energy of the system. This allows us to use its change as a very general criterion for the involution of the system, i.e., its degradation as it approaches the state of equilibrium, where $I = 0$:

$$dI = -\Sigma_i F_i \cdot dR_i \leq 0. \qquad (13)$$

Here the sign $<$ refers to the relaxation processes of the system; an equal sign - to a state of balance.

On the contrary, the increase in the system's inergy I due to its removal from equilibrium under the influence of external work can serve as a criterion for its evolution:

$$dI = -\Sigma_i F_i \cdot dR_i > 0. \qquad (14)$$

According to (3), the parameters ΔR_i can be found directly from the known density fields of the corresponding energy carrier Θ_i, and other parameters

© 2022 Global Journals

of nonequilibrium $Z_i=\Theta_i\Delta R_i$ and $X_i= - \partial U/\partial Z_i$ are determined from them. All three of these parameters can serve as non-entropic criteria for the evolution of the system [36]. The advantage of these criteria over entropy is that they are able to reflect the evolution of the system for each of its inherent degrees of freedom (mechanical, thermal, baric, chemical, electrical, etc.), and not only its approach to equilibrium, but also distance from it:

$$dX_i, dZ_i, dR_i< 0 \text{ (involution)}, \quad (15)$$

$$dX_i, dZ_i, dR_i> 0 \text{ (evolution)}. \quad (16)$$

This makes it possible to detect the opposite direction of processes not only in different degrees of freedom of the system, but also in its different parts (regions, phases and components) of the system. Since in isolated systems all processes are spontaneous, such an analysis makes meaningful the concept of self-organization of individual degrees of freedom of the system, which does not contradict thermodynamics due to the absence of such for an isolated system as a whole.

VII. Description of Energy Conversion Processes in Biosystems

The specificity of energy conversion processes in biosystems is the appearance of additional inter-relationships between the rates of dissimilar processes and the flows J_i and J_j of the converted and converted forms of energy. The presence of such a connection is easy to detect on the basis of the law of conservation of energy in the form (3), from which it follows that with a complete transformation of the i-th form of energy into the j-th

$$X_i \cdot J_i = -X_j \cdot J_j. \quad (17)$$

This relationship is reflected by the differential relationships of reciprocity, which are invariably anti-symmetric for energy conversion processes [15]:

$$\partial J_i/\partial X_j=L_{ij}= -\partial J_j/\partial X_i= -L_{ji}. \quad (18)$$

This (antisymmetric) nature of reciprocity relations is due to the different sign of the work performed by the forces X_i and X_j and does not depend, as shown in [12], on whether these forces belong to even or odd functions of time. In the particular case of linear systems, relations (12) transform into the Casimir antisymmetry conditions $L_{ij} = - L_{ji}$[2,3]. This means that in the linear approximation, the phenomenological laws of energy transformation take the form:

$$J_i =L_{ij}X_i - L_{ij}X_j. \quad (19)$$

$$J_j =L_{ji}X_i - L_{ji}X_j. \quad (20)$$

Unlike (6), these laws reflect a decrease in the flow of the primary energy carrier J_i as the overcome force X_j increases and approaches the "idle" mode. Therefore, it is these equations, and not the relations (6) postulated by L. Onsager, that should be called phenomenological (i.e., based on experience) laws.

Let us consider, as an example, an element of a muscle - a fibril, which has the ability to contract when a chemical reaction starts, that is, it converts chemical energy into mechanical energy. In accordance with this, we will take the flow of substances J_r participating in a given chemical reaction as the flow of the primary energy carrier J_i, and the rate of muscle contraction as the second flow J_j. Each of these flows, in accordance with (19) and (20), depends on both forces, the first of which X_i in this case is the negative gradient of the chemical affinity of the reaction – grad($A_r\xi_r$), and the other is the contraction force of the fibril X_j. Note that in the case when the chemical reaction goes to the end ($\xi_r = 1$), the force X_i is numerically equal to the standard affinity of the chemical reaction A_r. Since chemical reactions are usually described as scalar, in the future we will operate with the modules of forces and flows.

It is more convenient to represent laws (19) and (20) in a dimensionless form that does not contain phenomenological coefficients. For example, consider the regime of the so-called "isometric muscle contraction" when $J_j = 0$, as well as "unloaded muscle contraction" when $X_j = 0$. Expressing X_{jo} and J_{jk} in terms of phenomenological coefficients (assuming their constancy), we find under conditions of constancy of forces X_i:

$$X_j/X_{jo}+ J_j/J_{jk}= 1. \quad (21)$$

To confirm the applicability of these equations to biological systems, we will use the experimentally found kinetic Hill equations, which quite accurately describe the characteristics of muscles taken from various animal species [5]. The load characteristics of the muscle propellers built on their basis are shown in Figure 2.

Curves 1, 2, 3, 4 in this figure correspond to different degrees of nonlinearity of Hill's kinetic equations. This nonlinearity is usually explained by the relationship between the rates of both processes (flows $J_j$and J_j) [4]. In linear systems, the dependence of X_j/X_{jo}on J_j/J_{jk} in linear systems is expressed by a straight line intersecting the ordinate axes at $J_j/J_{jk}= 1$ and $X_j/X_j= 1$ (curve 1). It is easy to see that it is precisely this character that follows from the kinetic laws (15). Consequently, the work of the muscle and its element, the fibril, obeys the universal laws of energy dynamics, and the modes of isometric muscle contraction and its unloaded contraction are similar to the modes of short-

© 2022 Global Journals

circuiting and no-load and of a motor or a welding transformer.

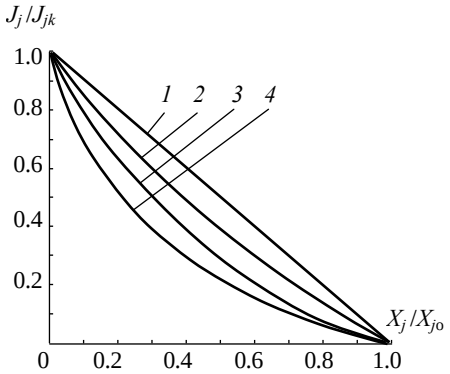

Figure 2: Load characteristic of the muscular propeller

Thus, the unity of the laws of energy transformation in technical and biological systems is revealed, which makes it possible to transfer the research results of some of them to others. At the same time, another reason for the inapplicability of consumer goods to biological energy converters is revealed. It consists in the fact that when forces and flows are found on the basis of expression (1) TIP, a limitation of the magnitude of their relative efficiency (less than 30%) arises, which is not characteristic of real energy converters (less than 30%) [37]. This limitation, however, is absent in the case of antisymmetric reciprocity relations. This confirms once again the inadmissibility of the formal transfer of the known provisions of the theory of irreversible processes to systems that perform useful work.

The independence of Eq. (21) from the structure and size of fibillae allows the theory of the similarity of muscle movers, similar to that for power plants [37]. This theory makes it possible to form a number of dimensionless criteria for the similarity of such systems. One of them, the "design criterion" $\Phi = R_{ij}R_{ji}/R_{ii}R_{jj}$, is analogous to the ratio of reactive and active resistances, known in radio engineering as the *Q*-factor of the circuit, and coincides (up to a temperature factor) with the "*Q*-factor" Φ, introduced A. Ioffe as a generalizing characteristic of thermoelectric generators (TEG). Its value fluctuates from zero to infinity ($0<\Phi<1$), increasing with a decrease in "active" resistances (from the side of dissipation forces) R_{ii} and R_{jj} and an increase in "reactive" resistances R_{ij} (from the side of the useful load). Like thermal resistances in the theory of heat transfer, these resistances depend on the properties of muscle tissues and their section, composition, etc.

Another dimensionless criterion $B = J_j/J_{jk} = 1 - X_j/X_{j0}$, called the "relative load", is composed of the boundary conditions specified by the value of the forces X_j, X_{j0} or flows J_j, J_{jk}. It changes from zero in the "idle" mode ("unloaded muscle contraction) to one in the" short circuit "mode (X_j=0). Using these criteria, expression (23) can be given the form of a criterion equation for the energy conversion process:

$$\eta_N=(1-B)/(1+1/B\Phi). \qquad (22)$$

Here $\eta_N = N_j/N_i$ is the efficiency of the process, expressed by the ratio of the output N_j and the input N_i power, and therefore we called it power. It generalizes the concept of relative efficiency η_{oi} in classical thermodynamics. This efficiency complements the well-known concept of taking into account the kinetics of the energy conversion process and therefore most fully reflects the perfection of the converter, that is, the degree to which it realizes the possibilities that nature provides.

The criterion equation (22) allows constructing a universal load characteristic expressing the dependence of this efficiency η_N on the power N_j and load B, as well as the perfection of the energy converter (Figure 3) [37]. The solid lines on it show the dependence of the efficiency η_N on the load criterion B at various values of the quality factor Φ, and the dash-dotted line shows the dependence on the load of its output power N_j. As follows from the figure, the efficiency of any power plant vanishes twice: at idle (B = 0) and in the "short circuit" mode (B = 1). In this case, the loads corresponding to the maximum efficiency and maximum power diverge the more noticeably, the more perfect the muscular mover. In the absence of any energy losses (from friction, heat release, all kinds of "leaks" of reagents, losses at idle run of the installation, etc., i.e., at $\Phi = \infty$), the power efficiency of the installation increases linearly with decreasing load, and at $B\rightarrow$ 0 reaches, as expected, unity. This case corresponds to the ideal Carnot machine, which has the highest thermodynamic efficiency. However, the power of the converter in this mode approaches zero. This indicates the existence of an optimum in terms of efficiency. A mode similar to the nominal mode of the power plant. The versatile features make it easy to find such a compromise. Thus, one more step is taken towards the approximation of the results of the theoretical analysis of the converter to reality.

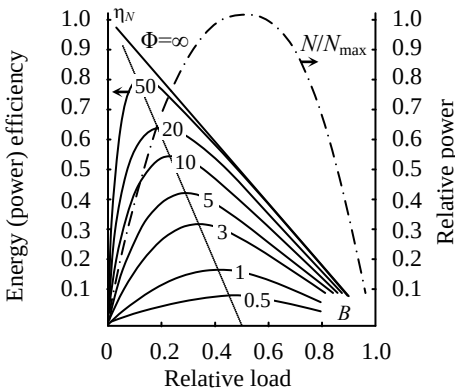

Figure 3: Universal load characteristics of linear energy converters systems

© 2022 Global Journals

VIII. The Principle of Survival" as the Basic Law of the Evolution of Biosystems

Let us apply the basic identity of energy dynamics (3) to the processes of evolution of biosystems. Introducing the missing nonequilibrium parameters X_i and ΔR_i into it allows us to obtain a number of nontrivial consequences for them [38]. One of them is the conclusion that after the isolation of the nonequilibrium system ($dU/dt = 0$) the processes of energy interconversion, obeying the condition

$$\Sigma_i X_i \cdot J_i = 0. \qquad (23)$$

Let us now take into account that a change in any parameter Z_i can be caused not only by relaxation of the i-th degree of freedom, but also by the performance of external W_i^e and internal W_i^u work by forces F_i and X_i. This circumstance can be expressed by the balance equations of the quantity Z_i, similar to the equations of entropy balance proposed by I. Prigogine:

$$dZ_i = d_e Z_i + d_u Z_i + d_i Z_i, \qquad (24)$$

where $d_e Z_i = đW_i^e/X_i$; $d_u Z_i = đW_i^u/X_i$; $d_i Z_i = đW_i^r/X_i < 0$ are the components of the total change in the parameter Z_i, caused by the performance of external W_i^e, internal W_i^u and dissipative W_i^r work, respectively.

Accordingly, the flow $J_i = dZ_i/dt$ as the generalized speed of any i-th process includes external J_i^e, reversible internal J_i^u and dissipative internal J_i^r components:

$$J_i = d_e Z_i/dt + d_u Z_i/dt + d_i Z_i/dt = J_i^e + J_i^u + J_i^r. \qquad (25)$$

In this case, condition (24) in isolated systems ($J_i^e = 0$) takes the form:

$$\Sigma_i X_i \cdot (J_i^u + J_i^r) = 0. \qquad (26)$$

According to this expression, as long as relaxation processes are going on in the system ($J_i^r \neq 0$), oppositely directed (anti-dissipative) processes of doing internal work “against equilibrium” will also take place in it. In energodynamics, this position is called the “principle of counter-directionality” of non-equilibrium processes, which can be regarded as a mathematical expressiIn this case, this principle means that the approach to equilibrium of some degrees of freedom of the system ($X_i \cdot J_i > 0$) is accompanied by the distance from it of other, j-th degrees of freedom ($X_i \cdot J_i < 0$). Hence follows the unity of the processes of evolution (complication) and involution (degradation) of non-equilibrium systems. Unlike classical thermodynamics, which cannot say anything about the rate of approach of a biosystem to equilibrium, energy dynamics allows us to raise the question of the rate of approach of the system to a state of equilibrium and the effect of the complexity of a biosystem and its remoteness from a state of equilibrium on the duration of its life. According to (3), under comparable conditions, the rate of relaxation of the system prescribed by the 2nd law of thermodynamics depends on the rate of reversible processes Jiu, with the necessity arising in it due to the principle of oppositely directed nonequilibrium processes. In this case, it is of undoubted interest to compare the speed of approaching equilibrium of two arbitrary biosystems of different complexity (with a different number of degrees of freedom).

If, in an arbitrary system, we somehow "freeze" chemical or any other processes associated with the performance of reversible internal work (that is, to direct $J_i u$ to zero), then the speed of its approach to equilibrium dU^r/dtwill become equal to

$$dI/dt = -\Sigma_i X_i \cdot J_i^r. \qquad (27)$$

Comparing (23) and (26), we find that their ratio is determined by the expression:

$$dU/dI = 1 + \Sigma_i X_i \cdot J_i^u / \Sigma_i X_i \cdot J_i^r. \qquad (28)$$

It is easy to see that this ratio can be either greater or less than one, depending on the sign of the sum $\Sigma_i X_i \cdot J_i^u$, since $\Sigma_i X_i \cdot J_i^r$ is always positive. If $\Sigma_i X_i \cdot J_i^u < 0$, that is, there is work “against equilibrium” (and forces X_i) in the system, then the speed of approach of such a system to equilibrium decreases in comparison with a system where such processes are absent:

$$dU/dI = 1 - \Sigma_i X_i \cdot J_i^u / \Sigma_i X_i \cdot J_i^r, \qquad (29)$$

and can become equal to zero when work "against equilibrium" becomes equal to work of a dissipative nature. This case corresponds to the onset of a stationary state. Among the macroprocesses in which such counter-directional changes of state take place is the so-called "active transport" of substances, which leads to the accumulation of reagents with a relatively high Gibbs energy in the corresponding organs. The same are the already mentioned processes of "ascending diffusion" in alloys, as well as the so-called "conjugate chemical reactions". Some of them, like the Belousov-Zhabotinsky cyclical reactions ("chemical clocks") or the process of the circulation of matter in the Universe, can continue indefinitely. All processes of this kind require a certain organization of the system and therefore arise only at a certain stage of their evolution. The life span of biosystems, as well as their reproductive period, depends on their intensity, which affects the evolution of the entire subsequent population of this type of bioorganisms.

© 2022 Global Journals

Here lies the key to understanding the general direction of the evolution of a biological system, understood as a transition from simple to complex. This direction of evolution is not something imposed by the "higher mind" or Darwinian "struggle for existence" - it is a consequence of purely physical reasons reflected in the energodynamic principle of "opposite direction" of nonequilibrium processes. Such are any processes leading to the ordering of the system, the acquisition of new properties by it (an increase in the number of degrees of freedom), the complication of the structure, etc.

At the same time, the "postponement" of the onset of equilibrium in biosystems, achieved due to the occurrence of reversible processes in them, is so close to the Darwinian idea of "struggle for existence" that it can also be called the "principle of survival" for clarity. This principle can be formulated briefly in the form of a statement: "Evolutionary processes occurring in biological systems are directed towards increasing the duration of their life." This provision is so general that it can be considered the basic law of biological evolution.

This law does not at all contradict classical thermodynamics and its second principle, which removes their "flagrant contradiction" noted by I. Prigogine. At the same time, he debunks the myth of “the emergence of order from chaos” [20], since it becomes clear that maintaining “order” requires the expenditure of work, the absence of which in isolated systems is inevitably accompanied by a decrease in their ordered energy. In other words, "order" in any part of the system (subsystem) arises not from ha-os, but due to a higher order in other parts of the system or in the surrounding force fields. For biological systems, these are radiation fields, flora and fauna, which have ordered forms of energy. This radically changes our worldview.

IX. Energodynamics and Darwinian Theory of Evolution

Let us now show that the well-known "triad" of Darwin's doctrine of evolution [] - adaptability, variability and heredity - are a consequence of the above formulated energy-dynamic law of evolution. Considering biological objects as non-equilibrium systems immersed in a nonequilibrium environment, energy dynamics deepens our understanding of equilibrium. It is one thing when both the system and the environment are homogeneous (that is, they lack both long-range and short-range force fields). Then their equilibrium corresponds to the termination of processes both in the environment and in the system. The condition for such external equilibrium is the equality of the corresponding potential (temperature, pressure, chemical, electrical, etc. potentials) in all parts of the system and the environment. The resulting forces X_i in this case are equal to zero, which corresponds to inaction. It is with this kind of external equilibrium that classical thermodynamics deals. However, the concept of force was alien to classical thermodynamics. Therefore, she distorted the meaning of the concept of equilibrium as an equal action of forces, replacing it with inaction (the absence of any processes).

A different kind of state occurs when both the system and the environment are heterogeneous and the thermodynamic forces X_i in them are nonzero. Then the external equilibrium means their equal action, which does not exclude the occurrence of internal processes in the system and in the environment. Thus, external balance does not at all mean the presence of complete (external and internal) balance. It is with this case that the thermodynamics of biological and ecological processes deals. Equilibrium establishment processes of this kind are adiabatic and therefore do not obey the entropic criteria of evolution and equilibrium. Meanwhile, it is these processes that are responsible for the evolution of biological systems in the direction of establishing a balance between them and the environment. This is Darwinian adaptability in its energy-dynamic understanding. In the course of such processes, the body acquires new properties (new degrees of freedom), which were absent in it in a state of internal balance. The lack of equilibrium with the environment is manifested in the presence of thermodynamic forces X_i, which generate a change in the state of both the system and its environment. This is the thermodynamic reason for the variability of organisms. The result of this process is the equality of the forces X_i in the system and the environment, and not their internal balance. Striving for such a balance by no means deprives the biosystem of the ability to perform useful external work and to internal interconversion of energy.

As follows from the principle of survival, partial equilibrium lengthens the time the system remains in a nonequilibrium state. Then, in the presence of inevitable mutations of the hereditary code, the degree of their probability increases. Thus, better "adapted" individuals acquire an advantage in the transmission of gene information. This is the energy-dynamic nature of heredity. It is characteristic that all three named basic provisions of the Darwinian doctrine of evolution turn out to be a consequence of a single criterion of "survival" - the minimum speed of the system approaching equilibrium.

In the "theory of neutrality" of evolution (L. Blumenfeld, 1977), energodynamics can explain the mechanism of elimination (preservation of random genetic changes), since the probability of this process from the standpoint of the "principle of survival" increases with the lengthening of the life of a better adapted (closer to external equilibrium) individual. In the theory of “jump-like evolution” (“punctualism”), energy

© 2022 Global Journals

dynamics can explain the jump-like increase in the rate of change of genes, since it recognizes the inevitability of "bifurcation" (branching of process trajectories) with distance from equilibrium. In the theory of "molecular evolution", energy dynamics is able to explain the change in the composition of living organisms in ontogenesis, since natural aging is accompanied by a decrease in their specific energy. Thus, energodynamics can serve as a touchstone for any of the evolutionary theories.

X. Conclusion

1. The reason for the "glaring contradiction" between equilibrium thermodynamics and the theory of biological evolution is the absence in its equations of time as a physical parameter and its inability to take into account the kinetics of real processes. This contradiction persists in the theory of irreversible processes, which excluded from consideration the reversible part of such processes.
2. Description of the state of nonequilibrium systems requires the introduction of intense X_i and extensive Z_i parameters of spatial in homogeneity, characterizing their deviation from equilibrium. These parameters have a number of advantages over entropy, reflecting the approach to equilibrium and the distance from it both for the system as a whole and for each of its inherent degrees of freedom separately.
3. The introduction of these parameters of spatial heterogeneity into thermodynamics reveals the occurrence in nonequilibrium systems of reversible processes of redistribution of energy carriers over the volume of the system and their opposite direction, reflecting the dialectical unity of opposites.
4. The use of these parameters X_i, Z_i and R_i as criteria for their evolution and involution reveals the inevitability of the simultaneous occurrence of these processes in different parts (regions, phases and components) of the nonequilibrium system and the interconversion of energy in them, accompanied not only by its relaxation, but and doing work "against equilibrium."
5. The processes of performing external and internal work in the muscle tissues of living organisms are subject to the same laws as the processes of energy conversion in various thermal and non-thermal machines. This makes it possible to create a theory of the similarity of muscular energy converters, which facilitates the selection of the optimal modes of their activity.
6. The course of oppositely directed processes in biological systems slows down their approach to equilibrium and makes it possible to formulate the "principle of their survival", according to which their self-organization leads to an increase in the duration of their life. This provision is so general that it can be considered the basic law of biological evolution.
7. The energy-dynamic theory of evolution confirms the main provisions of the Darwinian theory of evolution (adaptability, variability and heredity), explaining them, however, by natural causes. Thus, any contradictions between thermodynamics and the theory of biological evolution are eliminated.

References Références Referencias

1. *Де Groot S., Masur P.* Non-equilibrium Themdynmics. Amsterdam, 1962.
2. *Haase R.* Themdynmik der Irreverdiblen Processe. Darmstadt, 2963.
3. *Katchalsky A., Curran PF.* Nonequilibrium Thermodynamics in Biophysics. Harvard Univ. Press, Cambridge, 1967.
4. *Keplen SR., Essig E*. Bioenergetics and linear thermodynamics of irreversible processes. Moscow: Mir, 1968 (in Russian).
5. *Prigogine I*. Introduction to Thermodynamics of Irreversible Processes. -Springfield, 1955.
6. *Rudenko AP.* The theory of self-development of open catalytic systems. M., Science, 1969(in Russian).
7. *Rubin AB.* Thermodynamics of biological processes. Moscow State University, 1984(in Russian).
8. *Gladyshev G*. Thermodynamics Theory of the Evolution of Living Beings. New York: Nova Science Publishers, Inc., 1997(in Russian).
9. *Demirel Y*. Nonequilibrium Thermodynamics. Transport and Rate Processes in Physical, Chemical and Biological Systems, 3rd ed. Amsterdam, 2014.
10. *Driesch H.* Die Biologie als selbständige Grundwissenschaft, Leipzig 1893.
11. Schrödinger E. Was is Leben? München, 1951.
12. *Bauer E. Theoretical biology.* M.- Spb.1935(in Russian).
13. *Blumenfeld LA.* Problems of Biological Physics. M., Nauka, 1977(in Russian).
14. *Shnol SE.* Physicochemical factors of biological evolution. M., Science, 1979(in Russian).
15. *Antonov VF*. Physics and biophysics. Ed. 3rd. M.Media, 2010(in Russian).
16. *Nicolis G., Prigogine I.* Self-organization in nonequilibrium systems: From dissipative structures to ordering through fluctuations. Moscow: Mir, 1979(in Russian).
17. *Haken G.* Synergetics. M., Mir, 1980(in Russian).
18. *Berger P., Pomo I., Vidal K.* Order in chaos. Moscow: Mir, 1991(in Russian).
19. *Danilov YA., Kadomtsev BB.* What is synergetics. // Nonlinear waves. Self-organization-nation. Moscow: Nauka, 1983(in Russian).
20. *Prigogine I*. Order and Haos, Man's new dialog with Nature. London, 1984.

© 2022 Global Journals

21. *Bazarov IP*. Thermodynamics. Edn4. M., Vysshaya shkola, 1991 (in Russian).
22. *Boltzmann L.* Selected Works. Moscow: Nauka, 1984
23. *Etkin V. A.* Synthesis and new applications of the energy transfer and energy conversion theories. (Summary of thesis for doct. techn. sciences. //Moscow: State Techn. Univ. Press, 1998. (in Russian).
24. *Etkin V.* Thermokinetics (Synthesis of Heat Engineering Theoretical Grounds).Haifa, 2010; *Etkin VA*. Thermokinetics (thermodynamics of nonequilibrium processes of transfer and transformation of energy). Togliatti, 1999(in Russian).
25. *Etkin V.* Energodynamics (Thermodynamic Fundamentals of Synergetics). N. Y., Lulu Inc., 2011;*Etkin VA*. Energodynamics (synthesis of theories of energy transfer and transformation). St. Petersburg, Science, 2008(in Russian).
26. *Tomson W.* Mathematical and physical papers. Cambridge, 1882. V.1.
27. *Onsager L*. Reciprocal relations in irreversible processes. //Phys. Rev., 237(14)1931.405-426;238 (12)1931.2265-2279.
28. *Poincare H*. Revue generale des Sciences pures et appliquees, 19(1908).386-402.
29. *Gyarmatil*. Non-Equilibrium Thermodynamics. Field Theory and Variation Principles. Springer–Verlag, 1970.
30. *Etkin V.* On the Dialectic Unity of Evolution and Involution**.** //Global Journal of Science Frontier Research: A Physics and Space Science. 20(10)2020.9-16.
31. *Zhabotinsky AM.* Concentration fluctuations. Moscow: Nauka, 1974(in Russian).
32. *Prigogine I., Defey R.* Chemical thermodynamics. Novosibirsk: Science, 1966(in Russian).
33. *Shumon PP.* Diffusion in solids. Moscow: Metallurgy, 1966(in Russian).
34. *Etkin V.A.* Uniqueness of driving forces of irreversible processes. // Russian Journal of Physical Chemistry, 63(6). 1989. 918-919 (translated from Zhurnal Fizicheskoi Khimii, 63(1989). 1660-1662).
35. *Etkin V.A.* On the uniqueness of the driving forces of irreversible processes.//Journal. physical Chemistry, 63 (1989) 1660-1662(translated from Zhurnal Fizicheskoi Khimii, 66(5)1992. 1205 -1212.
36. *Etkin VA*. New **C**riteria of Evolution and Involution of the Isolated Systems. //International Journal of Thermodynamics, 21(2), 2018,120-126.
37. *Etkin VA*. Similarity Theory of Energy Conversion Processes.// International Journal of Energy and Power Engineering, 8(1). 2019.4-11.
38. *Etkin V.* Verifiable Forecasts of Energodynamics.// Scientific Israel- Technological Advan-tages", 16(1,2)2014.130-137; *Etkin VA.* Non-trivial consequences of energy dynamics (Collection of articles). Lulu Inc., 2020.
39. *Etkin V.* Principle of non-equilibrium processes counter directivity. //Reports by independent authors, 37(2016), 86 – 92.
40. *Darwin Ch.* On the Origin of Spices by Means of Natural Selection, or the Preservation of Favoured Races in the Struggle for Life . London: John Murra, 1859.

© 2022 Global Journals

Global Journal of Science Frontier Research: a
Physics and Space Science
Volume 22 Issue 6 Version 1.0 Year 2022
Type: Double Blind Peer Reviewed International Research Journal
Publisher: Global Journals
Online ISSN: 2249-4626 & Print ISSN: 0975-5896

Emerging Trends in Transmission Electron Microscopy for Medical Applications

By Dr. Alla Srivani, Gurram Vasanth, Dr. GVS Subbaroy Sharma, M. Srinivasa Rao, Dr. P Ramesh, Dr. A Raghavendra & Dr. G Krishna Kumari

East European University

Abstract- This paper is an overview of imaging methods used for research and diagnosis that appear in the literature. There are several types of scientific research and imaging modalities, including photography, microscopy, ultrasound, X-ray, computed tomography (CT), magnetic resonance imaging (MRI), and positron emission tomography (PET). The type of images used will depend on the part of the body the researcher wants to see in the image and the types of images readily available to the patient. For many years, medical imaging has played an important role in the early detection, diagnosis, and treatment of cancer and other diseases. In some cases, medical imaging tests are the first step in preventing the spread of cancer by detecting it early, and in many cases the cancer can be cured or eliminated. CT scans, MRIs, ultrasounds and X-ray imaging are very important tools in fighting various diseases. Medical imaging is also used to create accurate computer models of body systems, organs, tissues, and cells used in anatomy and physiology classes in medical school.

Keywords: medical physics, TEM, imaging, acceleration voltage, vacuume and medical imaging.

GJSFR-A Classification: DDC Code: 621.388 LCC Code: TK6630



Strictly as per the compliance and regulations of:

© 2022. Dr. Alla Srivani, Gurram Vasanth, Dr. GVS Subbaroy Sharma, M. Srinivasa Rao, Dr. P Ramesh, Dr. A Raghavendra & Dr. G Krishna Kumari. This research/review article is distributed under the terms of the Attribution-NonCommercial-NoDerivatives 4.0 International (CC BY-NC-ND 4.0). You must give appropriate credit to authors and reference this article if parts of the article are reproduced in any manner. Applicable licensing terms are at https://creativecommons.org/licenses/by-nc-nd/4.0/.

Emerging Trends in Transmission Electron Microscopy for Medical Applications

Dr. Alla Srivani [α], Gurram Vasanth [σ], Dr. GVS Subbaroy Sharma [ρ], M. Srinivasa Rao [Ω], Dr. P Ramesh [¥], Dr. A Raghavendra [§] & Dr. G Krishna Kumari [χ]

Abstract- This paper is an overview of imaging methods used for research and diagnosis that appear in the literature. There are several types of scientific research and imaging modalities, including photography, microscopy, ultrasound, X-ray, computed tomography (CT), magnetic resonance imaging (MRI), and positron emission tomography (PET). The type of images used will depend on the part of the body the researcher wants to see in the image and the types of images readily available to the patient. For many years, medical imaging has played an important role in the early detection, diagnosis, and treatment of cancer and other diseases. In some cases, medical imaging tests are the first step in preventing the spread of cancer by detecting it early, and in many cases the cancer can be cured or eliminated. CT scans, MRIs, ultrasounds and X-ray imaging are very important tools in fighting various diseases. Medical imaging is also used to create accurate computer models of body systems, organs, tissues, and cells used in anatomy and physiology classes in medical school.

Keywords: medical physics, TEM, imaging, acceleration voltage, vacuume and medical imaging.

I. Introduction

Scientific and diagnostic imaging is medical imaging used to create images of parts or the entire human/animal body for various clinical purposes, such as: B. Medical procedures and diagnostics or medicine, including the study of normal anatomy and function. Medical imaging in a broader sense is the subset of biological imaging that includes photography, microscopy, ultrasound, radiography, computed tomography (CT), magnetic resonance imaging (MRI), and positron emission tomography (PET) included. Detailed anatomical and physiological images of various Medical organs and tissues of the body for research, diagnostic and therapeutic purposes are used.

This post provides a detailed overview of medical imaging to outline past, present, and future aspects of the field.

Author α σ ρ Ω ¥ § χ: Vasireddy Venkatadri Institute of Technology, East European University, Mallareddy Engineering College (MREC-A), Annamalai University, Mallareddy Engineering College, NRI Engineering college. e-mail: vaniraghava2751982@gmail.com

II. Methodology

Acceleration Voltage is determined from 8 KV to 16 KV at different vacuum conditions for Advanced Materials

Sl.No	Vacuume (Kv)	Accelerating Voltage (Kv)
1	7	8
2	8	10
3	12	14
4	14	16

The overall structure of an electron microscope is similar to that of an optical microscope.

Sl. No	Vacuume (Kv)	Accelerating Voltage (Kv)
1	7	8
2	8	10
3	12	14
4	14	16

Light is replaced by electrons, and glass lenses are replaced by electromagnetic and electrostatic lenses.

Electron microscopes have an electron optical lens system similar to the glass lens in an optical microscope.

Mainly he has two types of electron microscopes. Between Transmission Electron Microscopy (TEM) and Scanning Electron Microscopy (SEM), TEM is the most commonly used. Electron microscopy allows the visualization of structures that are normally invisible to light microscopy. Electron microscopy can be used to visualize microorganisms, cells, large molecules, biopsy specimens, metals, and crystals. Modern electron microscopes use special digital cameras and frame grabbers to take electron micrographs and capture images.

Transmission electron microscopy is a technique developed to obtain much greater magnification, or detail, of specimens than conventional light microscopy. At the specimen it passes through, an image is formed from the interaction of electrons transferred through the sample. The image is magnified and focused onto an imaging device such as a

© 2022 Global Journals

fluorescent screen, a sheet of photographic film, or a sensor such as a CCD camera. , which is roughly analogous to a biological optical microscope.

TEM consists of an illumination system, a sample stage, an imaging system, and a vacuum system. Transmission electron microscopy is an important analytical method in physical, chemical and biological sciences.

TEM has applications in cancer research, virology, materials science, pollution, nanotechnology, and semiconductor research.

The seven most commonly used medical imaging modalities today are X-ray (that is, conventional radiography), CT, PET, SPECT, OI, US, and MRI. The first two (X-ray and CT) use high-energy photons to create 2D or 3D image sets of biological anatomy.

In contrast, nuclear medicine procedures such as PET and SPECT use small amounts of radiotracers involved in metabolic and signaling pathways in vivo and their distribution and abundance can be measured by the emitted radiation.

Finally, MRI, OI, and US use non-ionizing radiation for diagnostic purposes. H. Mechanical waves (US) in the MHz range, optical (OI), or magnetic fields (MRI) oscillating in the MHz range.

In general, most of the imaging modalities mentioned above, as well as therapeutic approaches, use electromagnetic radiation over a wide range of frequencies or energies. These parameters partially determine penetration depth, spatial resolution, specific absorption rate, etc. This affects the sensitivity and specificity of the medical imaging modalities used.

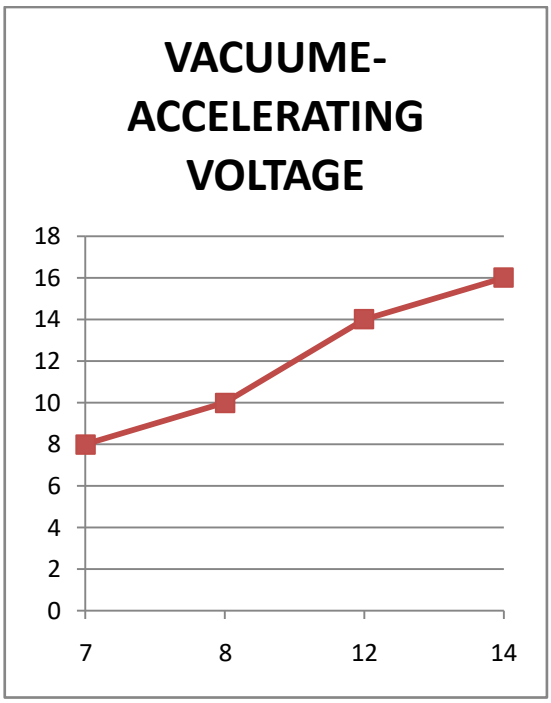

Fig. 1

III. Conclusion

Optical imaging (OI) often uses light from lasers or LEDs and allows imaging with high spatial resolution and good contrast, but the depth of tissue penetration is very limited. For these reasons, many optical imaging applications target cultured or fixed cell samples.

light microscopy is not only the method of choice in histopathology, but also the study of cell development and cell fate, gene expression analysis, cell-pathogen.

Interactions, cellular and intracellular signaling, metabolism, intercellular Also used for interaction analysis. Routine medical applications of optical imaging of target surfaces and transparencies of the human body (eg, dermatology, ophthalmology, various endoscopic procedures and dentistry).

Nevertheless, a number of additional optical imaging modalities have been developed to image normal and diseased patients and animals in clinical and pre-hospital settings. The OI is primarily used to image human skin, eyes, and other accessible parts of the body such as teeth, mucus, throat, and colon.

For this purpose, multi photon imaging and optical coherence tomography (OCT) are the most commonly used OI techniques. Moreover, the use of highly specific markers such as fluorescent tags and novel imaging probes facilitates the adoption of His OI for in vivo imaging.

3D optical imaging techniques include two-photon microscopy, OCT, light field microscopy, diffuse optical tomography, optical projection tomography, light sheet microscopy, and optical imaging. Acoustics is included. An approach that uses laser light for illumination and contrast is used in conjunction with ultrasonic detection. Super-resolution microscopy of OI was recently proposed, allowing non-invasive interrogation with a spatial resolution of less than 10 nm.

References Références Referencias

1. Keevil SF. Physics and medicine: a historical perspective. Lancet. (2012) 379:1517–24. doi: 10.1016/S0140-6736(11)60282-1.
2. Townsend D, Cheng Z, Georg D, Drexler W, Moser E. Grand challenges in biomedical physics. Front Physics. (2013). doi: 10.3389/fphy.2013.00001
3. Moser E, Laistler E, Schmitt F, Kontaxis G. Ultra-high field NMR and MRI—the role of magnet technology to increase sensitivity and specificity. Front Phys. (2017) 5:33. doi: 10.3389/fphy.2017.00033
4. Schnerr RS, Jansen JFA, Uludag K, Hofman PAM, Wildberger JE, van Oostenbrugge RJ, et al. Pulsatility of lenticulostriate arteries assessed by 7 tesla flow MRI—measurement, reproducibility, and applicability to aging effect. Front Physiol. (2017) 8:961. doi: 10.3389/fphys.2017.00961.

© 2022 Global Journals

5. Sarracanie M, Salameh N. Low-field MRI: how low can we go? A fresh view on an old debate. Front Phys. (2020) 8:172. doi: 10.3389/fphy.2020.00172
6. Stanciu SG, Silien C, Bianchini P. Editorial: advances in label free tissue imaging with laser scanning microscopy techniques. Front Phys. (2020) 8:17. doi: 10.3389/fphy.2020.00017
7. Cai F, Gao M, Li J, Lu W, Wu C. Compact dual-channel (Hyperspectral and Video) endoscopy. Front Phys. (2020) 8:110. doi: 10.3389/fphy.2020.00110
8. Oelschlegel AM, Goldschmidt J. Functional neuroimaging in rodents using cerebral blood flow SPECT. Front Phys. (2020) 8:152. doi: 10.3389/fphy.2020.00152
9. Jones JS, Small DM, Nishimura N. In vivo calcium imaging of cardiomyocytes in the beating mouse heart with multiphoton microscopy. Front Phys. (2018) 9:128. doi: 10.3389/fphys.2018.00969
10. Moran CM, Thomson AJW. Preclinical ultrasound imaging—a review of techniques and imaging applications. Front Phys. (2020) 8:124. doi: 10.3389/fphy.2020.00124
11. Goudot G, Mirault T, Khider L, Pedreira O, Cheng C, Porée J, et al. Carotid stiffness assessment with ultrafast ultrasound imaging in case of bicuspid aortic valve. Front Physiol. (2019) 10:1330. doi: 10.3389/fphys.2019.01330
12. Schlemmer A, Berg S, Lilienkamp T, Luther S, Parlitz U. Spatiotemporal permutation entropy as a measure for complexity of cardiac arrhythmia. Front Phys. (2018) 6:39. doi: 10.3389/fphy.2018.00039
13. Karhula SS, Finnil, ä M. A., Freedman JD, Kauppinen S, Valkealahti M, Lehenkari P, et al. Micro-scale distribution of CA4+ in ex vivo human articular cartilage detected with contrast-enhanced micro-computed tomography imaging. Front Phys. (2017) 5:38. doi: 10.3389/fphy.2017.00038

© 2022 Global Journals

This page is intentionally left blank

© 2022 Global Journals

Global Journal of Science Frontier Research: a Physics and Space Science
Volume 22 Issue 6 Version 1.0 Year 2022
Type: Double Blind Peer Reviewed International Research Journal
Publisher: Global Journals
Online ISSN: 2249-4626 & Print ISSN: 0975-5896

Gauge-Theoretic Study of Kundt Tube Experiment and Spontaneous Symmetry Transitions

By Tsutomu Kambe

University of Tokyo

Abstract- In the Kundt's experiment of acoustic resonance in closed tubes, two characteristic lengths were observed: one is the wave-length of the sound waves in resonance and the other the scale of dust striation. The latter has remained unresolved for its formation mechanism. Based on the Fluid Gauge Theory proposed recently by the author, formation mechanism of the dust striation is studied. When the sound is weak enough, the striation is unobserved. Once the wave intensity exceeds a threshold value, dust striations are formed. Formation of the dust striation is understood as a spontaneous transition of symmetry in the acoustics. According to the Theory, there is a transition of stress field within the fluid flow. Whereas the stress field is isotropic before transition, it becomes anisotropic after the transition. This is analogous to the spontaneous symmetry breaking known in the field theory. Lagrangian structures of both systems are verified to be analogous either.

GJSFR-A Classification: *DDC Code: 813.54 LCC Code: PS3564.I362*



Strictly as per the compliance and regulations of:

© 2022. Tsutomu Kambe. This research/review article is distributed under the terms of the Attribution-NonCommercial-NoDerivatives 4.0 International (CC BY-NC-ND 4.0). You must give appropriate credit to authors and reference this article if parts of the article are reproduced in any manner. Applicable licensing terms are at https://creativecommons.org/licenses/by-nc-nd/4.0/.

Gauge-Theoretic Study of Kundt Tube Experiment and Spontaneous Symmetry Transitions

Tsutomu Kambe

Abstract- In the Kundt's experiment of acoustic resonance in closed tubes, two characteristic lengths were observed: one is the wave-length of the sound waves in resonance and the other the scale of dust striation. The latter has remained unresolved for its formation mechanism. Based on the Fluid Gauge Theory proposed recently by the author, formation mechanism of the dust striation is studied. When the sound is weak enough, the striation is unobserved. Once the wave intensity exceeds a threshold value, dust striations are formed. Formation of the dust striation is understood as a spontaneous transition of symmetry in the acoustics. According to the Theory, there is a transition of stress field within the fluid flow. Whereas the stress field is isotropic before transition, it becomes anisotropic after the transition. This is analogous to the spontaneous symmetry breaking known in the field theory. Lagrangian structures of both systems are verified to be analogous either.

I. Introduction

In the middle of the 19th century, August Kundt carried out acoustic experiments to estimate sound speeds in various gases and materials, in laboratories very innovatively, from wave phenomena of sound resonance excited in closed tubes and published those observations in 1866 [1]. In this paper he reported an anomaly which has remained unresolved for a long time. The issue was as follows: there existed two characteristic scales, observed in his experiment. One is the wave-length of the sound wave in resonance within the tube, which was just the one being sought in his experiment. However embarrassingly to him, another characteristic scales were observed in his experiment, *i.e.* the dust striations formed in the resonant standing waves which were characterized with much shorter scales. Formation mechanism of the second dust striation has remained unresolved, *i.e.* without being given an appropriate interpretation on its physical mechanism.

After more than eighty years since then, in 1955 Robert Carman wrote a very informative review [8] for teachers of physics and explained compactly the *Kundt Tube Dust Striations*. Showing a beautiful sketch of striations, he noted that very few know what to say when a student asks why the dust figures in the tube are striated.

Most frequently offered explanations were that those were caused by higher harmonics of the resonant mode. But this was refuted by Dvorak [2] already in 1874. He argued that a very high overtone would be necessary to explain the observed wavelength of about 0.8cm for a typical resonant wavelength of about 11cm of Kundt's experiment. It is unconceivable in mechanics to assume that only one overtone is sufficiently stronger than any others to produce such distinct ripples.

Author: *Former Professor, University of Tokyo, Hongo, Bunkyo, Tokyo, Japan. e-mail: kambe@ruby.dti.ne.jp*
The main part of present study was presented orally at the Physics-2022 held at San Francisco, USA, on 18 - 21 July 2022.

© 2022 Global Journals

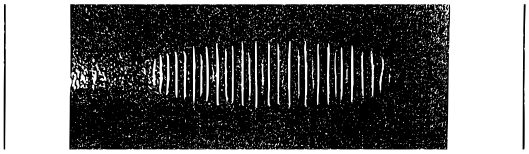

Fig. 1: Experimental picture of dust striation from Fig.7 of [7]. The two vertical bars on both sides are the part of Fig.7, signifying the length between them corresponds to $\frac{1}{2}\lambda_{\rm r}$.

In this regard, the experimental studies of Andrade ([5]∼[7]) are particularly noteworthy. Those were carried out prior to Carman's review (1955). In 1931, since it had passed already 65 years from the Kundt's work [1], the experimental devices of Andrade were renewed significantly with using electric oscillators and vibrating diaphragms, enabling steady-state conditions maintained during the observation of Andrade. Thus he was able to lower the resonance frequencies to 100 to 2300 cps (compared with previous values, 2500 $\sim$ 4000). As viewed from the present time, his key findings were two:

(i) A certain minimum velocity of the air particles is required for the ripple formation;

(ii) The inception of ripple formation corresponds to a spontaneous breakdown of the physical state of vortex-free flow in the tube.

The first signifies that there is a critical intensity of sound for the formation and the second implies that the ripple formation resulted from a spontaneous symmetry breaking. These findings are reviewed in the present study from the fluid-dynamic point of view on the basis of the Fluid Gauge Theory [13]. This is one of the main issues.

Kundt's experiment attracted interest of Rayleigh [4], who proposed that, within a sinusoidal standing wave excited powerfully in a pipe, steady streaming is generated in addition to the periodic oscillation by the action of the nonlinear mean Reynolds stress in collaboration with the dissipative dragging action of viscosity. Andrade [6] presented experimental photographs showing this steady streaming (Fig. 5(a)). In these backgrounds, Lighthill showed a diagram of the steady streaming ([11], Fig. 85) consisting of four cells of closed streamlines within a wavelength $\lambda_{\rm r}$, noting that this explains why dust particles tend to accumulate at the nodes and there are two nodes within $\lambda_{\rm r}$.

However, it is noted by Andrade [7] that the steady streaming is observed only under prolonged intensive sound waves. Lowering the intensity, but still above a critical intensity, he observed ripple-like striation with using minute cork particles. FIG.1 is its photo from [7], showing a number of ripple waves within a half wavelength $\frac{1}{2}\lambda_{\rm r}$. Kundt himself [1] used a number of minute Lycopodium dried spores as the dust particles, and described the structure of lateral striation as *ribs*, which were caused by the air in motion, not by other causes. Since then, very little is known about its formation mechanism.

The Kundt-tube experiments show us various interesting acoustic phenomena. Therefore, the present approach investigates the Kundt-tube experiments from diverse aspects: (a) *fluid-mechanically*, concerning stress fields, transition from a stress field to another, oscillatory boundary layers over the tube walls, or steady streaming as a nonlinear effect; (b) *gauge-theoretically.* concerning Lagrangians, gauge fields, or spontaneous symmetry transition.

First in the sections II and III, various phenomena observed in the experiments are presented compactly and then reviewed from a gauge-theoretic point of view, emphasizing that a transitional change of acoustic phenomena may be interpreted as spontaneous symmetry

© 2022 Global Journals

transition. Then in § IV, the *fluid gauge theory* is presented for its theoretical interpretation. Computer simulations are also presented to visualize non-trivial acoustic phenomena occurring within the flow fields in § III and IV, helped by the experimental picture (FIG.2) of the rotational eddy field visualized by Andrade [7].

In the flow fields studied here, there are three types of stress fields (§ IV-C) which are playing important roles in the acoustic phenomena: (A) *isotropic* stress field $\sigma^{jk}_{\rm I}(x^\nu)$ (non-dissipative), (B) *anisotropic* stress $\sigma^{jk}_{\rm A}(x^\nu)$ (non-dissipative), and (C) *viscous* stress $\sigma^{jk}_{\rm vis}(x^k)$ (anisotropic and dissipative). Traditional Eulerian fluid system is governed by the isotropic pressure stress $\sigma^{jk}_{\rm I}$. Depending on whether the stress field is isotropic $\sigma^{jk}_{\rm I}$ or anisotropic $\sigma^{jk}_{\rm A}$, the fluid current field $j^\mu(x^\mu)$ changes its character drastically. In fact , this is one of the main themes of the present study. The third viscous stress $\sigma^{jk}_{\rm vis}$ plays an important role in the Navier-Stokes system.

The viscous stress tensor has anisotropic components as well. The anisotropic components of viscous stress play essential roles in the study of fluid mechanics. Turbulence theory learns those and takes advantage of the anisotropic property of viscous stress. However, there exists an essential difference between the two fields of the viscous stress $\sigma^{jk}_{\rm vis}$ and the FGT anisotropic stress $\sigma^{\nu k}_{\rm A}$. The former is dissipative (shown in § IV (3)), while the latter is conservative because the mechanical systems derived from the action principle in terms of Lagrangians (§ IV, A and B) have Hamiltonian system of equations of motion which conserve the total mechanical energy (*cf.* [19] § 2.3; [20] § 2.3). Hence the present study emphasizes the importance of the conservative stress field $\sigma^{\nu k}_{\rm A}$. This is another theme of the present.

Section V reviews the theory of steady streaming generated by oscillatory boundary layers in the acoustic system, which is also observed in the Kundt's system [7].

Section VI investigates a similarity of spontaneous symmetry transitions occurring in two quite-different physical systems: (*a*) Kundt's acoustic system and (*b*) Higgs' mechanism ([21], [22]). It is quite unexpected finding that an analogy exists between the Lagrangian structures of both systems. Each system is described by a triplet of Lagrangians, each of which has similarity respectively. Most obvious similarity is seen in the forms of the Lagrangian describing interactions (see § VI).

II. Brief Description of Kundt's Experiment by Fluid Gauge Theory

The *present* study takes new fluid-mechanical view-points in order to describe the Kundt's experiment with physical terms. In particular, to explain the two experimental observations (*i*) and (*ii*) given in the Introduction, the *Fluid Gauge Theory* [13] is applied to those observations. The application has been found very successful. The outcomes obtained by the application have disclosed two innovative aspects of the Kundt's acoustic system. Such new findings are presented compactly in this section but detailed analyses are postponed to the following sections. The two innovative findings are as follow.

(I) Firstly, it is understood that the formation of dust striation in the Kundt's experiment tells a deep message. Namely, according to the theory [13], the *dust striation* shows an experimental evidence of existence of a background gauge field in the acoustics, characterized with much shorter scales of the striation. The theory predicts that trace of the background gauge field had been visualized with the dust striations.

(II) Secondly, by detailed examinations of the experiment and the theoretical structures, the Fluid Gauge Theory implies an unexpected finding that the formation mechanism of

© 2022 Global Journals

Kundt's dust striation is analogous to the spontaneous symmetry breaking, known in the Higgs mechanism. This is found by comparing the Lagrangian structure of the Fluid Gauge Theory with that of Higgs mechanism (see the section VI). Formation of Kundt's dust striation is in fact an acoustic analogue of *Spontaneous Symmetry Breaking* (Nambu [23]).

August Kundt [1] noted a remarkable statement in 1866 as follows: *As far as the origin of these transverse ribs is concerned, I refrain from any statement at this point. I would therefore prefer not to attempt its explanation at all, nor give an explanation, which I am forced to withdraw later.* Concerning the experimental evidence, this implies that he knew clearly the whole of phenomena, but realized that he was unable to find any appropriate theory to explain it.

As a possible theory, the Fluid Gauge Theory [13] is presented to explain the formation mechanism. The theory is formulated on the bases of two sets of 4-vector fields: (*i*) *Fluid current 4-vector* $j^\mu(x^\nu)$ and (*ii*) *Background gauge-field 4-covector* $a_\mu(x^\nu)$ $(\mu,\nu=0,1,2,3)$. Regarding the gauge field $a_\mu(x^\nu)$, a preliminary comment is given below in this section with detailed definitions postponed to later sections.

The Fluid Gauge Theory (FGT in short) is formulated in terms of relativistic Lagrangians, and hence the current 4-vector $j^\mu(x^\nu)$ is defined relativistically as follows:

$$j^\nu=\rho\,(c,\,\boldsymbol{v})=c\overline{\rho}u^\nu,\quad u^\nu\equiv \mathrm{d}x^\nu/\mathrm{d}\tau,\quad \overline{\rho}=\rho\sqrt{1-\beta^2}, \tag{1}$$

with c the light velocity, ρ the fluid mass density, $\boldsymbol{v}$ the fluid velocity in 3-space and $\beta\equiv|\boldsymbol{v}|/c$.[1] Concerning the Fluid-Mechanics, the *following* observation is instructive. Namely *there exist glimpses of linked structure of* $4d$*-space-time*, represented by $4d$ inner products:

$$\partial_\nu j^\nu=\partial_t\rho+\nabla\cdot(\rho\boldsymbol{v});\qquad j^\nu\partial_\nu=\rho\,(\partial_t+\boldsymbol{v}\cdot\nabla)\equiv\rho\,\mathrm{D}_t, \tag{2}$$

where $\partial_\nu=(c^{-1}\partial_t,\boldsymbol{\nabla})$, and $\mathrm{D}_t=\partial_t+\boldsymbol{v}\cdot\nabla$. The first is nothing but the expression leading to the *continuity equation* $(\partial_\nu j^\nu=0)$, and the second $\mathrm{D}_t\equiv\partial_t+\boldsymbol{v}\cdot\nabla$ the *material derivative*.

The reason why the gauge field $a_\mu(x^\nu)$ is introduced in the FGT theory is to ensure the continuity equation $\partial_\nu j^\nu=0$ which should be deduced from the action principle of invariant variation, instead of writing it *a priori*. Namely, the continuity equation is not given *a priori*, but is ensured owing to the existence of the gauge field $a_\mu(x^\nu)$.

Initially when the sound wave was weak, the system is governed by the traditional Eulerian system, but accompanying a *transparent* (invisible) gauge field a_ν (see below). As the wave intensity increases, the gauge field shows spontaneously its appearance at a transition when the field is colored with a rotational field superimposed on the transparent field. In fact, the traditional Eulerian system works only under such transparent gauge fields.

The present *Fluid Gauge Theory* [13] has been formulated according to the *gauge principle* of general gauge theory ([15], [16]), and the present theory extends the *isotropic* pressure stress fields σ_{I} of the traditional Eulerian fluid system to *anisotropic* stress fields σ_{Λ} at a transition caused by a certain physical mechanism (which will be considered in the section III, helped with computer simulations).

---

[1] $\mu,\nu=0,1,2,3$. The *overlined* value $\overline{\rho}$ denotes the proper value (*i.e.* the density ρ in the *rest frame* where the fluid is at rest). For the proper time τ, $\mathrm{d}\tau\equiv\sqrt{1-\beta^2}\,\mathrm{d}x^0$ where $x^\nu=(ct,\boldsymbol{x})$ with $x^0=ct$, t the time. and $\boldsymbol{x}=(x^1,x^2,x^3)$ a 3-vector notation. Following notations are used: $\mathrm{d}^3x\equiv\mathrm{d}x^1\mathrm{d}x^2\mathrm{d}x^3$, and $\boldsymbol{\nabla}=(\partial_k)$ where $\partial_k=\partial/\partial x^k$, $k=1,2,3$. The metric tensor is $\eta_{\mu\nu}=\eta^{\mu\nu}=\mathrm{diag}(-1,1,1,1)$.

© 2022 Global Journals

III. Transition of States

Let us consider *fluid-dynamic* aspects of the Kundt's experiment by examining the stress fields. Suppose that the air in a closed tube is excited with resonant sound waves. During the initial period when the sound intensity is weak, main part of the air motion executes longitudinal oscillation, which is vortex-free and irrotational. This is described very nicely by the Euler's system of an ideal fluid without viscosity. However, as the sound intensity increases, presence of minute dust particles scattered over the lower tube-wall acts as source of eddy, providing rotational component to the main part. This plays a certain role of trigger that prompts the state transition.

a) Transition is prompted by fluid-mechanical processes

As the sound intensity increases in the tube, the *rms* velocity $\overline{u} = \langle |\boldsymbol{u}_m|^2 \rangle^{1/2}$ of the air motion increases where $|\boldsymbol{u}_m|$ is a representative magnitude of velocity of air-gas molecules. Presence of dust particles within intense acoustic field favors transition of the stress field within the oscillating air to another stress field of different characteristics. Suppose that there exist small external objects acting as roughness on the wall. When the air is flowing fast over the roughness surface, its boundary layer separates from the solid roughness surface if an effective Reynolds number of the fluid motion is sufficiently high to enable the flow separation, as verified experimentally in [6]. Then, shearing rotational flows are supplied within the fluid, inducing eddying fluid motion within a broader space region. This was studied experimentally by Andrade ([5] $\sim$ [7]).

In 1930s, Andrade carried out detailed studies on the Kundt's experiment with updated devices at his times. From his earlier studies, he concluded on the basis of the Reynolds numbers observed experimentally that the periodic air motion about an obstacle produced eddying motion. This rotational motion was mixed and combined with the surrounding irrotational oscillating motion in the pipe. Concerning all the previous experiments carried out not only by himself but also by other previous workers, he commented that the air motion previously had been assumed tacitly to be irrotational, but actually the motion had been rotational.

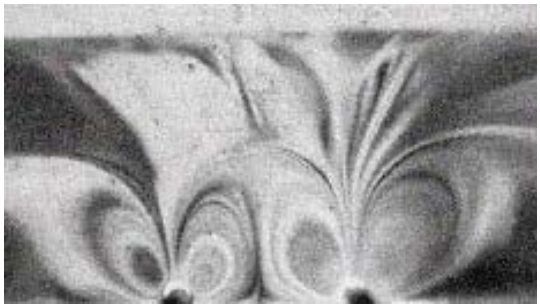

Fig. 2: Photo of eddies visualized with smoke ([7], Fig.27). On the lower wall two thin cylinders (seen dark) were placed and the upper wall seen as white belt.

Figure 2 shows one of the many photos in the paper [7], visualizing eddy pattern (with using tobacco smoke) generated by a pair of thin cylinders placed at the bottom transversally (perpendicular to the sheet) within the resonant longitudinal (*left-right*) air motion. Andrade gave a plenty of experimental evidences in [7] of existence of eddying motions generated by obstacles in the field or roughness elements on the lower wall. In the absence of roughness

© 2022 Global Journals

or obstacles, the air oscillation should be longitudinal and mainly irrotational external to thin boundary layers (caused by the non-slip condition of viscosity effect).

Hinted by the experimental evidences of Andrade, we can make a following observation on the acoustic field of Kundt's experiment. Those experimental evidences imply that there must have been a *transition* in the acoustic field when the sound intensity was made increased.

b) Prediction of the FGT theory

In the traditional Fluid Mechanics, the fluid is said to be *ideal* if its mechanical energy is conserved during its motion, and said *dissipative* if its kinetic energy is lost into heat energy by the action of viscosity. The equation of motion of the air (assumed to be an ideal non-dissipative fluid as an idealization) is given by the form:

$$\rho\, \mathrm{D}_t v^k = -\partial_k p, \qquad k = 1, 2, 3, \tag{3}$$

where p is the pressure, v^k is the k-th component of the fluid velocity, and the operator $\mathrm{D}_t \equiv \partial_t + \boldsymbol{v} \cdot \nabla$ is the material derivative defined by (2).

In the present problem of the state transition, we are interested in the stress field $\sigma^{jk}(\boldsymbol{x})$ within the space of acoustic resonance, By using it, the above equation of motion can be rewritten as

$$\rho\, \mathrm{D}_t v^k = \partial_j \sigma_{\mathrm{I}}^{jk}, \quad \sigma_{\mathrm{I}}^{jk} = -p\, \delta^{jk}, \qquad (j, k = 1, 2, 3), \tag{4}$$

where σ_{I}^{jk} is the stress tensor representing the *Isotropic* pressure stress.[2] The equation (4), or equivalently (3), is nothing but the Euler's equation of motion.

The Fluid Gauge Theory (briefly described in §II) predicts transition of the stress field in the fluid in motion. This implies that the form of σ_{I}^{jk} given in (4) may take another form at a certain transition. There are three types of stress fields (to be considered below in the current issue): (A) *isotropic* stress field $\sigma_{\mathrm{I}}^{jk}(x^\nu)$ (non-dissipative), (B) *anisotropic* stress $\sigma_{\mathrm{A}}^{jk}(x^\nu)$ (non-dissipative), and (C) *viscous* stress $\sigma_{\mathrm{vis}}^{jk}(x^k)$ (anisotropic and dissipative). As mentioned briefly in the section II, the traditional Eulerian fluid system, governed by the isotropic pressure stress σ_{I}^{jk}, works under transparent gauge fields.

When sound intensity is weak, Euler's equation of motion (4) is valid, with the stress field represented by the isotropic stress σ_{I}^{jk}. Interestingly, the same Eulerian Fluid system is valid in the Fluid Gauge Theory when the gauge field a_ν is transparent, *i.e.* when a_ν is expressed as $\partial_\nu \Psi(x^\mu)$. This finding gives a hint to develop a new theory.

In the Kundt's experiment of acoustic resonance, when the sound intensity was increased, minute dust-like particles of random dispersion showed unexpected behaviors under the acoustic field. The cluster of dust particles arranged themselves spontaneously and formed transversal rib-like structure having much smaller scale than the wavelength λ_{r} of resonant waves. This is understood as *spontaneous symmetry transition.*

[2] A tensor of the form $p\,\delta^{jk}$ is said an isotropic tensor, since the metric tensor in the $3d$ cartesian space is given by the isotropic tensors: $\delta^{jk} = \delta_{jk} = \mathrm{diag}(1, 1, 1)$. Then, raising the lower index of ∂_k is simply done by $\partial^k = \delta^{kl}\partial_l$. Then the equation (3) can be rewritten as $\rho\, \mathrm{D}_t v^k = -\partial^k p$.

© 2022 Global Journals

An extension from the transparent gauge field $a_\nu^{(0)} = \partial_\nu \Psi$ to general gauge field a_ν, *i.e.* general 4-vector field $a_\nu(x^\mu)$, is enabled by the *principle of local gauge invariance* according to the General Gauge Theory ([13], [15], [16]). This is described in the section IV. In fact, the new general gauge field a_ν enforces transition of the stress field from the *isotropic* $\sigma_{\rm I}^{jk}$ to *anisotropic* stress field $\sigma_{\rm A}^{jk}$ of the system, given by (21) $\sim$ (23). This is called the *Fluid Gauge Theory* (in short, *FGT*). The former stress field $\sigma_{\rm I}^{jk}$ has affinity with *irrotational* velocity field under the transparent field $a_\nu^{(0)}$, while the latter stress field $\sigma_{\rm A}^{jk}$ is receptive with *rotational* (eddying) velocity field in combination with the colored field $a_\nu(x^\mu)$. This is consistent with what is explained in the above paragraph for the experimental visualization of the rib-like structure of dust particles existing in the acoustic field, called the *spontaneous symmetry transition*.

c) Comparison of Flow Fields before and after the Transition

In order to see the difference of the flow fields before and after the transition of stress field, let us carry out simple model analyses in this section. Consider a fluid in $2d$ (x, y)-channel with the channel axis taken to the x-direction and its width H to the normal y-direction.

Before the transition, the motion is governed by the equation (4) under the isotropic pressure stress $\sigma_{\rm I}^{jk}$. In this analysis, no-slip condition is applied on both of the upper and lower walls, so that the viscous stress term $\sigma_{\rm vis}^{jk}$ is added[3]. The equation of motion takes the following form, *i.e.* the Navier-Stokes equation:

$$\rho\, {\rm D}_t v^k = \partial_j \sigma_{\rm I}^{jk} + \partial_j \sigma_{\rm vis}^{jk}\,. \tag{5}$$

The fluid motion is assumed to be *unidirectional* : $\boldsymbol{v} = (u(t, y), 0, 0)$. Instead of sound oscillation in the channel, an analogous problem is chosen by taking special boundary conditions with the lower wall $y = 0$ being in motion under no-slip condition (moving in its own plane), while the upper wall $y = H$ is kept at rest. More precisely, the lower wall is given a time periodic motion of a period T and a space-periodic tangential motion of wavelength λ_g, and its x velocity is given by[4]

$$u = u_w \sin 2\pi(x/\lambda_g)\, \cos 2\pi(t/T).$$

To see the characteristic features of fluid motion before the transition, the equation (5) was solved under the stresses, $\sigma_{\rm I}^{jk} + \sigma_{\rm vis}^{jk}$, satisfying the boundary conditions mentioned above.

Next, after the transition, according to the last paragraph of section (b), the *anisotropic* stress field $\sigma_{\rm A}^{jk}$ is newly added and the total stress field takes the form $\sigma_{\rm I}^{jk} + \sigma_{\rm A}^{jk} + \sigma_{\rm vis}^{jk}$, where the form of $\sigma_{\rm A}^{jk}$ is defined by (22) and (23) in the next section IV. Hence the equation of motion (4) is replaced by

$$\rho\, {\rm D}_t v^k = \partial_\nu \sigma_{\rm I}^{\nu k} + \partial_\nu \sigma_{\rm A}^{\nu k} + \partial_j \sigma_{\rm vis}^{jk}. \tag{6}$$

To see the fluid motion after the transition, the equation (6) was solved under the same driving condition at the lower wall $y = 0$ while taking passive condition at the upper wall, taking reflection-less boundary condition allowing slip.

[3] $\sigma_{\rm vis}^{jk} = 2\eta\,(e_{jk} - \frac{1}{3}\,\Delta\,\delta_{jk})$. where η is a viscosity coefficient, $e_{jk} = \frac{1}{2}\,(\partial_j u_k + \partial_k u_j)$ and $\Delta = e_{kk}$.

[4] where $u_w/c_s = 1.5 \times 10^{-3}$ and $c_g/c_s = 0.031$ for c_s sound speed (344 m/s at 20° C) and c_g speed of gauge field.

© 2022 Global Journals

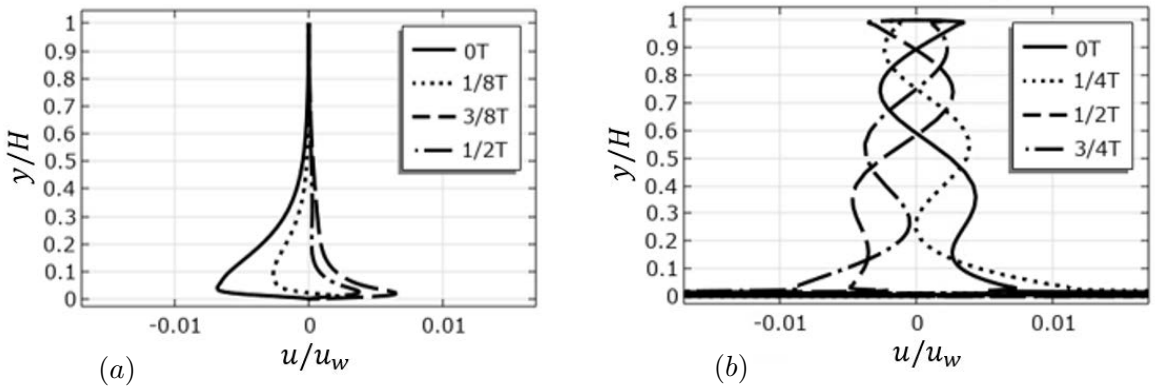

Fig. 3: Comparison of velocity fields generated by different stress fields at $x/\lambda_g = 0.45$: (a) before the transition and (b) after the transition. See Appendix B 4 for more details.

Figure 3 compares the flow developments before (left) and after (right) the transition in 2d (x, y)-channel within a period T of oscillation. The figure on the left is the Stokes-type oscillatory layer (Eulerian + viscosity: under transparent gauge field), while that on the right is the wavy layer in FGT system (FGT+viscosity under general colored gauge field).

Difference of the features of both fields is remarkable. This impressive difference has been caused by the transition of internal stress field from the isotropic $\sigma_{\rm I}^{jk}$ to the anisotropic $\sigma_{\rm A}^{jk}$, which may be called as *Spontaneous Symmetry Transition*.

d) Effect of the anisotropic stress field $\sigma_{\rm (ani)}^{jk}$

Under the influence of anisotropic stress field $\sigma_{\rm A}^{jk}$, the acoustic field is modified spontaneously. In the Kundt's experiment, when the sound intensity was increased, the cluster of minute dust particles arranged themselves spontaneously forming rib-like structure of much smaller scale than the resonant wavelength $\lambda_{\rm r}$.

On the basis of the FGT theory, computer simulation has been carried out. Figure 4 shows computed streamlines in the acoustic field averaged over a cycle of sound oscillation. Striking similarity is observed between the two of FIG.2 and FIG.4, concerning the envelope curves seen at the central lower part of the figures, both of which enclose a pair of eddies with their heights reaching half of the channel height. This is remarkable because the experimental photo of FIG.2 was taken in 1930s by Andrade ([5]∼[7]) visualizing the flow pattern by tobacco smoke, while the computed envelope line of FIG.4 has been obtained in

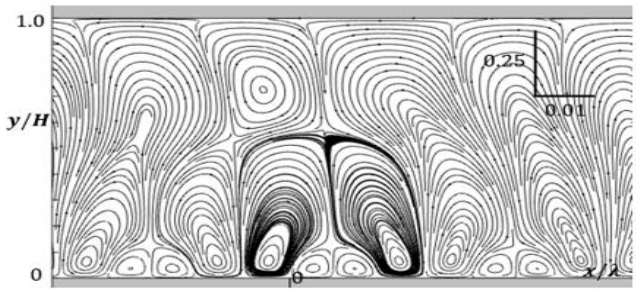

Fig. 4: Streamlines computed from the velocity field of FGT theory averaged over a cycle of acoustic oscillation .

© 2022 Global Journals

this year by the FGT theory presented next in the secction IV, or by the governing system of equations (21) ∼ (23) of § IV C - 2 , [5] under the time separation of ninety years.

Another point to be remarked is that this structure was sketched and shown as the figure 2 of [7], in order to illustrate formation of small intermediate ridges (libs) of dust which are seen in FIG.1 as shorter vertical lines between longer ones. In FIG.4, the shorter line corresponds to the innermost eddy-pair surrounded by outer larger pair of eddies. In FIG.2, there must be a separation bubble of eddies although it is hard to recognize.

Thus it is understood that longitudinal (*left-right*) sequential array of transversal eddies of FIG.4 are responsible for formation of the Kundt's dust striation.

IV. Fluid Gauge Theory (FGT)

The *Fluid Gauge Theory* [13] has been proposed to improve representation of the stress fields within fluid flows including strong turbulence, by extending the isotropic pressure stress field $\sigma_{\rm I}^{\nu k}$ to anisotropic stress field $\sigma_{\rm A}^{\nu k}$. As explained in the previous sections II and III for the formation mechanism of Kundt's dust striations, it is remarkable that this new gauge theory is found to explain most appropriately the fluid mechanical aspects of what are happening in the resonance tube of Kundt's experiment. Therefore, its detailed theoretical structure is presented in this section.

a) Lagrangians

Total Lagrangian $\mathcal{L}^{\rm FGT}$ proposed by the FGT theory [13] for the fluid system consists of three parts, $\mathcal{L}^{\rm FGT} = \mathcal{L}_{\rm fluid} + \mathcal{L}_{\rm int} + \mathcal{L}_a$:

$$\mathcal{L}_{\rm fluid} = -c^{-1}(c^2 + \overline{\epsilon}(\overline{\rho}))\,\overline{\rho}, \tag{7}$$

$$\mathcal{L}_{\rm int} = c^{-1} j^\nu\, a_\nu\,, \tag{8}$$

$$\mathcal{L}_a = -(4\mu c)^{-1} f^{\nu\lambda}\, f_{\nu\lambda}, \tag{9}$$

$$f_{\nu\lambda} \equiv \partial_\nu a_\lambda - \partial_\lambda a_\nu, \qquad \overline{\rho} \equiv \rho\sqrt{1-\beta^2}\,, \tag{10}$$

where $\beta \equiv |\boldsymbol{v}|/c$, and *overlined* values denote proper values. The action of the system $S^{\rm FGT}$ is defined by

$$S^{\rm FGT} \equiv \int \mathcal{L}^{\rm FGT} {\rm d}\Omega = \int \Big[\mathcal{L}_{\rm fluid} + \mathcal{L}_{\rm int} + \mathcal{L}_a\Big]{\rm d}\Omega, \tag{11}$$

where ${\rm d}\Omega = c\,{\rm d}t\,{\rm d}^3x$. The first $\mathcal{L}_{\rm fluid}$ is the Lagrangian of a perfect fluid (*i.e.* an ideal fluid). In fact, in non-relativistic limit as $\beta \to 0$, the expression of $\mathcal{L}_{\rm fluid}\, c\,{\rm d}^3x$ per unit mass ($m_1 \equiv \rho\,{\rm d}^3x = 1$) reduces to the non-relativistic Lagrangian, $L_{nr} \equiv \frac{1}{2}\,m_1 v^2 - \epsilon$ (with ϵ the specific internal energy), neglecting the rest-mass energy $-m_1c^2$. Hence it is seen that the Lagrangian $\mathcal{L}_{\rm fluid}$ is a relativistic version extended from the classic non-relativistic form L_{nr}.

The third $\mathcal{L}_a$ is the Lagrangian of the gauge field represented in a form satisfying local gauge invariance with respect to the gauge field a_ν as well as ensuring current conservation. The middle $\mathcal{L}_{\rm int}$ represents the interaction between the current j^ν and the gauge field a_ν.

[5] This test simulation was done by $-\partial_t \boldsymbol{d} + \nabla \times \boldsymbol{h} = \rho\boldsymbol{v}$ (see (16)) for the gauge field a_ν and the equation of motion (6) with additional viscosity stress $\sigma_{\rm vis}^{jk}$, under the approximation $|\rho'/\rho| \ll 1$ and $|\nabla\phi/\partial_t \boldsymbol{a}| \ll 1$.

© 2022 Global Journals

Equations of motion are deduced from the action principle and the force field is represented in terms of the stress field σ.

b) Governing equations

To find the equations of motion, the action principle is applied to $S^{\rm FGT}$, by assuming the gauge field a_ν given and vary only the position coordinate x_p^k of fluid particles moving with the velocity $v^k = {\rm D}_t x_p^k$ along their trajectories ($k = 1, 2, 3$). In the non-relativistic limit as $\beta \to 0$, the equation of motion is deduced by the action principle as

$$\rho\, {\rm D}_t v^k = -\partial^k p + \rho f^{k\nu}\, v_\nu, \quad (k = 1, 2, 3), \tag{12}$$

(*cf.* Eq.(2.30) of [13]) from the combination of two Lagrangians $\mathcal{L}_{\rm fluid}$ and $\mathcal{L}_{\rm int}$, since the third $\mathcal{L}_a$ is invariant in this variation. By the $(0, 3)$-notation, we have $v_\nu = (-c, \boldsymbol{v})$ and $v^\nu = (c, \boldsymbol{v})$ with $\boldsymbol{v}$ being a 3-vector, and $\nu = 0, 1, 2, 3$ must be taken in (12).

To find the equations governing the gauge field a_ν, we vary only the field a_ν with assuming the fluid motion $j^\nu = \rho v^\nu$ given. From the action principle, we obtain

$$\frac{\partial}{\partial x^\lambda} f^{\nu\lambda} = \mu\, j^\nu \tag{13}$$

(see Eq.(2.32) of [13]) with $j^\nu = (\rho\, c, \boldsymbol{j})$ and $\boldsymbol{j} = \rho \boldsymbol{v}$, where μ is a control parameter (introduced in (9)) to denote the degree of mutual interaction.

The equation of current conservation can be derived from this, which is directly connected with the gauge-invariant property of the Lagrangian $\mathcal{L}_a$ (see [14], § II (a)). This is analogous to the electromagnetic fields. In fact, applying the divergence operator ∂_ν on the equation (13), one obtains $0 = \partial_\nu \partial_\lambda f^{\nu\lambda} = \mu\, \partial_\nu j^\nu$. The middle side of total summation with respect to ν and λ vanishes because of the anti-symmetry of $f^{\nu\lambda}$ and the symmetry of $\partial_\nu \partial_\lambda$ with respect to ν and λ. Hence, the current conservation equation is deduced:

$$\partial_\nu j^\nu = 0, \quad \Rightarrow \quad \partial_t \rho + \nabla \cdot (\rho \boldsymbol{v}) = 0, \tag{14}$$

(see (2)). The third Lagrangian $\mathcal{L}_a$ ensures the *mass conservation*.

Introducing the $(0, 3)$-notation for a_ν too (like below (12)) by $a_\nu = (-\overline{\phi}, \boldsymbol{a})$ where $\overline{\phi} \equiv \phi/c$ for ϕ a scalar field, we define new two 3-vector fields $\boldsymbol{e}$ and $\boldsymbol{b}$ by

$$\boldsymbol{e} \equiv -\partial_t \boldsymbol{a} - \nabla \phi, \qquad \boldsymbol{b} \equiv \nabla \times \boldsymbol{a}. \tag{15}$$

Then, these enable the equation (13) transformed into a pair of equations analogous to the Maxwell equations of *Electromagnetism*. In fact, with defining $\boldsymbol{d}$ and $\boldsymbol{h}$ by $\boldsymbol{d} = \epsilon \boldsymbol{e}$ and $\boldsymbol{h} = \boldsymbol{b}/\mu$ with using $\epsilon \equiv 1/(\mu\, c^2)$, the equation (13) gives a pair of Maxwell equations:

$$-\partial_t \boldsymbol{d} + \nabla \times \boldsymbol{h} = \boldsymbol{j}, \qquad \nabla \cdot \boldsymbol{d} = \rho, \tag{16}$$

(Eq.(3.18) of [13]). Definition (15) gives another pair of Maxwell equations (Eq.(3.20) of [13]):

$$\partial_t \boldsymbol{b} + \nabla \times \boldsymbol{e} = 0, \qquad \nabla \cdot \boldsymbol{b} = 0. \tag{17}$$

In summary, it is found that the fluid current field $j^\mu(x^\mu)$ changes its character drastically, depending on whether the gauge field a_ν is derived from a scalar potential $\Psi(x^\mu)$ (*i.e.* $a_\nu = \partial_\nu \Psi$) or takes an intrinsic 4-vector form $a_\nu(x^\mu)$ yielding non-vanishing $f_{\mu\nu} (= \partial_\mu a_\nu - \partial_\nu a_\mu)$ field.

© 2022 Global Journals

c) Three stress fields in fluid-flow fields

There are three types of stress fields within the fluid flows: (A) *isotropic* stress field $\sigma^{jk}_{\rm I}(x^\nu)$ (non-dissipative), (B) *anisotropic* stress $\sigma^{jk}_{\rm A}(x^\nu)$ (non-dissipative), and (C) *viscous* stress $\sigma^{jk}_{\rm vis}(x^k)$ (anisotropic and dissipative). As mentioned previously, the traditional Eulerian fluid system is governed by the isotropic pressure stress $\sigma^{jk}_{\rm I}$. According to the FGT theory, on the other hand, the corresponding case of isotropic pressure stress $\sigma^{jk}_{\rm I}$ is accompanied by a transparent gauge field which is derived from a scalar potential $\Psi(x^\mu)$ (*i.e.* $a_\nu = \partial_\nu\Psi$).

Depending on whether the stress field is $\sigma^{jk}_{\rm I}$ (isotropic) or $\sigma^{jk}_{\rm A}$ (anisotropic), the fluid current field $j^\mu(x^\mu)$ changes its character drastically. In the latter case, the gauge field $a_\nu(x^\mu)$ takes intrinsic 4-vector form yielding non-vanishing $f_{\mu\nu}(= \partial_\mu a_\nu - \partial_\nu a_\mu)$. The third viscous stress $\sigma^{jk}_{\rm vis}$ plays an important role in the traditional Navier-Stokes system. Below, we look into the three stress fields in details.

(1) *Isotropic stress field* $\sigma^{jk}_{\rm I}$ *and transparent gauge field* $\partial_\nu\Psi$

If $a_\nu = \partial_\nu\Psi$, the field tensor $f_{\mu\nu}$ defined by (10) takes the form, $f_{\mu\nu} = \partial_\mu\partial_\nu\Psi - \partial_\nu\partial_\mu\Psi$. Hence $f_{\mu\nu} \equiv 0$. Then, the third Lagrangian $\mathcal{L}_a$ vanishes identically, while the action principle applied to the remaining pair of Lagrangians ($\mathcal{L}_{\rm fluid}$, $\mathcal{L}_{\rm int}$) yield the equation (12) of the Eulerian fluid system since its derivation was independent of $\mathcal{L}_a$. The equation (12) under $f^{\mu\nu} = 0$ reduces to

$$\rho\, {\rm D}_t v^k = \partial_j \sigma^{jk}_{\rm I}, \quad \sigma^{jk}_{\rm I} = -p\,\delta^{jk}, \qquad j,k = 1,2,3. \tag{18}$$

This is the same as (4).[6]

The equation (13) must be discarded here because both of $\mathcal{L}_a$ and $f_{\mu\nu}$ vanishes. However, a wonderful feature of this gauge theory is that the mass conservation equation is still deduced from the action principle under $a_\nu = \partial_\nu\Psi$. Varying the field $\Psi \to \Psi + \delta\Psi$ in $\mathcal{L}_{\rm int}$ of (8) with assuming the fluid current j^ν fixed, the action variation is given by $\delta S^{\rm FGT} = c^{-1}\int j^\nu\,\partial_\nu(\delta\Psi)\,{\rm d}\Omega$, which is transformed as

$$\delta S^{\rm FGT} = -\,c^{-1}\int \partial_\nu j^\nu\,\delta\Psi\;{\rm d}\Omega + \int \partial_\nu\Big(j^\nu\delta\Psi\Big){\rm d}\Omega. \tag{19}$$

The second is integrated once, leading to vanishing boundary integrals. Requiring $\delta S^{\rm FGT} = 0$ for arbitrary $\delta\Psi$ results in (from (19)):

$$\partial_\nu j^\nu = \partial_t\rho + \nabla\cdot(\rho\boldsymbol{v}) = 0. \tag{20}$$

Thus, it is found in the particular case $a_\nu = \partial_\nu\Psi$ that the fluid system, described by the action $S^{\rm FGT}$, reduces to the *Eulerian system* described by the Euler's equation of motion (18) and the continuity equation (20). The gauge field $a_\nu = \partial_\nu\Psi$ exits, but not observable. This may be said that the gauge field is *transparent*.

(2) *Anisotropic stress field* $\sigma^{jk}_{\rm A}$ *and colored gauge field* a_ν

Suppose that the gauge field a_ν makes a transition from the *transparent* field $\partial_\nu\Psi$ to general vector-potential a_ν yielding colored non-vanishing $f_{\mu\nu}$.[7] Its experimental evidence

[6] With the metric tensor $\delta_{jk} = \delta^{jk} = {\rm diag}(1,1,1)$, we have $\sigma_{jk} = \eta_{ja}\eta_{kb}\sigma^{ab} = \sigma^{jk}$.

[7] The "colored" is equivalent to "$f_{\mu\nu}$ non-vanishing". Non-dissipative anisotropic stress $\sigma^{jk}_{\rm A}$ was introduced first by [18]. Detailed analysis was done by [19] from *fluid-dynamics* view-point. Reinterpretation was given by [20] from the *gauge invariance*.

© 2022 Global Journals

was given in the section III. This causes corresponding transition of stress tensor σ^{jk} within the flow field from the isotropic stress $\sigma^{jk}_{\rm I} = -p\,\delta^{jk}$ to a new stress field with additional anisotropic part $\sigma^{jk}_{\rm A}$. Rewriting the second force term on the right of (12) as $\rho f^{k\nu}\, v_\nu = \partial_\nu \sigma^{\nu k}_{\rm A}$, the equation becomes

$$\rho\, {\rm D}_t v^k = \partial_\nu \sigma^{\nu k}_{\rm I} + \partial_\nu \sigma^{\nu k}_{\rm A}, \tag{21}$$

where

$$\sigma^{jk}_{\rm A} = e^j d^k + b^j h^k - w_e\,\delta^{jk}, \qquad w_e \equiv \tfrac{1}{2}\,(\boldsymbol{e},\boldsymbol{d}) + \tfrac{1}{2}\,(\boldsymbol{h},\boldsymbol{b}) \tag{22}$$

$$\sigma^{00}_{\rm A} = -w_e, \qquad \sigma^{0k}_{\rm A} = -c(\boldsymbol{d}\times\boldsymbol{b})^k, \tag{23}$$

for $j,k = 1,2,3$ and $\nu = 0,1,2,3$. Definitions of $\boldsymbol{d}$ and $\boldsymbol{h}$ are given in the paragraph above (16). Using (22) and (23), the second force term $\partial_\nu \sigma^{\nu k}_{\rm A}$ can be given another expression:

$$\partial_\nu \sigma^{\nu k}_{\rm A} = \rho\,(\boldsymbol{f}_{\rm L})^k, \quad \boldsymbol{f}_{\rm L} \equiv \boldsymbol{e} + \boldsymbol{v}\times\boldsymbol{b}, \tag{24}$$

This may be termed as *fluid-Lorentz* force, and the stress tensor $\sigma^{\nu k}_{\rm A}$ is analogous to the Maxwell stress of Electromagnetism.

The anisotropic stress field $\sigma^{\nu k}_{\rm A}$ was introduced in [13]. In the current fluid mechanics, the stress $\sigma^{\nu k}_{\rm A}$ is still out of consideration. As a matter of fact, the viscous stress tensor $\sigma^{jk}_{\rm vis}$, considered in the next item (3), is used in the current theory of fluid mechanics. The viscous stress tensor has anisotropic components as well. At the times of 1953 and 1967 when George Batchelor published his textbooks ([9], [10]), the anisotropic components of viscous stress might be useful in his study of fluid-dynamics and turbulence (see (3) below).

However, there exists an essential difference between the two fields of the viscous stress $\sigma^{jk}_{\rm vis}$ and the FGT stress $\sigma^{\nu k}_{\rm A}$. The former is dissipative as shown in (3), while the latter is conservative because the mechanical systems derived from the action principle in terms of Lagrangians (like those of the sections a) and b) of § IV) have Hamiltonian system of equations of motion which conserve the total mechanical energy. Hence the present study emphasizes the importance of the field $\sigma^{\nu k}_{\rm A}$.

(3) *Viscous stress tensor $\sigma^{jk}_{\rm vis}$ and boundary layers*

Concerning the expression $\sigma^{jk}_{\rm I} = -p\,\delta^{jk}$, George Batchelor (the author of the book [10]) describes in its §3.3: "*There is no reason to expect these results to be valid for a fluid in motion*". The author's point is that the law $\sigma^{jk}_{\rm I} = -p\,\delta^{jk}$ is valid in a fluid at rest. He continues: "*The simple notion of a pressure acting equally in all directions is lost in most cases of a fluid in motion.*" And, "*Tangential stresses are non-zero in general.*" The pressure is defined originally by the thermodynamics and the thermodynamic equations of state refer to equilibrium conditions, whereas the state of a fluid in motion are not in exact thermodynamic equilibrium.

It is convenient to regard the stress tensor σ_{ij} as the sum of an isotropic part $-p\delta_{ij}$ and a remaining non-isotropic part d_{ij}:

$$\sigma_{ij} = -p\delta_{ij} + d_{ij}, \tag{25}$$

where, assuming $d_{ii} = 0$, we have $p = -\frac{1}{3}\,\sigma_{ii}$, and the non-isotropic part d_{ij} may be termed the *deviatoric stress tensor*. Here the $p = -\frac{1}{3}\,\sigma_{ii}$ has a mechanical significance, generalizing the elementary notion of pressure, but reducing to the fluid pressure when the fluid is at rest.

© 2022 Global Journals

Traditional fluid mechanics assumes that the deviatoric stress d_{ij} is originated by non-uniformity of the flow field, and seeks a linear local relation between the stress d_{ij} and local velocity gradients $\partial u_j/\partial x_i$. It is a usual custom to rewrite the velocity gradient $\partial u_j/\partial x_i = \partial_i u_j$ as

$$\partial_i u_j = e_{ij} + \xi_{ij}, \qquad e_{ij} = \tfrac{1}{2}\,(\partial_i u_j + \partial_j u_i), \tag{26}$$

$$\xi_{ij} = \tfrac{1}{2}\,(\partial_i u_j - \partial_j u_i) = \tfrac{1}{2}\,\varepsilon_{ijk}\,\omega_k, \qquad \omega_k = \varepsilon_{kij}\partial_i u_j, \tag{27}$$

where ε_{kij} is the alternating tensor[8]. According to the detailed tensor analysis (in §3.3 of [10], : deleting contribution from the term ξ_{ij} after all), the deviatoric stress is given by

$$d_{ij} = 2\eta\,(e_{ij} - \tfrac{1}{3}\,\Delta\,\delta_{ij}), \qquad \Delta \equiv e_{kk} = \operatorname{div}\boldsymbol{u}, \tag{28}$$

satisfying $d_{ii} = 0$, where η is a viscosity coefficient. Thus, we find[9]

$$\sigma^{jk}_{\rm vis} = 2\eta\,(e_{jk} - \tfrac{1}{3}\,\Delta\,\delta_{jk}). \tag{29}$$

Then the equation of motion is given by the form of well-known Navier-Stokes equation:

$$\rho\,\mathrm{D}_t v^k = -\partial_k p + \partial_j \sigma^{jk}_{\rm vis}\,. \tag{30}$$

In a special case where the divergence $\Delta = \operatorname{div}\boldsymbol{v}$ is not significant, the above Navier-Stokes equation takes the following form

$$\rho = \rho_0 + \rho', \quad p = p_0 + p', \qquad p' = c_{\rm s}^2\,\rho', \tag{31}$$

$$\rho\,\partial_t u_k + \rho\,u_j\partial_j u_k = -\partial_k p + \eta\nabla^2 u_k\,. \tag{32}$$

$$\rho\,u_j\partial_j u_k \approx \partial_j(\rho_0\,u_j u_k) = \partial_j R_{jk}, \quad R_{jk} = \rho_0\,u_j u_k \tag{33}$$

where v^k and ρ are replaced approximately with u_k and a constant ρ_0 when $\Delta = \partial_k v^k \approx \partial_k u_k$ is not significant.

In order to find the energy dissipated into heat by the motion of a viscous fluid (or *equivalently*, the heat energy gained by the fluid internally), one must define the thermodynamic state of the fluid, which is characterized with the density ρ, pressure p, specific internal energy ε (per unit mass), specific entropy s and specific enthalpy h, and temperature T. There is a unidirectional transfer of mechanical energy by the viscosity to the internal energy ε, *i.e.* irreversible dissipation into heat.

According to the texts ([10], [12]), the amount of heat gained by unit volume of the fluid is given by the following expression (see Appendix A), which can be shown to be non-negative:

$$\sigma^{jk}_{\rm vis}\;\partial_k v_j = 2\eta\,(e_{jk} - \tfrac{1}{3}\,\Delta\,\delta_{jk})(e_{jk} - \tfrac{1}{3}\,\Delta\,\delta_{jk}) \quad (\geq 0), \tag{34}$$

where the heat conduction effect owing to non-uniform temperature ($\nabla T \neq 0$) is omitted. [*cf.* § 3.4 of [10] or § 49 of [12]. The latter text shows additional non-negative $\zeta\Delta^2$ to (34) from ζ.]

[8] $\varepsilon_{ijk} = 0$ unless i, j, k are all different, with its value $+1$ or -1 according as i, j, k in cyclic order or not.

[9] The textbook [12] adds one more term with the second (bulk) viscosity ζ: $\zeta\,\Delta\,\delta_{jk}$ stemming from the finite time response of molecular processes. Note that there is no distinction whether the indices are upper or lower in the present. See the note below (18).

© 2022 Global Journals

V. Steady Streaming by Powerful Excitation

Suppose that the acoustic waves in a closed tube were initially weak. The system is governed by the Eulerian system, but accompanying a transparent (invisible) gauge field $\partial_\nu \Psi$ (described in § III. B). As the wave intensity increases, the gauge field shows its appearance spontaneously at a transition when the field is colored with general rotational field superimposed on the transparent field. This is consistent with the Fluid Gauge Theory, which predicts the trace of background gauge field visualized by the Kundt's dust striations.

Furthermore, if there is a prolonged powerful acoustic excitation, *steady streaming* is generated within the tube filled with standing waves. A number of experimental photographs showing the steady streaming were presented by Andrade [6], which were observed under powerful excitation (FIG.5). The steady streaming is generated by the combined action of the nonlinear Reynolds stress and the viscous shear effect causing acoustic energy dissipation (see (38) given below). [*cf.* § 4.7 of [11]]. Lowering the intensity, but still above a critical intensity, he observed ripple-like striations.

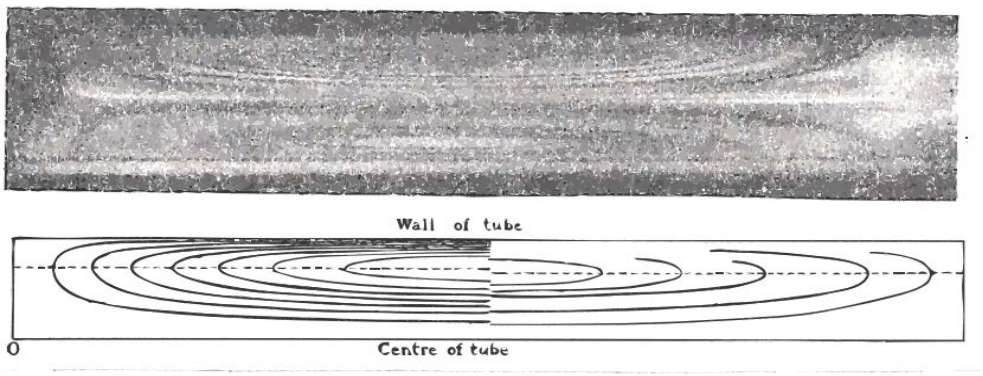

Fig. 5: Steady streamings of a single quarter-wave-length circulation in the Kundt tube experiment, shown by (a) Photograph (upper) taken for $600Hz$ sound resonance visualized with smoke by Andrade (FIG.13 of [6]), and (b) Streamlines (lower) between a pair of a node (left) and antinode (right): the curves on the right-hand half side were reproduced by reading the drift motion of smoke particles, while the curves on the left-hand half side are theoretical streamlines computed from Rayleigh's formula (FIG.5 of [6] and Ryleigh formula shown at pgae 453). .

Citing the descriptions in the well-known classics [4] in 1890s, Rayleigh wrote his philosophical view on the acoustic problem initiated by Kundt [1] in §352 of [4]: "*One of the most curious consequences of viscosity is the generation in certain cases of regular vortices.* [*Of this an example, discovered by Dvorak [3], has already been mentioned in §260.*] *In a theoretically inviscid fluid, no such effect could occur (§240); and, even when viscosity enters, the phenomenon is one of the second order, dependent, that is, upon the square of the motion.* ..... "

Suppose that oscillations of the acoustic pressure are expressed as $p(t,x) = e^{i\omega t} f(x)$ in a closed tube. Resonant sound waves in the tube generate a steady streaming motion there. Such effect can occur by the action of Reynolds stress $\overline{\rho u_j u_k}$ when the acoustic energy dissipation takes place in thin boundary layers on the tube walls, where the overline signifies an average over a wave period, *i.e.* a mean value. The mean force $\overline{F}_k$ with which waves act on a fluid element results from the gradient of Reynolds stress $\overline{R}_{jk} = \rho_0 \overline{u_j u_k}$, represented by $\overline{F}_k = -\partial_j(\rho_0 \overline{u_j u_k})$ from (33). Taking time average of (32) in the main part of sound waves (*i.e.* external to the viscous boundary layer) where the viscous effect of $\sigma^{\rm vis}_{jk}$ is not significant, one obtains the mean equation of motion:

© 2022 Global Journals

$$\rho_0\,\partial_t\,\overline{u}_k = \overline{F}_k - \partial_k\overline{p},$$

which reduces to $\overline{F}_k - \partial_k\overline{p} = 0$ since $\partial_t\overline{u}_k$ vanishes by the time derivative. Thus, we obtain the mean equation valid in the main part external to thin viscous boundary layers:

$$\partial_k\overline{p} \;=\; \overline{F}_k\,, \quad \overline{F}_x = -\partial_j\overline{R}_{jx} = -\partial_x(\rho_0\,\overline{uu}) - \partial_y(\rho_0\,\overline{uv}), \tag{35}$$

where $\overline{R}_{jk} = \rho_0\,\overline{u_j u_k}$. In this main wave part, there is balance of the two mean effects (gradients) of the pressure and the Reynolds stress. This implies the place where there is a driving force of the steady streaming. In fact, *departure* of the mean force $\partial_j\overline{R}_{jk}$ within the thin boundary layer from its external value $\partial_j(\overline{R}_{jk})_{\rm ex} = \partial_j(\rho_0\,\overline{u_j u_k})_{\rm ex}$ generates streaming, because the external mean pressure $\overline{p}_{\rm ex}$ is unchanged, *i.e.* uniform approximately across thin boundary layer (see, *e.g.* §5.7 of [10]).

Hence the external mean pressure gradient $\partial_x\overline{p}_{\rm ex}$ is given by $\overline{F}_x$ of (35). rewritten as

$$\partial_x\overline{p}_{\rm ex} = (\overline{F}_x)_{\rm ex} = -\partial_j(\overline{R}_{jx})_{\rm ex} = -\partial_x(\rho_0\,\overline{uu})_{\rm ex} - \partial_y(\rho_0\,\overline{uv})_{\rm ex}, \tag{36}$$

Within the boundary layer, the mean force $\overline{F}_x$ is given by the negative of $\partial_j\overline{R}_{jx}$ where $\overline{R}_{xx} = \rho_0\,\overline{u^2}$ and $\overline{R}_{yx} = \overline{R}_{xy} = \rho_0\,\overline{uv}$, which depart from those with the lower suffix "ex".[10]

A steady streaming $\overline{u}^{\rm st}$ is generated by the viscous shear force $\partial_y\,\sigma^{\rm vis}_{yx} \approx \eta\,\partial_y^2\,\overline{u}^{\rm st}$ being in balance with two other forces, *i.e.* (i) gradient of mean Reynolds stress $\partial_j\overline{R}_{jx}$ and (ii) that of mean external pressure $\partial_x\overline{p}_{\rm ex}$:

$$\eta\,\partial_y^2\,\overline{u}^{\rm st} - \partial_j\overline{R}_{jx} - \partial_x\overline{p}_{\rm ex} = 0. \tag{37}$$

Substituting the expression for $\partial_x\overline{p}_{\rm ex}$ of (36) and using the definition of $\partial_j\overline{R}_{jx}$, one can rewrite it as

$$\nu\,\partial_y^2\,\overline{u}^{\rm st} = \big(\partial_x\,\overline{u^2} - \partial_x(\overline{u^2})_{\rm ex}\big) + \big(\partial_y\big(\overline{uv}\big) - \partial_y\big(\overline{uv}\big)_{\rm ex}\big), \tag{38}$$

where $\nu \equiv \eta/\rho_0$. To evaluate the 2nd order terms on the right hand side of (38), the expressions of u and v must be found from the linear theory of oscillatory boundary layers in the tube. It is reminded that the equations for the mean stream has been derived from the full nonlinear equations (32) and (33).

The mean equation (38) is linear with respect to the variable $\overline{u}^{\rm st}$ on the left hand side, so that one can represent it as a linear combination $\overline{u}^{\rm st} = (\overline{u}^{\rm st})_{uu} + (\overline{u}^{\rm st})_{uv}$, each of which satisfies the following equations:

$$\nu\,\partial_y^2\,(\overline{u}^{\rm st})_{uu} = \partial_x\,\overline{u^2} - \partial_x(\overline{u^2})_{\rm ex} \tag{39}$$

$$\nu\,\partial_y^2\,(\overline{u}^{\rm st})_{uv} = \partial_y\big(\overline{uv}\big) - \partial_y\big(\overline{uv}\big)_{\rm ex} \tag{40}$$

The linear theory of *Oscillatory Boundary Layers* is presented in the Appendix B. The axial x-velocity $u(t, x, y,)$ is given by (B16) of the Appendix B 3 as

[10] The mean streaming $\overline{u}^{\rm st}$ is generated by departure of $\overline{R}_{jx}$ from the external values $(\overline{R}_{jx})_{\rm ex}$, which is in balance with the external pressure gradient $\overline{p}_{\rm ex}$, keeping uniform across the thin boundary layer.

© 2022 Global Journals

$$u(t,x,y,) = u_{\rm ex}(x)\ \Re\big[\tilde{P}(t)\ F_\kappa(y)\ \big], \qquad \tilde{P}(t) \equiv e^{i\omega t}. \tag{41}$$

$$F_\kappa(y) \equiv 1 - \exp\{-(i\,\omega/\nu)^{1/2}\,y\} = 1 - \exp\{-(1+i)\,\kappa\,y\}, \tag{42}$$

$$u_{\rm ex}(x) \equiv U_0\ \cos kx, \tag{43}$$

from the linear theory of the acoustic resonance under the oscillatory pressure gradient $P \equiv -\partial p_e/\partial x = u_{\rm ex}(x)\Re\big[P_0\,e^{i\omega t}\big]$, where $P_0 = \rho_0\,i\,\omega$, $\kappa \equiv \sqrt{\omega/2\nu}$, and $u_{\rm ex}(x)$ is a real function of x. Note that $(i\,\omega/\nu)^{1/2}\,y = (1+i)\,\kappa\,y$.

From this u-solution, the y-component $v(t,x,y,)$ is found as

$$v(t,x,y,) = u'_{\rm ex}(x)\,\Re\ \big[(\nu/(i\,\omega))^{1/2}\tilde{P}(t)\ F_\kappa(y)\ \ \big], \tag{44}$$

where $u'_{\rm ex}(x) = {\rm d}u_{\rm ex}/{\rm d}x$. (*cf.* Eq. (205) and (206) of Chap.4 of [11]).

It is shown in the linear theory of Appendix **??** that the above expressions of u and v satisfy the linearized equation of continuity: $\partial_t\rho_{\rm ex} + \rho_0(\partial_x u + \partial_y v) = 0$. From (41) and (44), one can find time-averages of the wo products $\overline{uv}$ and $\overline{u^2}$ to be used for (39) and (40).

First, we consider $\overline{uv}$ and the equation (40). Taking a product of the real parts of (41) and (44), one obtains after taking its time average:

$$\overline{uv} = \tfrac{1}{2}\,(\nu/2\omega)^{1/2}\ u_{\rm ex}(x)\,u'_{\rm ex}(x)\ \Big|\ F_\kappa(y)\ \Big|^2, \tag{45}$$

and its external value is $(\overline{uv})_{\rm ex} = \frac{1}{2}\,(\nu/2\omega)^{1/2}\ u_{\rm ex}(x)\,u'_{\rm ex}(x)$ as $\kappa y \to \infty$. Integrating (40) with y twice, the mean streaming $\overline{u}^{\rm st}_{\overline{uv}}$ generated by the departure of $\overline{uv}$ from the external value in the oscillating boundary layer is given by

$$\begin{aligned}\overline{u}^{\rm st}_{\overline{uv}} &= \nu^{-1}\int_0^y \Big[\overline{uv} - (\overline{uv})_{\rm ex}\Big]\,{\rm d}y \\ &= \nu^{-1}\frac{1}{2}\,\frac{\nu}{\omega}\,\frac{1}{\sqrt{2}}\ u_{\rm ex}(x)\,u'_{\rm ex}(x)\ \int_0^y \Big[\,|\ F_\kappa(y)\ |^2 - 1\Big]\,{\rm d}(\kappa y),\end{aligned} \tag{46}$$

where $\kappa \equiv \sqrt{\omega/2\nu}$. At the external edge of the boundary layer as $\zeta \equiv \kappa y$ tends to ∞, the integral in the last expression can be estimated as

$$\int_0^\zeta \Big[\big|1 - \exp\{-(1+i)\,\zeta_*\}\big|^2 - 1\Big]\,{\rm d}\zeta_* \quad \to \quad -1/\sqrt{2} \quad (\text{as } \zeta \to \infty).$$

Hence, the steady streaming generated by $\overline{uv}$ at the edge external to the boundary layer is

$$\overline{u}^{\rm st}_{\overline{uv}} \ = \ -\frac{1}{4\omega}\,u_{\rm ex}(x)\,u'_{\rm ex}(x) \tag{47}$$

[11] $\overline{u^2} = \frac{1}{2}\,(u_{\rm ex})^2|F_\kappa|^2$ and $|F_\kappa|^2 = 1 - 2e^{-\kappa y}\,\cos\kappa y + e^{-2\kappa y}$. This is because $u^2 = (u_{\rm ex})^2\ \Re\big[\tilde{P}(t)\,F_\kappa(y)\ \big]^2 = \Re\big[e^{i\omega t}\,F_\kappa(y)\ \big]^2 = (1/4)(u_{\rm ex})^2\ (e^{i\omega t}\,F_\kappa + e^{-i\omega t}\,\hat{F}_\kappa)^2 = (1/4)\,(e^{2i\omega t}\,F_\kappa^2 + e^{-2i\omega t}\,\hat{F}_\kappa^2 + 2|e^{i\omega t}|\,|F_\kappa|^2\,)$ where $\hat{F}_\kappa$ is the complex conjugate of F_κ. Taking time average $<\ \cdot\ >_{\rm av}$, we have $< e^{\pm 2i\omega t} >_{\rm av} = 0$ and $|e^{i\omega t}| = 1$. $\partial_x\overline{p}_{uu} = -(1/4)u_{\rm ex}^2\ \delta,\ \ \delta = 1/\kappa$

© 2022 Global Journals

Secondly, there is one more contribution from the component $\overline{uu}$ of Reynolds stress. The steady stream $(\overline{u}^{\rm st})_{uu}$ generated by $\overline{uu}$ is found from the equation (39). Taking a double product of the real part of u given by (41), one obtains after taking its time average:[11]

$$\overline{uu} = \tfrac{1}{2}\, u_{\rm ex}^2\ |F_\kappa(y)|^2 \tag{48}$$

and its external value is $(\overline{uu})_{\rm ex} = \frac{1}{2}\, u_{\rm ex}^2$ since $|F_\kappa(y)|^2 \to 1$ as $\kappa y \to \infty$. Substituting these values of $\overline{uu}$ and $(\overline{uu})_{\rm ex}$ to the right hand side of (39) and integrating with respect to y, we have

$$\nu\, \partial_y\, (\overline{u}^{\rm st})_{uu} = \frac{1}{2\kappa}\, ({\rm d}u_{\rm ex}^2(x)/{\rm d}x)\ \int_0^\zeta \big[-2e^{-\zeta}\cos\zeta + e^{-2\zeta}\big]\, {\rm d}\zeta - \rho_0^{-1}\partial_x \overline{p}_{uu}. \tag{49}$$

where the last term $-\rho_0^{-1}\partial_x \overline{p}_{uu}$ is a function of x only, which is arbitrary in general, but its functional form is fixed by the argument just below.

Requiring the influence of viscous friction force vanishing externally from the boundary layer, $\nu\, \partial_y\, (\overline{u}^{\rm st})_{uu} \to 0$ as $\zeta = \kappa y \to \infty$, the counter pressure force $-\rho_0^{-1}\partial_x (\overline{p}_{uu})_{\rm ex}$ owing to the Reynolds stress $\overline{uu}$ must be given by $(1/4\kappa)({\rm d}u_{\rm ex}^2(x)/{\rm d}x)$ at the edge of the boundary layer. Then, deleting the counter pressure force, we have

$$\nu\, \partial_y\, (\overline{u}^{\rm st})_{uu} = \frac{1}{2\kappa}\, u_{\rm ex}\, u'_{\rm ex}\, \big[-e^{-2\zeta} + 2e^{-\zeta}(\cos\zeta - \sin\zeta)\big]. \tag{50}$$

Integrating this with respect to ζ for entire range $[0,\, \infty]$, we obtain the steady streaming generated by $\overline{uu}$ at the edge external to the boundary layer:

$$(\overline{u}^{\rm st})_{uu} = \nu^{-1}\frac{1}{2}\frac{1}{\kappa^2}\, u_{\rm ex}\, u'_{\rm ex}\, \big(-\frac{1}{2}\big) = -\frac{1}{2\omega}\, u_{\rm ex}(x)\, u'_{\rm ex}(x). \tag{51}$$

since $1/\kappa^2 = 2\nu/\omega$. Summing up this term $(\overline{u}^{\rm st})_{uu}$ with $(\overline{u}^{\rm st})_{uv}$ of (47), we find finally the total value:

$$(\overline{u}^{\rm st})_{\rm total} = (\overline{u}^{\rm st})_{uu} + (\overline{u}^{\rm st})_{uv} = -\frac{3}{4}\ \frac{1}{\omega}\ u_{\rm ex}(x)\, u'_{\rm ex}(x). \tag{52}$$

(*cf.* Eq. (215) of Chap.4 of [11]).

VI. Spontaneous Symmetry Transitions: Kundt's System and Higgs' Mechanism

An analogy exists in the Lagrangian structures in two physical systems between Kundt's symmetry transition and Higgs' mechanism. Let us consider the Higgs' mechanism from the *abelian gauge theory* [21, 22]. Suppose that a massive charged scalar field $\phi\, (= \phi_1 + i\phi_2)$ is interacting with an electromagnetic field A_μ (a massless vector boson). Its Lagrangian is given by $\mathcal{L} = \mathcal{L}_\phi + \mathcal{L}_A$:

© 2022 Global Journals

$$\mathcal{L}_\phi = (\mathrm{D}^\mu\phi)^*\mathrm{D}_\mu\phi - \mu^2\phi^*\phi - \lambda(\phi^*\phi)^2, \quad \mathrm{D}_\mu \equiv \partial_\mu - ieA_\mu, \tag{53}$$

$$\mathcal{L}_A = -(1/4)F_{\mu\nu}F^{\mu\nu}, \quad F_{\mu\nu} = \partial_\mu A_\nu - \partial_\nu A_\mu, \tag{54}$$

where e is the electric charge, $\lambda(>0)$ being a constant parameter, and another parameter μ^2 taking positive or negative values (according to the tradition of field theory). The Lagrangian $\mathcal{L}_\phi$ is invariant under the local U(1) transformation.

For $\mu^2 > 0$, the Lagrangian describes physics of a massless gauge field A_μ coupled with a complex scalar field ϕ of mass μ with ϕ^4 self-interaction. This corresponds to the case of our transparent gauge field considered in § IV c) (1), where the *transparent gauge field* corresponds to the *massless gauge boson* in this analogy, while the *particle field* ϕ corresponds to *fluid current field*.

For $\mu^2 < 0$, the field will acquire a vacuum expectation value $\phi_0 = \langle\phi\rangle_0 = v/\sqrt{2}$ ($v^2 = -\mu^2/\lambda > 0$), and new symmetries emerge. As traditional, let us take the minimum ϕ_0 along the direction of the real part of ϕ and expand the ϕ-field in its vicinity: $\phi(x) = (1/\sqrt{2})(v + \phi_1(x) + i\,\phi_2(x))$. Substituting this form, the Lagrangian $\mathcal{L} = \mathcal{L}_A + \mathcal{L}_\phi$ can be rearranged as $\mathcal{L} \equiv \mathcal{L}^{\mathrm{Higgs}} = \mathcal{L}_\phi^{(m)} + \mathcal{L}_{\mathrm{intG}} + \mathcal{L}_A^{(m)}$, where

$$\mathcal{L}_\phi^{(m)} = \tfrac{1}{2}\,(\partial_\mu\phi_1)^2 + \tfrac{1}{2}\,(\partial_\mu\phi_1)^2 - \tfrac{1}{2}\,m_\phi^2\phi_1^2, \tag{55}$$

$$\mathcal{L}_{\mathrm{intG}} = m_A\,A_\mu\partial^\mu\phi_2 \ \ (\text{a Goldstone-mode term}), \tag{56}$$

$$\mathcal{L}_A^{(m)} = -(1/4)\,F_{\mu\nu}F^{\mu\nu} + \tfrac{1}{2}\,m_A^2 A_\mu A^\mu, \tag{57}$$

where $m_\phi^2 = 2v^2\lambda$ and $m_A = ev$. The third $\mathcal{L}_A^{(m)}$ describes the gauge field A_μ which acquired a mass term proportional to m_A^2. One can see similarity of the above triplet of Lagrangians, $[\mathcal{L}_\phi^{(m)}, \mathcal{L}_{\mathrm{intG}}, \mathcal{L}_A^{(m)}]$ in each form with the triplet of FGT Lagrangians, $[\mathcal{L}_{\mathrm{fluid}}, \mathcal{L}_{\mathrm{int}}, \mathcal{L}_a]$ given by (7), (8) and (9).

Most obvious similarity is seen in the forms of $\mathcal{L}_{\mathrm{intG}}$ of (56) and $\mathcal{L}_{\mathrm{int}} = c^{-1}j^\nu\,a_\nu$ of (8), comparing those from the viewpoint of the *de Broglie* concept for the momentum associated with $\partial^\mu\phi_2$ of (56), in which the factor $A_\mu\partial^\mu\phi_2$ is analogous to $a_\nu j^\nu$ of $\mathcal{L}_{\mathrm{int}}$. Next, the first member $\mathcal{L}_\phi^{(m)}$ describes the massive scalar particle field ϕ, while its FGT counterpart $\mathcal{L}_{\mathrm{fluid}}$ describes the massive fluid current.

In the beginning, the Lagrangian $\mathcal{L}_A$ described the massless gauge boson, which has been transformed to $\mathcal{L}_A^{(m)}$ having a mass term $\frac{1}{2}\,m_A^2 A_\mu A^\mu$ after the transition. Corresponding FGT Lagrangian is $\mathcal{L}_a$ of (9), and the FGT gauge field a_ν is governed by the equation (13): $\partial_\lambda f^{\nu\lambda} = \mu\,j^\nu$. Obviously, the field tensor $f^{\nu\lambda}$ is controlled and *colored* by the fluid current j^ν giving an inertial effect (*i.e.* an inertial influence) on the evolution of the gauge field a_ν.

VII. Summary

In the Kundt tube experiment [1], an interesting anomaly is known, *i.e.* there existed two characteristic scales observed in the experiment. One is the wave-length λ_r of the sound

© 2022 Global Journals

wave in resonance within the tube, and the other is the dust striations formed in the resonant standing wave characterized with much shorter longitudinal scales ℓ. Formation mechanism of the second dust striations has remained unresolved for a long time.

Fluid Gauge Theory has been proposed to explain the formation mechanism of the dust striation. The new fluid theory is based on the concepts of the gauge theories in Physics. Although certain fluid motions are described by both of the traditional Eulerian equations and the new Fluid Gauge Theory, there is a difference between the two. The flow field of the FGT theory is now accompanied by a gauge field behind it. In this case, the pressure stress field is *isotropic*, the gauge field is transparent and the flow field is mainly irrotational. However, the invisible gauge field acts to guarantee the law of mass conservation.

Fluid Gauge Theory [13] eventually allows transition of the isotropic pressure stress field existing in the Eulerian field to anisotropic stress field. Correspondingly, the flow field becomes rotational and the trace of gauge field is visualized by eddies. In this case too, the mass conservation is ensured by the action of the background gauge field. Owing of this, the FGT theory does not set the continuity equation *a priori* from the outset. Transition of the stress field from the isotropic to anisotropic occurs spontaneously. The transition from irrotational flow field to rotational one is often caused by the action of viscosity (existing in real fluids).

Fluid Gauge Theory can represent new mechanism of transverse rotational waves of a characteristic length scale ℓ, which coexists in the field of longitudinal irrotational acoustic waves in resonance of another scale λ_r. This is the case of the dust striation. Since the oscillation frequencies of both modes share the same excitation frequency, the difference of the two longitudinal scales might be associated with the difference of respective phase velocity: one is c_s (the sound velocity of irrotational waves) and the other c_g (the velocity of rotational waves of gauge field). Thus, we have $\ell/\lambda_r = c_g/c_s$. Before the transition, there existed only the longitudinal irrotational acoustic waves. This is understood as a symmetry transition in the acoustic system according to the Fluid Gauge Theory. The larger acoustic scale of the resonance mode is that described by the Eulerian system. The second new smaller scales are generated by rotational eddy modes, predicted by the Fluid Gauge Theory.

It is surprising that the Lagrangian representation of the Fluid Gauge Theory has disclosed the similarity of two phenomena observed in quite different physical fields: one is the spontaneous formation of dust striation in the Kundt's acoustic experiment and the other the Higgs Mechanism of the particle physics. It is a quite unexpected finding that an analogy exists between the Lagrangian structures of both systems: Kundt and Higgs. Each system is described by a triplet of Lagrangians, each of which has similarity respectively. Most obvious similarity is seen in the forms of the Lagrangian describing interactions (see § VI).

When there is a prolonged powerful acoustic excitation, *steady streaming* is generated within the tube filled with standing waves. The steady streaming is generated by the combined action of the nonlinear Reynolds stress and the viscous shear effect. Andrade [6] presented experimental photographs showing this steady streaming. However, this was observed under prolonged intensive sound waves. Lowering the intensity, but still above a critical intensity, he observed ripple-like striation with using minute cork particles.

Finally, it is emphasized the *dust striation* is a visualized trace of a background rotational gauge field existing in the acoustic field of longitudinal irrotational waves. The formation mechanism of dust striation is understood as a spontaneous transition of symmetry in the acoustics, analogous to that known in the field theory.

© 2022 Global Journals

Appendix

Appendix A: Energy equation and Entropy equation of a viscous fluid

Suppose a viscous fluid in motion with its thermodynamic state characterized with the density ρ, pressure p, specific internal energy ε, specific entropy s and specific enthalpy h (specific denoting per unit mass), and temperature T. The continuity equation (20) and the equation of motion (30) are

$$\partial_t \rho + \nabla \cdot (\rho \boldsymbol{v}) = 0, \qquad \rho\, \partial_t v_k + \rho\, \boldsymbol{v} \cdot \nabla v_k = -\partial_k p + \partial_j \sigma^{jk}_{\rm vis}\,. \tag{A1}$$

The stress $\sigma^{jk}_{\rm vis}$ is rewritten as $\sigma^{\rm (vis)}_{jk}$ below.

Energy density (per unit volume) of the fluid in motion with velocity $\boldsymbol{v} = (v_k)$ is given by $E = \frac{1}{2}\,\rho v^2 + \rho\varepsilon$. Total energy flux F_k passing through unit area in a fluid per unit time to the x_k-direction is given by $F_k = \rho v_k(\frac{1}{2}\,v^2 + h) - v_j\,\sigma^{\rm (vis)}_{jk} - \kappa\partial_k T$ where κ is the thermal conductivity (from [12], §49). According to the general law of physics, the conservation of energy is expressed by $\partial_t E = -\partial_k F_k$. Namely, we have

$$\partial_t(\tfrac{1}{2}\,\rho v^2 + \rho\varepsilon) = -\partial_k\left(\,\rho v_k(\tfrac{1}{2}\,v^2 + h) - v_j\,\sigma^{\rm (vis)}_{jk}\,\right). \tag{A2}$$

where the thermal conduction effect ($\kappa\partial_k T$) is omitted for simplicity because this section is concerned with only the mechanism of viscous dissipation of kinetic energy $\frac{1}{2}\,\rho v^2$ and associated increases of the internal energy ε and entropy s.

According to §49 of [12], using the continuity equation and equation of motion of (A1) helped by thermodynamic relations[12], the left-hand side of (A2) can be transformed to

$$\partial_t(\tfrac{1}{2}\,\rho v^2 + \rho\varepsilon) = -\partial_k\left(\,\rho v_k(\tfrac{1}{2}\,v^2 + h) - v_j\,\sigma^{\rm (vis)}_{jk}\,\right)$$

$$+\rho\,T\,(\partial_t s + \boldsymbol{v}\cdot\nabla s) - \sigma^{\rm (vis)}_{jk}\;\partial_k v_j\;. \tag{A3}$$

Comparing both of the right-hand side of (A2) and (A3), the second line of (A3) must vanish. Hence we have the entropy equation,

$$\rho\,T\left(\partial_t s + \boldsymbol{v}\cdot\nabla s\right) = \sigma^{\rm (vis)}_{jk}\;\partial_k v_j\,, \tag{A4}$$

in addition to the energy equation (A2). The quantity $\sigma^{\rm (vis)}_{jk}\;\partial_k v_j$ on the right-hand side is shown to be positive by (34) in the main text (§ IV. C. (3)).

The above result states that the total energy is conserved by the equation (A2) if the heat energy is taken into account, where the heat energy is transformed from the kinetic energy and an associated increase of the entropy s is given by the equation (A4) characterizing the thermodynamic state of the fluid.

Lastly, it would be instructive to consider that the last term $-v_j\,\sigma^{\rm (vis)}_{jk}$ on the right of (A2) is regarded as a energy flux (*i.e.* a rate of working) due to the viscosity action. Consider a

[12] Enthalpy: $h = \varepsilon + p/\rho$; Differentials of state variables: $\mathrm{d}\varepsilon = T\,\mathrm{d}s + (p/\rho^2)\,\mathrm{d}\rho$; $\partial_t\varepsilon = T\,\partial_t s + (p/\rho^2)\,\partial_t\rho$, and $\partial_t\rho = -\partial_k(\rho v_k)$. Time derivatives: $\partial_t(\frac{1}{2}\,\rho v^2) = \rho v_k\partial_t v_k = \rho v_k(-v_k\partial_k v_k - v_k\partial_k p + v_k\partial_j\sigma^{\rm (vis)}_{jk})$, $\partial_t(\rho\varepsilon) = \rho\partial_t\varepsilon + \varepsilon\partial_t\rho = \rho T\partial_t s + h\,\partial_t\rho = \rho T\partial_t s - h\,\partial_k(\rho v_k)$. $\rho v_k\partial_k\varepsilon = \rho v_k T\,\partial_k s + (p/\rho)v_k\partial_k\rho$.

© 2022 Global Journals

fluid volume $\mathcal{V}$ surrounded by a closed surface $\mathcal{S}$. The rate at which a work W is done to outside fluid across the surface $\mathcal{S}$ by the fluid in $\mathcal{V}$ with the viscous stress $\sigma^{(\mathrm{vis})}_{jk}$ is given by

$$W = \int_{\mathcal{S}} v_j\, \sigma^{(\mathrm{vis})}_{jk}\, n_k \mathrm{d}S = \int_{\mathcal{V}} \partial_k (v_j \sigma^{(\mathrm{vis})}_{jk})\, \mathrm{d}V = \int_{\mathcal{V}} \Big[\, v_j\, \partial_k \sigma^{(\mathrm{vis})}_{jk} + \big(\partial_k v_j\big)\, \sigma^{\mathrm{vis}}_{jk} \Big] \mathrm{d}V$$

$$= \int_{\mathcal{V}} v_k F^{(\mathrm{vis})}_k\, \mathrm{d}V + \int_{\mathcal{V}} \big[\, (\partial_k v_j) \sigma^{(\mathrm{vis})}_{jk} \big] \mathrm{d}V, \qquad F^{(\mathrm{vis})}_k \equiv \partial_j \sigma^{(\mathrm{vis})}_{jk}\,. \tag{A5}$$

where $\sigma^{(\mathrm{vis})}_{jk} = \sigma^{(\mathrm{vis})}_{kj}$, and n_k is unit outward normal to the enclosing surface $\mathcal{S}$. Since the work W is done to external fluid, the work to the fluid inside $\mathcal{S}$ is $W_{\mathrm{in}} = -W$. This implies the term $-v_j\, \sigma^{(\mathrm{vis})}_{jk}$ denotes the work (an energy flux) within the fluid itself.

The integrand $v_k F^{(\mathrm{vis})}_k$ in the first integral of (A5) denotes the mechanical work done by the viscous force $F^{(\mathrm{vis})}_k = \partial_j \sigma^{jk}_{\mathrm{vis}}$ of (A1), while the integrand $(\partial_k v_j)\, \sigma^{(\mathrm{vis})}_{jk}$ in the second integral denotes the energy dissipated into heat by the viscous action. The last is nothing but the expression of the right-hand side of (A4), confirming the consistence of the theory.

Appendix B: Oscillatory Boundary Layers

In order to see the difference and transition of the stress fields before and after certain spontaneous change, simple model analyses are presented in this Appendix B.

Let us consider a fluid in $2d$ (x, y)-channel with the channel axis to the x-direction and its width H to the normal y-direction. Not only the sound oscillation in the channel, but also other special conditions are imposed to consider analogous model problems. The fluid is supposed to be under pressure p_e, which is either uniform (with uniform fluid density ρ_0) in the first case B 1, or subjected to a pressure gradient $P \equiv -\partial p_e/\partial x$ in the x-direction which is uniform spatially but oscillates sinusoidally in time $P(t)$ in the second case B 2. Regarding the boundary conditions, the upper wall $y = H$ is kept at rest, while the lower wall $y = 0$ is in motion or at rest depending on each case. The fluid observes the no-slip condition on both walls.

In the third case B 3, P is $P(t, x)$, periodic both temporally and spatially, and the fluid follows the no-slip condition on both walls at rest. Representative velocity u' of fluid flow is assumed very small compared to the sound speed c_s, and the density change $\Delta\rho$ is related to the pressure change Δp isentropically, with the specific entropy s being fixed:

$$\Delta p = c_s^2\, \Delta\rho, \qquad c_s^2 = \partial p/\partial\rho\big|_{s:\mathrm{fixed}}. \tag{B1}$$

The relative density change $\Delta\rho/\rho_0$ is small,[13], of the order of 10^{-3}.

Before the transition, the motion is governed by the equation (18) under the isotropic pressure stress σ^{jk}_{I}. However in this model analysis, no-slip condition is applied on both of the upper and lower walls, so that the viscous stress term $\sigma^{jk}_{\mathrm{vis}}$ is included in the equation of motion. Furthermore, the fluid motion is assumed to take *unidirectional* velocity field, $\boldsymbol{v}_{\mathrm{uni}} = (u(y,t), 0, 0)$, governed by the Navier-Stokes equation (30).

[13] The equation (B2) can be written as $\rho\,\partial_t u \approx -\partial_x p_e$ out of thin viscous boundary layer. Using $\rho\partial_t u \approx \rho_0 i\omega u' = i\rho_0 k c_g u'$ and $\partial_x p_e = (\partial p_e/\partial\rho)\partial_x\rho \approx c_s^2 ik\rho'$. Then, $|\rho'/\rho_0| \approx |u'/c_s|(c_g/c_s) \approx 10^{-3}$.

© 2022 Global Journals

For the unidirectional flow field $\boldsymbol{v}_{\rm uni}$, the NS-eq.(30) reduces to

$$\rho\,\partial_t u = P + \rho\,\nu\,\partial_y^2 u\,, \qquad P = -\partial p_e/\partial x, \quad \nu \equiv \eta/\rho. \tag{B2}$$

Let us now consider the above three cases, step by step, in order to arrive at desired expressions, with improving boundary conditions imposed at the lower wall and with-and-without pressure oscillation.

1. *Lower wall oscillates in its own plane while upper wall kept at rest*

First, the lower wall makes a time periodic motion of a period T with its x-velocity U_w represented by the real part of $u_w e^{i\omega t}$ with $\omega = 2\pi/T$ the angular frequency:

$$U_w(t) = \Re[u_w\, e^{i\omega t}] = u_w\, \cos 2\pi(t/T), \tag{B3}$$

where u_w is real and denotes the amplitude of wall oscillation. Namely the wall is moving in its own plane with a sinusoidal oscillation. The solution $u(y,t)$ satisfying (B2) is given by

$$u(y,t) = \Re\Big[u_w\, e^{i\omega t}\, \frac{\sinh[K(1-Y)]}{\sinh K}\Big]; \quad Y = \frac{y}{H}, \quad \frac{K}{H} = \Big(\frac{i\omega}{\nu}\Big)^{1/2} = \sqrt{\frac{\omega}{2\nu}}(1+i). \tag{B4}$$

One can easily check that this satisfies not only the equation (B2) under $P = 0$, but the boundary conditions at $y = 0$ and H as well.

As $H \to \infty$, this tends to the solution found by Stokes:

$$u(y,t) \to \Re\big[u_w\, e^{i\omega t} \exp\,[-(i\,\omega/\nu)^{1/2}\, y]\ \big], \tag{B5}$$

This solution represents an oscillating motion adjacent to the wall, called the *Stokes' oscillatory boundary layer* (see §4.3 of [10], or §4.7 of [11]). This is generated by the viscous dragging effect caused by the oscillating boundary wall at $y = 0$. The viscous dragging is expressed by the exponential factor:

$$\exp\,[-(i\,\omega/\nu)^{1/2}\, y] = \exp\,[-(\omega/2\nu)^{1/2}\, y] \cdot \exp\,[-i(\omega/2\nu)^{1/2}\, y]$$

since $\sqrt{i} = (1+i)/\sqrt{2}$. The effective thickness $\delta_{\rm vis}$ of the viscous layer is found from the first factor $\exp\,[-(1/\delta_{\rm vis})\, y]$ where $\delta_{\rm vis} = \sqrt{2\nu/\omega}$. The second factor $\exp\,[-i\,(y/\delta_{\rm vis})]$, combined with the time factor $e^{i\omega t}$ of (B5), represents a wave propagating away from the wall: $\exp\,[i(\omega t - (y/\delta_{\rm vis})\,)\,]$.

The thickness $\delta_{\rm vis} = \sqrt{2\nu/\omega}$ is found very small, compared with an experimental channel width $H \approx 5\,cm$, if we take the experimental frequency $f = \omega/(2\pi)$ of the order $10^3\,s^{-1}$ and the air kinematic viscosity $\nu_{\rm air} = 0.15\,cm^2 s^{-1}$ (at normal conditions): $\delta_{\rm vis} \approx 10^{-2}\,cm$, and $H/\delta_{\rm vis} \approx 10^3$.

2. *Time-periodic oscillation of pressure gradient with walls at rest*

In the previous section B 1, the time periodic oscillation $e^{i\omega t}$ is imposed uniformly to the lower wall. Here, instead of the wall motion, a pressure oscillation is applied to the whole fluid (in the channel) uniformly with $P(t) = P_0\, e^{i\omega t}$ at all points, with the static condition $U_w = 0$ applied at the wall boundaries.

© 2022 Global Journals

First, we consider the case $H \to \infty$ and use the solution (B5) in order to find a solution of the present case. Far away from the lower wall ($y/\delta_{\rm vis} \gg 1$), the viscous dragging effect by the no-slip condition at the wall $y = 0$ decays exponentially as $y/\delta_{\rm vis}$ increases, and the equation (B2) tends to be approximated by $\rho\,\partial_t u = P(t)$. Assuming $u \propto e^{i\omega t}$, this is solved by $u_\infty = (\rho\, i\,\omega)^{-1} P(t)$, where $\partial_t u = i\omega u$ is used.

Regarding the full equation (B2), let us assume $u(y,t)$ having the time factor $e^{i\omega t}$ and write as $u(y,t) - u_\infty = u_\infty\, f(y)$ by using unknown function $f(y)$, the equation (B2) can be written as $(\rho\, i\omega)\,\big(u_\infty + u_\infty\, f(y)\big) = (\rho\, i\,\omega) u_\infty + \rho\,\nu\, u_\infty \partial_y^2 f$ with using $P = (\rho\, i\omega)\, u_\infty$. This reduces to an ordinary differential equation for $f(y)$:

$$f''(y) - (i\omega/\nu)\, f(y) = 0. \tag{B6}$$

where the boundary conditions are: $f(0) = -1$ to satisfy $u(0,t) = 0$ and $f(\infty) = 0$ to satisfy $u(0,t) = u_\infty$. Thus, the solution $u(y,t)$ of (B2), tending to u_∞ as $y/\delta_{\rm vis} \to \infty$, is given by

$$u(y,t) = \Re\big[(\rho\, i\,\omega)^{-1} P(t)\ [1 - \exp\{-(i\,\omega/\nu)^{1/2}\, y\}]\ \big], \quad P(t) = P_0\, e^{i\omega t}. \tag{B7}$$

This solution (B7) has been found for the infinite fluid layer with $H \to \infty$. However, in view of the estimate given in the last paragraph of B 1 where $H/\delta_{\rm vis} \approx 10^3$, one may use (B7) for a finite H with sufficient accuracy. This solution (B7) can be used practically as the $u(y,t)$ for the lower half $0 < y \le \frac{1}{2} H$ of the channel under the oscillation pressure gradient P (simulating an acoustic oscillation),

3. *Pressure oscillation both time-periodic and space-periodic*

Here, in addition to the time periodic motion (of period T), a space-periodic structure (with a wavelength λ_g)[14] is imposed for the pressure gradient $P \equiv -\partial p_e/\partial x$ to the x-direction, represented as[15]

$$P_+(t,x) = P_0\, e^{i\omega t}\ e^{+ikx}, \qquad \omega = 2\pi/T, \quad k = 2\pi/\lambda_g, \tag{B8}$$

with the condition $U_w = 0$ applied at the wall boundaries. The solution $u(t,x,y)$ to

$$\rho\,\partial_t u = P_+ + \rho\,\nu\,\partial_y^2 u\,, \qquad P_+ = -\partial p_e/\partial x, \tag{B9}$$

(equivalent to (B2)), tending to $U^\dagger_{\rm ex}(t,x)$ as $y/\delta_{\rm vis} \to \infty$, is given by

$$u_+(t,x,y) = \Re\big[U^\dagger_{\rm ex}(t,x)\ F(y)\big], \qquad U^\dagger_{\rm ex}(t,x) = (\rho\, i\,\omega)^{-1} P_+(t,x), \tag{B10}$$

$$F(y) = 1 - \exp\{-(i\,\omega/\nu)^{1/2}\, y\}. \tag{B11}$$

[14] The wavelength λ_g is defined by $c_g\, T$, where c_g is the phase speed of the gauge field a_ν and T denotes the same period of sound vibration. For the sound speed $c_s = 344$ m/s (at 20° C), the sound wavelength λ_s is given by $c_s\, T$, and the following parameters are used: $c_g/c_s = \lambda_g/\lambda_s = 0.031$ and $u_w/c_g = 0.05$.

[15] The suffices "+" or "†" denote the expressions derived from the x-space periodicity e^{+ikx}. This is to discriminate those derived from the e^{-ikx} periodicity to be given next.

© 2022 Global Journals

Corresponding y-component $v_+(t,x,y)$ is given by

$$v_+(t,x,y) = \Re\big[\ (\nu/i\omega)^{1/2}\ \big(\partial U^\dagger_{\rm ex}/\partial x\big)\ F(y)\big], \tag{B12}$$

We can calculate $\partial_x u_+ + \partial_y v_+$, which is found as

$$\partial_x u_+ + \partial_y v_+ = \Re\big[\partial_x U^\dagger_{\rm ex}\ \big((1-e^{-\kappa y}) + e^{-\kappa y}\big)\big] = \Re\big[\partial_x U^\dagger_{\rm ex}\big] = \Re\big[-ik/(\rho\, i\,\omega) P^\dagger_{\rm ex}\big]$$

$$= \Re\big[-(1/\rho_0)\, i\omega \rho^\dagger_{\rm ex}\big] = -(1/\rho_0)\,\partial_t \rho^\dagger_{\rm ex}. \tag{B13}$$

since $P^\dagger_{\rm ex} = -\partial_x p^\dagger_{\rm ex} = ik(c_s^2 \rho^\dagger_{\rm ex}) = i(\omega^2/k)\rho^\dagger_{\rm ex}$ and $\omega = kc_s$. The last expression implies the following linearized continuity equation:

$$\partial_t \rho^\dagger_{\rm ex} + \rho_0(\partial_x u_+ + \partial_y v_+) = 0. \tag{B14}$$

Next, under another pressure gradient given by $P_-(t,x) = P_0\, e^{i\omega t}\ e^{-ikx}$, one can easily find the solution $u_-(t,x,y)$ with the parallel analysis, represented as

$$u_-(t,x,y) = \Re\big[U^-_{\rm ex}(t,x)\ F(y)\big], \qquad U^-_{\rm ex}(t,x) = (\rho\, i\,\omega)^{-1} P_-(t,x), \tag{B15}$$

Thus, we can give a representation of the external x-velocity in a resonant sound wave by the linear combination of $u_+(t,x,y)$ and $u_-(t,x,y)$:

$$u_{\rm res}(t,x,y) = u_+ + u_- = \Re\big[U^\dagger_{\rm ex}(t,x)\ F(y)\big] + \Re\big[U^-_{\rm ex}(t,x)\ F(y)\big]$$

$$= \Re\big[\, u_{\rm ex}(x)\ e^{i\omega t}\ F(y)\big], \quad u_{\rm ex}(x) = \frac{2}{i\,\rho_0\,\omega}\, P_0\, \cos\, kx. \tag{B16}$$

4. *Lower wall tangential oscillation both time-periodic and space-periodic*

Lower wall oscillates tangentially with both time-periodic $e^{i\omega t}$ and space-periodic $\cos\, kx$, with a period T ($\omega = 2\pi/T$) and a wave-length $\lambda_g = 2\pi/k$. The wall velocity $u|_{y=0}$ is

$$U_w(t,x) = \Re[u_w\, \cos\, kx\, e^{i\omega t}] = u_w\, \cos\, kx\, \cos 2\pi(t/T), \quad k = 2\pi/\lambda_g, \tag{B17}$$

where u_w is real, denoting the amplitude of wall oscillation. Figure 3 compares two velocity fields generated by two different stress fields for the same wall motion of (B17). The figure (a) on the left is the Stokes-type oscillatory layer (Eulerian + viscosity: under transparent gauge field):

$$u(t,x,y,) = u_w\, \cos\, kx\ \ \Re\big[e^{i\omega t}\, \exp\{-(i\,\omega/\nu)^{1/2}\, y\}\big], \tag{B18}$$

derived from (41) $\sim$ (43) of § V, with deleting $u_{\rm ex}(x)$ and the sign reversed.

Next, the figure (b) on the right is the wavy layer obtained from the FGT system (FGT+viscosity under vectorial (colored) gauge field a_ν). One can see remarkable difference between the two fields.

© 2022 Global Journals

Acknowledgments

The author would like to express gratitude to the Royal Society and the journal *Philosophical Transactions of the Royal Society* for permission to use the FIG.1 and FIG.2 cited from [7] and FIG.5 cited from [6], both paper published ninety years ago.

The finite element analysis of the present study was carried out by the courtesy of Mr. Masanori Hashiguchi (Professional Engineer Japan; Former researcher of *i*CFD). Concerning the financial support to carry out the present study, the author would like to express heartfelt thanks to Mr. Kousuke Umadume, President of Institute of Japan Ship Model (WASEN).

References Références Referencias

1. August Kundt, Ueber eine neue Art akustischer Staubfiguren und über die Anwendung derselben zur Bestimmung der Schallgeschwindigkeit in festen Körpern und Gasen, Ann. der Physik & Chemie, vol.127, 497 - 523 (1866).
2. Dvorak, Ann. der Physik, vol.153, 102 - 115 (1874);
3. V. Dvorak, Ann. der Physik, vol.157, 42 - 73 (1876).
4. J. W. S. Rayleigh, *The Theory of Sound*, Vol. Two (1896).
5. E. N. Da C. Andrade, Phenomena in a sounding tube, Nature, p.438, March 21 (1931).
6. E. N. Da C. Andrade, On the circulations caused by the vibration of air in a tube, Proc. Roy. Soc. A134, 445 - 470 (1931).
7. E. N. Da C. Andrade, On the groupings and general behaviour of solid particles under the influence of air vibrations in tubes, Phil. Trans. Roy. Soc. A230, 413-445 (1932).
8. R. A. Carman, Kundt Tube Dust Striations, American J. of Phys. 23, 505 - 507 (1955)
9. G. K. Batchelor, *The Theory of Homogeneous Turbulence,* Cambridge University Press (1953).
10. G. K. Batchelor, *An Introduction to Fluid Dynamics,* Cambridge University Press (1967).
11. James Lighthill, *Waves in fluids,* Cambridge University Press (1978).
12. L.D. Landau and E.M. Lifshitz, *Fluid Mechanics* (Pergamon Press, 2nd ed.) (1987).
13. T. Kambe, Fluid Gauge Theory. Global Journal of Sci. Front. Res. A, vol.21 (4), 113-147 (2021)
14. T. Kambe, Gauge symmetries in physical fields (Review), Global Journal of Sci. Front. Res. A, vol.21 (4), 1- 44.
15. R. Utiyama, Invariant theoretical interpretation of interaction, Phys. Rev. 101, 1597 - 1607(1956).
16. R. Utiyama, Introduction to General Gauge *Field Theory* [book in Japanese], (Iwanami, Tokyo) (1987).
17. Kambe T., New representation of rotational flow fields satisfying Euler's equation of an ideal compressible fluid, *Fluid Dyn. Res.* 45, 015505 (16pp) (2013).
18. Scofield D. F. and Pablo Huq, Fluid dynamical Lorentz force law and Poynting theorem – derivation and implications. *Fluid Dyn. Res.,* 46, 055514 (22pp) (2014).
19. Kambe T., New scenario of turbulence theory and wall-bounded turbulence: Theoretical significance, Geophys. *Astrophys. Fluid Dyn.* 111, 448-507, (2017).

© 2022 Global Journals

20. Kambe T 2020 New perspectives on mass conservation law and waves in fluid mechanics, *Fluid Dyn. Res.* 52, 1 - 34 (2020).
21. Djouadi A. 2008: The anatomy of electro-weak symmetry breaking, I: The Higgs boson in the standard model, Phys. Rept. 457: 1-216; LPT-Orsay-05-18,
22. Laura Reina 2011: lectures on Higgs-Boson Physics, Proc. of TASI 2011, arXiv: 1208.5504 [hep-ph].
23. Y. Nambu, Spontaneous Symmetry Breaking in Particle Physics: A Case of Cross Fertilization, Nobel Lecture (2008).

Note Added in Proof:

The spontaneous symmetry breaking (SSB) is explained by the Nobel Laureate *Yoichiro NAMBU* in his Nobel Lecture [23] in 2008: "*Spontaneous Symmetry Breaking in Particle Physics: A Case of Cross Fertilization*", in which the following illustrative example is given:

> "$\cdots$ In fact, it (*SSB*) is a very familiar one in our daily life. For example, consider an elastic straight rod (*of circular cross-section*) standing vertically. It has a rotational symmetry; it looks the same from any horizontal direction. But if one applies increasing pressure (*pressing stress*) to squeeze it, it will bend in some direction, and the symmetry is lost. The bending can occur in principle in any (*horizontal*) direction since all directions are equivalent. But you do not see it unless you repeat the experiment many times. This is SSB. $\cdots\cdots$ "

One can compare this example with our case of spontaneous symmetry transition in the Kundt's experiment. The initial state of the elastic straight rod (of circular cross-section) standing vertically corresponds, in our case, to the acoustic pure resonance of wavelength λ_r in a closed tube, which is governed by the Euler's equation of motion in a tranparent gauge field $a_\nu^{(0)} = \partial_\nu \Psi$.

As the acoustic intensity increases, the gauge field a_ν shows spontaneously its appearance at a transition when the field a_ν is colored with a characteristic wave-length ℓ of transverse rotational waves, coexisting in the irrotational resonant acoustic waves of wave-length λ_r. The length ℓ is not unique, but depends on the fluid state concerning distributioin and degree of the rotational component of the background fluid motion. This is analogous to the case of rod bending. The horizontal direction of bending depends on the internal microscopic structure within the elastic rod.

Thus, it is understood that the elastic rod could be an illustrative example to our Kundt's experiment as well.

© 2022 Global Journals

Global Journals Guidelines Handbook 2022

www.GlobalJournals.org

Memberships

Fellows/Associates of Science Frontier Research Council

FSFRC/ASFRC Memberships



Introduction

FSFRC/ASFRC is the most prestigious membership of Global Journals accredited by Open Association of Research Society, U.S.A (OARS). The credentials of Fellow and Associate designations signify that the researcher has gained the knowledge of the fundamental and high-level concepts, and is a subject matter expert, proficient in an expertise course covering the professional code of conduct, and follows recognized standards of practice. The credentials are designated only to the researchers, scientists, and professionals that have been selected by a rigorous process by our Editorial Board and Management Board.

Associates of FSFRC/ASFRC are scientists and researchers from around the world are working on projects/researches that have huge potentials. Members support Global Journals' mission to advance technology for humanity and the profession.

FSFRC

Fellow of Science Frontier Research Council

FELLOW OF SCIENCE FRONTIER RESEARCH COUNCIL is the most prestigious membership of Global Journals. It is an award and membership granted to individuals that the Open Association of Research Society judges to have made a 'substantial contribution to the improvement of computer science, technology, and electronics engineering.

The primary objective is to recognize the leaders in research and scientific fields of the current era with a global perspective and to create a channel between them and other researchers for better exposure and knowledge sharing. Members are most eminent scientists, engineers, and technologists from all across the world. Fellows are elected for life through a peer review process on the basis of excellence in the respective domain. There is no limit on the number of new nominations made in any year. Each year, the Open Association of Research Society elect up to 12 new Fellow Members.

Benefit

To the institution

Get letter of appreciation

Global Journals sends a letter of appreciation of author to the Dean or CEO of the University or Company of which author is a part, signed by editor in chief or chief author.



Exclusive Network

Get access to a closed network

A FSFRC member gets access to a closed network of Tier 1 researchers and scientists with direct communication channel through our website. Fellows can reach out to other members or researchers directly. They should also be open to reaching out by other.

Career | Credibility | Exclusive | Reputation



Certificate

Receive a print ed copy of a certificate

Fellows receive a printed copy of a certificate signed by our Chief Author that may be used for academic purposes and a personal recommendation letter to the dean of member's university.

Career | Credibility | Exclusive | Reputation



Designation

Get honored title of membership

Fellows can use the honored title of membership. The “FSFRC” is an honored title which is accorded to a person’s name viz. Dr. John E. Hall, Ph.D., FSFRC or William Walldroff, M.S., FSFRC.

Career | Credibility | Exclusive | Reputation

Recognition on the Platform

Better visibility and citation

All the Fellow members of FSFRC get a badge of "Leading Member of Global Journals" on the Research Community that distinguishes them from others. Additionally, the profile is also partially maintained by our team for better visibility and citation. All fellows get a dedicated page on the website with their biography.

Career | Credibility | Reputation

© Copyright by Global Journals | Guidelines Handbook

Future Work

Get discounts on the future publications

Fellows receive discounts on future publications with Global Journals up to 60%. Through our recommendation programs, members also receive discounts on publications made with OARS affiliated organizations.

Career | Financial



GJ Internal Account

Unlimited forward of Emails

Fellows get secure and fast GJ work emails with unlimited forward of emails that they may use them as their primary email. For example,
john [AT] globaljournals [DOT] org.

Career | Credibility | Reputation



Premium Tools

Access to all the premium tools

To take future researches to the zenith, fellows and associates receive access to all the premium tools that Global Journals have to offer along with the partnership with some of the best marketing leading tools out there.

Financial

Conferences & Events

Organize seminar/conference

Fellows are authorized to organize symposium/seminar/conference on behalf of Global Journal Incorporation (USA). They can also participate in the same organized by another institution as representative of Global Journal. In both the cases, it is mandatory for him to discuss with us and obtain our consent. Additionally, they get free research conferences (and others) alerts.

Career | Credibility | Financial

Early Invitations

Early invitations to all the symposiums, seminars, conferences

All fellows receive the early invitations to all the symposiums, seminars, conferences and webinars hosted by Global Journals in their subject.

Exclusive



Publishing Articles & Books

Earn 60% of sales proceeds

Fellows can publish articles (limited) without any fees. Also, they can earn up to 60% of sales proceeds from the sale of reference/review books/literature/ publishing of research paper. The FSFRC member can decide its price and we can help in making the right decision.

Exclusive | Financial

Reviewers

Get a remuneration of 15% of author fees

Fellow members are eligible to join as a paid peer reviewer at Global Journals Incorporation (USA) and can get a remuneration of 15% of author fees, taken from the author of a respective paper.

Financial

Access to Editorial Board

Become a member of the Editorial Board

Fellows may join as a member of the Editorial Board of Global Journals Incorporation (USA) after successful completion of three years as Fellow and as Peer Reviewer. Additionally, Fellows get a chance to nominate other members for Editorial Board.

Career | Credibility | Exclusive | Reputation

And Much More

Get access to scientific museums and observatories across the globe

All members get access to 5 selected scientific museums and observatories across the globe. All researches published with Global Journals will be kept under deep archival facilities across regions for future protections and disaster recovery. They get 10 GB free secure cloud access for storing research files.

ASSOCIATE OF SCIENCE FRONTIER RESEARCH COUNCIL

ASSOCIATE OF SCIENCE FRONTIER RESEARCH COUNCIL is the membership of Global Journals awarded to individuals that the Open Association of Research Society judges to have made a 'substantial contribution to the improvement of computer science, technology, and electronics engineering.

The primary objective is to recognize the leaders in research and scientific fields of the current era with a global perspective and to create a channel between them and other researchers for better exposure and knowledge sharing. Members are most eminent scientists, engineers, and technologists from all across the world. Associate membership can later be promoted to Fellow Membership. Associates are elected for life through a peer review process on the basis of excellence in the respective domain. There is no limit on the number of new nominations made in any year. Each year, the Open Association of Research Society elect up to 12 new Associate Members.

To the institution

Get letter of appreciation

Global Journals sends a letter of appreciation of author to the Dean or CEO of the University or Company of which author is a part, signed by editor in chief or chief author.



Exclusive Network

Get access to a closed network

A ASFRC member gets access to a closed network of Tier 1 researchers and scientists with direct communication channel through our website. Associates can reach out to other members or researchers directly. They should also be open to reaching out by other.

Career | Credibility | Exclusive | Reputation



Certificate

Receive a print ed copy of a certificate

Associates receive a printed copy of a certificate signed by our Chief Author that may be used for academic purposes and a personal recommendation letter to the dean of member's university.

Career | Credibility | Exclusive | Reputation



Designation

Get honored title of membership

Associates can use the honored title of membership. The “ASFRC” is an honored title which is accorded to a person’s name viz. Dr. John E. Hall, Ph.D., ASFRC or William Walldroff, M.S., ASFRC.

Career | Credibility | Exclusive | Reputation

Recognition on the Platform

Better visibility and citation

All the Associate members of ASFRC get a badge of "Leading Member of Global Journals" on the Research Community that distinguishes them from others. Additionally, the profile is also partially maintained by our team for better visibility and citation. All associates get a dedicated page on the website with their biography.

Career | Credibility | Reputation

© Copyright by Global Journals | Guidelines Handbook

Future Work

Get discounts on the future publications

Associates receive discounts on the future publications with Global Journals up to 60%. Through our recommendation programs, members also receive discounts on publications made with OARS affiliated organizations.

Career | Financial



GJ Internal Account

Unlimited forward of Emails

Associates get secure and fast GJ work emails with unlimited forward of emails that they may use them as their primary email. For example,
john [AT] globaljournals [DOT] org.

Career | Credibility | Reputation



Premium Tools

Access to all the premium tools

To take future researches to the zenith, fellows receive access to almost all the premium tools that Global Journals have to offer along with the partnership with some of the best marketing leading tools out there.

Financial

Conferences & Events

Organize seminar/conference

Associates are authorized to organize symposium/seminar/conference on behalf of Global Journal Incorporation (USA). They can also participate in the same organized by another institution as representative of Global Journal. In both the cases, it is mandatory for him to discuss with us and obtain our consent. Additionally, they get free research conferences (and others) alerts.

Career | Credibility | Financial

Early Invitations

Early invitations to all the symposiums, seminars, conferences

All associates receive the early invitations to all the symposiums, seminars, conferences and webinars hosted by Global Journals in their subject.

Exclusive



Publishing Articles & Books

Earn 30-40% of sales proceeds

Associates can publish articles (limited) without any fees. Also, they can earn up to 30-40% of sales proceeds from the sale of reference/review books/literature/publishing of research paper.

Exclusive | Financial

Reviewers

Get a remuneration of 15% of author fees

Associate members are eligible to join as a paid peer reviewer at Global Journals Incorporation (USA) and can get a remuneration of 15% of author fees, taken from the author of a respective paper.

Financial

And Much More

Get access to scientific museums and observatories across the globe

All members get access to 2 selected scientific museums and observatories across the globe. All researches published with Global Journals will be kept under deep archival facilities across regions for future protections and disaster recovery. They get 5 GB free secure cloud access for storing research files.

© Copyright by Global Journals | Guidelines Handbook

Associate	Fellow	Research Group	Basic
$4800 **lifetime designation**	$6800 **lifetime designation**	$12500.00 **organizational**	APC **per article**
Certificate, LoR and Momento **2** discounted publishing/year **Gradation** of Research **10** research contacts/day **1 GB** Cloud Storage **GJ** Community Access	**Certificate,** LoR and Momento **Unlimited** discounted publishing/year **Gradation** of Research **Unlimited** research contacts/day **5 GB** Cloud Storage **Online Presense** Assistance **GJ** Community Access	**Certificates,** LoRs and Momentos **Unlimited** free publishing/year **Gradation** of Research **Unlimited** research contacts/day **Unlimited** Cloud Storage **Online Presense** Assistance **GJ** Community Access	**GJ** Community Access

Preferred Author Guidelines

We accept the manuscript submissions in any standard (generic) format.

We typeset manuscripts using advanced typesetting tools like Adobe In Design, CorelDraw, TeXnicCenter, and TeXStudio. We usually recommend authors submit their research using any standard format they are comfortable with, and let Global Journals do the rest.

Alternatively, you can download our basic template from https://globaljournals.org/Template.zip

Authors should submit their complete paper/article, including text illustrations, graphics, conclusions, artwork, and tables. Authors who are not able to submit manuscript using the form above can email the manuscript department at submit@globaljournals.org or get in touch with chiefeditor@globaljournals.org if they wish to send the abstract before submission.

Before and during Submission

Authors must ensure the information provided during the submission of a paper is authentic. Please go through the following checklist before submitting:

1. Authors must go through the complete author guideline and understand and *agree to Global Journals' ethics and code of conduct,* along with author responsibilities.
2. Authors must accept the privacy policy, terms, and conditions of Global Journals.
3. Ensure corresponding author's email address and postal address are accurate and reachable.
4. Manuscript to be submitted must include keywords, an abstract, a paper title, co-author(s') names and details (email address, name, phone number, and institution), figures and illustrations in vector format including appropriate captions, tables, including titles and footnotes, a conclusion, results, acknowledgments and references.
5. Authors should submit paper in a ZIP archive if any supplementary files are required along with the paper.
6. Proper permissions must be acquired for the use of any copyrighted material.
7. Manuscript submitted *must not have been submitted or published elsewhere* and all authors must be aware of the submission.

Declaration of Conflicts of Interest

It is required for authors to declare all financial, institutional, and personal relationships with other individuals and organizations that could influence (bias) their research.

Policy on Plagiarism

Plagiarism is not acceptable in Global Journals submissions at all.

Plagiarized content will not be considered for publication. We reserve the right to inform authors' institutions about plagiarism detected either before or after publication. If plagiarism is identified, we will follow COPE guidelines:

Authors are solely responsible for all the plagiarism that is found. The author must not fabricate, falsify or plagiarize existing research data. The following, if copied, will be considered plagiarism:

- Words (language)
- Ideas
- Findings
- Writings
- Diagrams
- Graphs
- Illustrations
- Lectures

- Printed material
- Graphic representations
- Computer programs
- Electronic material
- Any other original work

Authorship Policies

Global Journals follows the definition of authorship set up by the Open Association of Research Society, USA. According to its guidelines, authorship criteria must be based on:

1. Substantial contributions to the conception and acquisition of data, analysis, and interpretation of findings.
2. Drafting the paper and revising it critically regarding important academic content.
3. Final approval of the version of the paper to be published.

Changes in Authorship

The corresponding author should mention the name and complete details of all co-authors during submission and in manuscript. We support addition, rearrangement, manipulation, and deletions in authors list till the early view publication of the journal. We expect that corresponding author will notify all co-authors of submission. We follow COPE guidelines for changes in authorship.

Copyright

During submission of the manuscript, the author is confirming an exclusive license agreement with Global Journals which gives Global Journals the authority to reproduce, reuse, and republish authors' research. We also believe in flexible copyright terms where copyright may remain with authors/employers/institutions as well. Contact your editor after acceptance to choose your copyright policy. You may follow this form for copyright transfers.

Appealing Decisions

Unless specified in the notification, the Editorial Board's decision on publication of the paper is final and cannot be appealed before making the major change in the manuscript.

Acknowledgments

Contributors to the research other than authors credited should be mentioned in Acknowledgments. The source of funding for the research can be included. Suppliers of resources may be mentioned along with their addresses.

Declaration of funding sources

Global Journals is in partnership with various universities, laboratories, and other institutions worldwide in the research domain. Authors are requested to disclose their source of funding during every stage of their research, such as making analysis, performing laboratory operations, computing data, and using institutional resources, from writing an article to its submission. This will also help authors to get reimbursements by requesting an open access publication letter from Global Journals and submitting to the respective funding source.

Preparing your Manuscript

Authors can submit papers and articles in an acceptable file format: MS Word (doc, docx), LaTeX (.tex, .zip or .rar including all of your files), Adobe PDF (.pdf), rich text format (.rtf), simple text document (.txt), Open Document Text (.odt), and Apple Pages (.pages). Our professional layout editors will format the entire paper according to our official guidelines. This is one of the highlights of publishing with Global Journals—authors should not be concerned about the formatting of their paper. Global Journals accepts articles and manuscripts in every major language, be it Spanish, Chinese, Japanese, Portuguese, Russian, French, German, Dutch, Italian, Greek, or any other national language, but the title, subtitle, and abstract should be in English. This will facilitate indexing and the pre-peer review process.

The following is the official style and template developed for publication of a research paper. Authors are not required to follow this style during the submission of the paper. It is just for reference purposes.

Manuscript Style Instruction (Optional)

- Microsoft Word Document Setting Instructions.
- Font type of all text should be Swis721 Lt BT.
- Page size: 8.27" x 11'", left margin: 0.65, right margin: 0.65, bottom margin: 0.75.
- Paper title should be in one column of font size 24.
- Author name in font size of 11 in one column.
- Abstract: font size 9 with the word "Abstract" in bold italics.
- Main text: font size 10 with two justified columns.
- Two columns with equal column width of 3.38 and spacing of 0.2.
- First character must be three lines drop-capped.
- The paragraph before spacing of 1 pt and after of 0 pt.
- Line spacing of 1 pt.
- Large images must be in one column.
- The names of first main headings (Heading 1) must be in Roman font, capital letters, and font size of 10.
- The names of second main headings (Heading 2) must not include numbers and must be in italics with a font size of 10.

Structure and Format of Manuscript

The recommended size of an original research paper is under 15,000 words and review papers under 7,000 words. Research articles should be less than 10,000 words. Research papers are usually longer than review papers. Review papers are reports of significant research (typically less than 7,000 words, including tables, figures, and references)

A research paper must include:

a) A title which should be relevant to the theme of the paper.
b) A summary, known as an abstract (less than 150 words), containing the major results and conclusions.
c) Up to 10 keywords that precisely identify the paper's subject, purpose, and focus.
d) An introduction, giving fundamental background objectives.
e) Resources and techniques with sufficient complete experimental details (wherever possible by reference) to permit repetition, sources of information must be given, and numerical methods must be specified by reference.
f) Results which should be presented concisely by well-designed tables and figures.
g) Suitable statistical data should also be given.
h) All data must have been gathered with attention to numerical detail in the planning stage.

Design has been recognized to be essential to experiments for a considerable time, and the editor has decided that any paper that appears not to have adequate numerical treatments of the data will be returned unrefereed.

i) Discussion should cover implications and consequences and not just recapitulate the results; conclusions should also be summarized.
j) There should be brief acknowledgments.
k) There ought to be references in the conventional format. Global Journals recommends APA format.

Authors should carefully consider the preparation of papers to ensure that they communicate effectively. Papers are much more likely to be accepted if they are carefully designed and laid out, contain few or no errors, are summarizing, and follow instructions. They will also be published with much fewer delays than those that require much technical and editorial correction.

The Editorial Board reserves the right to make literary corrections and suggestions to improve brevity.



Format Structure

It is necessary that authors take care in submitting a manuscript that is written in simple language and adheres to published guidelines.

All manuscripts submitted to Global Journals should include:

Title

The title page must carry an informative title that reflects the content, a running title (less than 45 characters together with spaces), names of the authors and co-authors, and the place(s) where the work was carried out.

Author details

The full postal address of any related author(s) must be specified.

Abstract

The abstract is the foundation of the research paper. It should be clear and concise and must contain the objective of the paper and inferences drawn. It is advised to not include big mathematical equations or complicated jargon.

Many researchers searching for information online will use search engines such as Google, Yahoo or others. By optimizing your paper for search engines, you will amplify the chance of someone finding it. In turn, this will make it more likely to be viewed and cited in further works. Global Journals has compiled these guidelines to facilitate you to maximize the web-friendliness of the most public part of your paper.

Keywords

A major lynchpin of research work for the writing of research papers is the keyword search, which one will employ to find both library and internet resources. Up to eleven keywords or very brief phrases have to be given to help data retrieval, mining, and indexing.

One must be persistent and creative in using keywords. An effective keyword search requires a strategy: planning of a list of possible keywords and phrases to try.

Choice of the main keywords is the first tool of writing a research paper. Research paper writing is an art. Keyword search should be as strategic as possible.

One should start brainstorming lists of potential keywords before even beginning searching. Think about the most important concepts related to research work. Ask, “What words would a source have to include to be truly valuable in a research paper?” Then consider synonyms for the important words.

It may take the discovery of only one important paper to steer in the right keyword direction because, in most databases, the keywords under which a research paper is abstracted are listed with the paper.

Numerical Methods

Numerical methods used should be transparent and, where appropriate, supported by references.

Abbreviations

Authors must list all the abbreviations used in the paper at the end of the paper or in a separate table before using them.

Formulas and equations

Authors are advised to submit any mathematical equation using either MathJax, KaTeX, or LaTeX, or in a very high-quality image.

Tables, Figures, and Figure Legends

Tables: Tables should be cautiously designed, uncrowned, and include only essential data. Each must have an Arabic number, e.g., Table 4, a self-explanatory caption, and be on a separate sheet. Authors must submit tables in an editable format and not as images. References to these tables (if any) must be mentioned accurately.

Figures

Figures are supposed to be submitted as separate files. Always include a citation in the text for each figure using Arabic numbers, e.g., Fig. 4. Artwork must be submitted online in vector electronic form or by emailing it.

Preparation of Eletronic Figures for Publication

Although low-quality images are sufficient for review purposes, print publication requires high-quality images to prevent the final product being blurred or fuzzy. Submit (possibly by e-mail) EPS (line art) or TIFF (halftone/ photographs) files only. MS PowerPoint and Word Graphics are unsuitable for printed pictures. Avoid using pixel-oriented software. Scans (TIFF only) should have a resolution of at least 350 dpi (halftone) or 700 to 1100 dpi (line drawings). Please give the data for figures in black and white or submit a Color Work Agreement form. EPS files must be saved with fonts embedded (and with a TIFF preview, if possible).

For scanned images, the scanning resolution at final image size ought to be as follows to ensure good reproduction: line art: >650 dpi; halftones (including gel photographs): >350 dpi; figures containing both halftone and line images: >650 dpi.

Color charges: Authors are advised to pay the full cost for the reproduction of their color artwork. Hence, please note that if there is color artwork in your manuscript when it is accepted for publication, we would require you to complete and return a Color Work Agreement form before your paper can be published. Also, you can email your editor to remove the color fee after acceptance of the paper.

Tips for Writing a Good Quality Science Frontier Research Paper

Techniques for writing a good quality Science Frontier Research paper:

1. Choosing the topic: In most cases, the topic is selected by the interests of the author, but it can also be suggested by the guides. You can have several topics, and then judge which you are most comfortable with. This may be done by asking several questions of yourself, like "Will I be able to carry out a search in this area? Will I find all necessary resources to accomplish the search? Will I be able to find all information in this field area?" If the answer to this type of question is "yes," then you ought to choose that topic. In most cases, you may have to conduct surveys and visit several places. Also, you might have to do a lot of work to find all the rises and falls of the various data on that subject. Sometimes, detailed information plays a vital role, instead of short information. Evaluators are human: The first thing to remember is that evaluators are also human beings. They are not only meant for rejecting a paper. They are here to evaluate your paper. So present your best aspect.

2. Think like evaluators: If you are in confusion or getting demotivated because your paper may not be accepted by the evaluators, then think, and try to evaluate your paper like an evaluator. Try to understand what an evaluator wants in your research paper, and you will automatically have your answer. Make blueprints of paper: The outline is the plan or framework that will help you to arrange your thoughts. It will make your paper logical. But remember that all points of your outline must be related to the topic you have chosen.

3. Ask your guides: If you are having any difficulty with your research, then do not hesitate to share your difficulty with your guide (if you have one). They will surely help you out and resolve your doubts. If you can't clarify what exactly you require for your work, then ask your supervisor to help you with an alternative. He or she might also provide you with a list of essential readings.

4. Use of computer is recommended: As you are doing research in the field of science frontier then this point is quite obvious. Use right software: Always use good quality software packages. If you are not capable of judging good software, then you can lose the quality of your paper unknowingly. There are various programs available to help you which you can get through the internet.

5. Use the internet for help: An excellent start for your paper is using Google. It is a wondrous search engine, where you can have your doubts resolved. You may also read some answers for the frequent question of how to write your research paper or find a model research paper. You can download books from the internet. If you have all the required books, place importance on reading, selecting, and analyzing the specified information. Then sketch out your research paper. Use big pictures: You may use encyclopedias like Wikipedia to get pictures with the best resolution. At Global Journals, you should strictly follow here.



© Copyright by Global Journals | Guidelines Handbook

6. Bookmarks are useful: When you read any book or magazine, you generally use bookmarks, right? It is a good habit which helps to not lose your continuity. You should always use bookmarks while searching on the internet also, which will make your search easier.

7. Revise what you wrote: When you write anything, always read it, summarize it, and then finalize it.

8. Make every effort: Make every effort to mention what you are going to write in your paper. That means always have a good start. Try to mention everything in the introduction—what is the need for a particular research paper. Polish your work with good writing skills and always give an evaluator what he wants. Make backups: When you are going to do any important thing like making a research paper, you should always have backup copies of it either on your computer or on paper. This protects you from losing any portion of your important data.

9. Produce good diagrams of your own: Always try to include good charts or diagrams in your paper to improve quality. Using several unnecessary diagrams will degrade the quality of your paper by creating a hodgepodge. So always try to include diagrams which were made by you to improve the readability of your paper. Use of direct quotes: When you do research relevant to literature, history, or current affairs, then use of quotes becomes essential, but if the study is relevant to science, use of quotes is not preferable.

10. Use proper verb tense: Use proper verb tenses in your paper. Use past tense to present those events that have happened. Use present tense to indicate events that are going on. Use future tense to indicate events that will happen in the future. Use of wrong tenses will confuse the evaluator. Avoid sentences that are incomplete.

11. Pick a good study spot: Always try to pick a spot for your research which is quiet. Not every spot is good for studying.

12. Know what you know: Always try to know what you know by making objectives, otherwise you will be confused and unable to achieve your target.

13. Use good grammar: Always use good grammar and words that will have a positive impact on the evaluator; use of good vocabulary does not mean using tough words which the evaluator has to find in a dictionary. Do not fragment sentences. Eliminate one-word sentences. Do not ever use a big word when a smaller one would suffice.

Verbs have to be in agreement with their subjects. In a research paper, do not start sentences with conjunctions or finish them with prepositions. When writing formally, it is advisable to never split an infinitive because someone will (wrongly) complain. Avoid clichés like a disease. Always shun irritating alliteration. Use language which is simple and straightforward. Put together a neat summary.

14. Arrangement of information: Each section of the main body should start with an opening sentence, and there should be a changeover at the end of the section. Give only valid and powerful arguments for your topic. You may also maintain your arguments with records.

15. Never start at the last minute: Always allow enough time for research work. Leaving everything to the last minute will degrade your paper and spoil your work.

16. Multitasking in research is not good: Doing several things at the same time is a bad habit in the case of research activity. Research is an area where everything has a particular time slot. Divide your research work into parts, and do a particular part in a particular time slot.

17. Never copy others' work: Never copy others' work and give it your name because if the evaluator has seen it anywhere, you will be in trouble. Take proper rest and food: No matter how many hours you spend on your research activity, if you are not taking care of your health, then all your efforts will have been in vain. For quality research, take proper rest and food.

18. Go to seminars: Attend seminars if the topic is relevant to your research area. Utilize all your resources.

19. Refresh your mind after intervals: Try to give your mind a rest by listening to soft music or sleeping in intervals. This will also improve your memory. Acquire colleagues: Always try to acquire colleagues. No matter how sharp you are, if you acquire colleagues, they can give you ideas which will be helpful to your research.

20. Think technically: Always think technically. If anything happens, search for its reasons, benefits, and demerits. Think and then print: When you go to print your paper, check that tables are not split, headings are not detached from their descriptions, and page sequence is maintained.

21. Adding unnecessary information: Do not add unnecessary information like "I have used MS Excel to draw graphs." Irrelevant and inappropriate material is superfluous. Foreign terminology and phrases are not apropos. One should never take a broad view. Analogy is like feathers on a snake. Use words properly, regardless of how others use them. Remove quotations. Puns are for kids, not grunt readers. Never oversimplify: When adding material to your research paper, never go for oversimplification; this will definitely irritate the evaluator. Be specific. Never use rhythmic redundancies. Contractions shouldn't be used in a research paper. Comparisons are as terrible as clichés. Give up ampersands, abbreviations, and so on. Remove commas that are not necessary. Parenthetical words should be between brackets or commas. Understatement is always the best way to put forward earth-shaking thoughts. Give a detailed literary review.

22. Report concluded results: Use concluded results. From raw data, filter the results, and then conclude your studies based on measurements and observations taken. An appropriate number of decimal places should be used. Parenthetical remarks are prohibited here. Proofread carefully at the final stage. At the end, give an outline to your arguments. Spot perspectives of further study of the subject. Justify your conclusion at the bottom sufficiently, which will probably include examples.

23. Upon conclusion: Once you have concluded your research, the next most important step is to present your findings. Presentation is extremely important as it is the definite medium though which your research is going to be in print for the rest of the crowd. Care should be taken to categorize your thoughts well and present them in a logical and neat manner. A good quality research paper format is essential because it serves to highlight your research paper and bring to light all necessary aspects of your research.

Informal Guidelines of Research Paper Writing

Key points to remember:

- Submit all work in its final form.
- Write your paper in the form which is presented in the guidelines using the template.
- Please note the criteria peer reviewers will use for grading the final paper.

Final points:

One purpose of organizing a research paper is to let people interpret your efforts selectively. The journal requires the following sections, submitted in the order listed, with each section starting on a new page:

The introduction: This will be compiled from reference matter and reflect the design processes or outline of basis that directed you to make a study. As you carry out the process of study, the method and process section will be constructed like that. The results segment will show related statistics in nearly sequential order and direct reviewers to similar intellectual paths throughout the data that you gathered to carry out your study.

The discussion section:

This will provide understanding of the data and projections as to the implications of the results. The use of good quality references throughout the paper will give the effort trustworthiness by representing an alertness to prior workings.

Writing a research paper is not an easy job, no matter how trouble-free the actual research or concept. Practice, excellent preparation, and controlled record-keeping are the only means to make straightforward progression.

General style:

Specific editorial column necessities for compliance of a manuscript will always take over from directions in these general guidelines.

To make a paper clear: Adhere to recommended page limits.



Mistakes to avoid:

- Insertion of a title at the foot of a page with subsequent text on the next page.
- Separating a table, chart, or figure—confine each to a single page.
- Submitting a manuscript with pages out of sequence.
- In every section of your document, use standard writing style, including articles ("a" and "the").
- Keep paying attention to the topic of the paper.
- Use paragraphs to split each significant point (excluding the abstract).
- Align the primary line of each section.
- Present your points in sound order.
- Use present tense to report well-accepted matters.
- Use past tense to describe specific results.
- Do not use familiar wording; don't address the reviewer directly. Don't use slang or superlatives.
- Avoid use of extra pictures—include only those figures essential to presenting results.

Title page:

Choose a revealing title. It should be short and include the name(s) and address(es) of all authors. It should not have acronyms or abbreviations or exceed two printed lines.

Abstract: This summary should be two hundred words or less. It should clearly and briefly explain the key findings reported in the manuscript and must have precise statistics. It should not have acronyms or abbreviations. It should be logical in itself. Do not cite references at this point.

An abstract is a brief, distinct paragraph summary of finished work or work in development. In a minute or less, a reviewer can be taught the foundation behind the study, common approaches to the problem, relevant results, and significant conclusions or new questions.

Write your summary when your paper is completed because how can you write the summary of anything which is not yet written? Wealth of terminology is very essential in abstract. Use comprehensive sentences, and do not sacrifice readability for brevity; you can maintain it succinctly by phrasing sentences so that they provide more than a lone rationale. The author can at this moment go straight to shortening the outcome. Sum up the study with the subsequent elements in any summary. Try to limit the initial two items to no more than one line each.

Reason for writing the article—theory, overall issue, purpose.

- Fundamental goal.
- To-the-point depiction of the research.
- Consequences, including definite statistics—if the consequences are quantitative in nature, account for this; results of any numerical analysis should be reported. Significant conclusions or questions that emerge from the research.

Approach:

- Single section and succinct.
- An outline of the job done is always written in past tense.
- Concentrate on shortening results—limit background information to a verdict or two.
- Exact spelling, clarity of sentences and phrases, and appropriate reporting of quantities (proper units, important statistics) are just as significant in an abstract as they are anywhere else.

Introduction:

The introduction should "introduce" the manuscript. The reviewer should be presented with sufficient background information to be capable of comprehending and calculating the purpose of your study without having to refer to other works. The basis for the study should be offered. Give the most important references, but avoid making a comprehensive appraisal of the topic. Describe the problem visibly. If the problem is not acknowledged in a logical, reasonable way, the reviewer will give no attention to your results. Speak in common terms about techniques used to explain the problem, if needed, but do not present any particulars about the protocols here.

The following approach can create a valuable beginning:

- Explain the value (significance) of the study.
- Defend the model—why did you employ this particular system or method? What is its compensation? Remark upon its appropriateness from an abstract point of view as well as pointing out sensible reasons for using it.
- Present a justification. State your particular theory(-ies) or aim(s), and describe the logic that led you to choose them.
- Briefly explain the study's tentative purpose and how it meets the declared objectives.

Approach:

Use past tense except for when referring to recognized facts. After all, the manuscript will be submitted after the entire job is done. Sort out your thoughts; manufacture one key point for every section. If you make the four points listed above, you will need at least four paragraphs. Present surrounding information only when it is necessary to support a situation. The reviewer does not desire to read everything you know about a topic. Shape the theory specifically—do not take a broad view.

As always, give awareness to spelling, simplicity, and correctness of sentences and phrases.

Procedures (methods and materials):

This part is supposed to be the easiest to carve if you have good skills. A soundly written procedures segment allows a capable scientist to replicate your results. Present precise information about your supplies. The suppliers and clarity of reagents can be helpful bits of information. Present methods in sequential order, but linked methodologies can be grouped as a segment. Be concise when relating the protocols. Attempt to give the least amount of information that would permit another capable scientist to replicate your outcome, but be cautious that vital information is integrated. The use of subheadings is suggested and ought to be synchronized with the results section.

When a technique is used that has been well-described in another section, mention the specific item describing the way, but draw the basic principle while stating the situation. The purpose is to show all particular resources and broad procedures so that another person may use some or all of the methods in one more study or referee the scientific value of your work. It is not to be a step-by-step report of the whole thing you did, nor is a methods section a set of orders.

Materials:

Materials may be reported in part of a section or else they may be recognized along with your measures.

Methods:

- Report the method and not the particulars of each process that engaged the same methodology.
- Describe the method entirely.
- To be succinct, present methods under headings dedicated to specific dealings or groups of measures.
- Simplify—detail how procedures were completed, not how they were performed on a particular day.
- If well-known procedures were used, account for the procedure by name, possibly with a reference, and that's all.

Approach:

It is embarrassing to use vigorous voice when documenting methods without using first person, which would focus the reviewer's interest on the researcher rather than the job. As a result, when writing up the methods, most authors use third person passive voice.

Use standard style in this and every other part of the paper—avoid familiar lists, and use full sentences.

What to keep away from:

- Resources and methods are not a set of information.
- Skip all descriptive information and surroundings—save it for the argument.
- Leave out information that is immaterial to a third party.



© Copyright by Global Journals | Guidelines Handbook

Results:

The principle of a results segment is to present and demonstrate your conclusion. Create this part as entirely objective details of the outcome, and save all understanding for the discussion.

The page length of this segment is set by the sum and types of data to be reported. Use statistics and tables, if suitable, to present consequences most efficiently.

You must clearly differentiate material which would usually be incorporated in a study editorial from any unprocessed data or additional appendix matter that would not be available. In fact, such matters should not be submitted at all except if requested by the instructor.

Content:

- Sum up your conclusions in text and demonstrate them, if suitable, with figures and tables.
- In the manuscript, explain each of your consequences, and point the reader to remarks that are most appropriate.
- Present a background, such as by describing the question that was addressed by creation of an exacting study.
- Explain results of control experiments and give remarks that are not accessible in a prescribed figure or table, if appropriate.
- Examine your data, then prepare the analyzed (transformed) data in the form of a figure (graph), table, or manuscript.

What to stay away from:

- Do not discuss or infer your outcome, report surrounding information, or try to explain anything.
- Do not include raw data or intermediate calculations in a research manuscript.
- Do not present similar data more than once.
- A manuscript should complement any figures or tables, not duplicate information.
- Never confuse figures with tables—there is a difference.

Approach:

As always, use past tense when you submit your results, and put the whole thing in a reasonable order.

Put figures and tables, appropriately numbered, in order at the end of the report.

If you desire, you may place your figures and tables properly within the text of your results section.

Figures and tables:

If you put figures and tables at the end of some details, make certain that they are visibly distinguished from any attached appendix materials, such as raw facts. Whatever the position, each table must be titled, numbered one after the other, and include a heading. All figures and tables must be divided from the text.

Discussion:

The discussion is expected to be the trickiest segment to write. A lot of papers submitted to the journal are discarded based on problems with the discussion. There is no rule for how long an argument should be.

Position your understanding of the outcome visibly to lead the reviewer through your conclusions, and then finish the paper with a summing up of the implications of the study. The purpose here is to offer an understanding of your results and support all of your conclusions, using facts from your research and generally accepted information, if suitable. The implication of results should be fully described.

Infer your data in the conversation in suitable depth. This means that when you clarify an observable fact, you must explain mechanisms that may account for the observation. If your results vary from your prospect, make clear why that may have happened. If your results agree, then explain the theory that the proof supported. It is never suitable to just state that the data approved the prospect, and let it drop at that. Make a decision as to whether each premise is supported or discarded or if you cannot make a conclusion with assurance. Do not just dismiss a study or part of a study as "uncertain."

Research papers are not acknowledged if the work is imperfect. Draw what conclusions you can based upon the results that you have, and take care of the study as a finished work.

- You may propose future guidelines, such as how an experiment might be personalized to accomplish a new idea.
- Give details of all of your remarks as much as possible, focusing on mechanisms.
- Make a decision as to whether the tentative design sufficiently addressed the theory and whether or not it was correctly restricted. Try to present substitute explanations if they are sensible alternatives.
- One piece of research will not counter an overall question, so maintain the large picture in mind. Where do you go next? The best studies unlock new avenues of study. What questions remain?
- Recommendations for detailed papers will offer supplementary suggestions.

Approach:

When you refer to information, differentiate data generated by your own studies from other available information. Present work done by specific persons (including you) in past tense.

Describe generally acknowledged facts and main beliefs in present tense.

The Administration Rules

Administration Rules to Be Strictly Followed before Submitting Your Research Paper to Global Journals Inc.

Please read the following rules and regulations carefully before submitting your research paper to Global Journals Inc. to avoid rejection.

Segment draft and final research paper: You have to strictly follow the template of a research paper, failing which your paper may get rejected. You are expected to write each part of the paper wholly on your own. The peer reviewers need to identify your own perspective of the concepts in your own terms. Please do not extract straight from any other source, and do not rephrase someone else's analysis. Do not allow anyone else to proofread your manuscript.

Written material: You may discuss this with your guides and key sources. Do not copy anyone else's paper, even if this is only imitation, otherwise it will be rejected on the grounds of plagiarism, which is illegal. Various methods to avoid plagiarism are strictly applied by us to every paper, and, if found guilty, you may be blacklisted, which could affect your career adversely. To guard yourself and others from possible illegal use, please do not permit anyone to use or even read your paper and file.

Criterion for Grading a Research Paper (Compilation) by Global Journals

Please note that following table is only a Grading of "Paper Compilation" and not on "Performed/Stated Research" whose grading solely depends on Individual Assigned Peer Reviewer and Editorial Board Member. These can be available only on request and after decision of Paper. This report will be the property of Global Journals.

Topics	Grades		
	A-B	**C-D**	**E-F**
Abstract	Clear and concise with appropriate content, Correct format. 200 words or below	Unclear summary and no specific data, Incorrect form Above 200 words	No specific data with ambiguous information Above 250 words
Introduction	Containing all background details with clear goal and appropriate details, flow specification, no grammar and spelling mistake, well organized sentence and paragraph, reference cited	Unclear and confusing data, appropriate format, grammar and spelling errors with unorganized matter	Out of place depth and content, hazy format
Methods and Procedures	Clear and to the point with well arranged paragraph, precision and accuracy of facts and figures, well organized subheads	Difficult to comprehend with embarrassed text, too much explanation but completed	Incorrect and unorganized structure with hazy meaning
Result	Well organized, Clear and specific, Correct units with precision, correct data, well structuring of paragraph, no grammar and spelling mistake	Complete and embarrassed text, difficult to comprehend	Irregular format with wrong facts and figures
Discussion	Well organized, meaningful specification, sound conclusion, logical and concise explanation, highly structured paragraph reference cited	Wordy, unclear conclusion, spurious	Conclusion is not cited, unorganized, difficult to comprehend
References	Complete and correct format, well organized	Beside the point, Incomplete	Wrong format and structuring

INDEX

A

Acceleration · 25, 69
Alleviate · 2
Atrium · 55

B

Blatant · 50

C

Contradiction · 1, 50

E

Ecliptic · 30, 45
Elivination · 1, 50

L

Luminary · 40

P

Paddle · 32
Prigogine · 52, 54, 58, 62, 64, 65, 67

S

Smearing · 40
Spontaneous · 1, 73, 77, 83, 92, 103
Striations. · 73
Strive · 33

T

Tranparent · 103

V

Ventricle · 55





Global Journal of Science Frontier Research

Visit us on the Web at www.GlobalJournals.org | www.JournalofScience.org
or email us at helpdesk@globaljournals.org

ISSN 9755896



© Global Journals